UNIVERSITY OF SÃO PAULO
POLYTECHNIC SCHOOL

GUSTAVO PEREIRA ZAGO

Novel natural-based polymers for dewatering of iron ore tailings

São Paulo
2022

GUSTAVO PEREIRA ZAGO

Novel natural-based polymers for dewatering iron ore tailings

Corrected Version

Thesis presented to the Escola Politécnica da Universidade de São Paulo to obtain the degree of Doctor of Science.

São Paulo
2022

GUSTAVO PEREIRA ZAGO

Novel natural-based polymers for dewatering iron ore tailings

Corrected Version

Thesis presented to the Escola Politécnica da Universidade de São Paulo to obtain the degree of Doctor of Science.

Concentration Field: Chemical Engineering

Advisor: Prof. Dr. Reinaldo Giudici

Co-advisor: Prof. Joao B. Soares

São Paulo
2022

Este exemplar foi revisado e corrigido em relação à versão original, sob responsabilidade única do autor e com a anuência de seu orientador.

São Paulo, 17 de outubro de 2022

Assinatura do autor: _____

Assinatura do orientador: _____

Catalogação-na-publicação

Pereira Zago, Gustavo
Novel natural-based polymers for dewatering iron ore tailings / G. Pereira Zago -- versão corr. -- São Paulo, 2022.
146 p.

Tese (Doutorado) - Escola Politécnica da Universidade de São Paulo. Departamento de Engenharia Química.

1.FLOCULAÇÃO 2.MINERAÇÃO DE MINERAIS INDUSTRIAIS 3.RECURSOS NATURAIS 4.DESAGUAMENTO I.Universidade de São Paulo. Escola Politécnica. Departamento de Engenharia Química II.t.

ACKNOWLEDGMENTS

First, I would like to express my gratitude to my advisor, Dr. Reinaldo Giudici. He has been supportive, kind and has given me excellent guidance and encouragement throughout my research and graduate studies.

I would like to express my sincere gratitude to my co-advisor, Dr. Joao Soares, who has given valuable time, advice, and considerable contribution to the writing of this thesis. This thesis would not have been possible without his assistance and guidance. Having had the opportunity to work with Dr. Soares in his group at the University of Alberta was a great experience for me.

To my mother for her support and guidance throughout this process.

Thank you to all my friends for their unquestionable good times shared and your support in overcoming the difficulties encountered during this time.

Last but not least, I would like to thank everyone who contributed to this project.

“Your beliefs become your thoughts,
Your thoughts become your words,
Your words become your actions,
Your actions become your habits,
Your habits become your values,
Your values become your destiny.”

— Mahatma Gandhi

RESUMO

ZAGO, Gustavo Pereira. **Novel natural-based polymers for dewatering of iron ore tailings**. 2022. 132 p. Tese (Doutorado em Ciências) - Departamento de Engenharia Química da Escola Politécnica, Universidade de São Paulo, São Paulo, 2022.

Em resposta ao crescimento da demanda por produtos minerais, os rejeitos de minério contendo particulados finos continuam sendo intensamente acumulados, e não existem esforços suficientes para que sejam processados. O volume e a composição dos rejeitos dependem principalmente do tipo de minério e dos processos de beneficiamento utilizados. Nas últimas décadas, a intensa exploração resultou na disponibilidade de minerais com baixas concentrações de metais e composições muito complexas. Para serem processados, eles requerem mais água e, consequentemente geram mais rejeitos. Assim, para que a indústria mineral seja sustentável, devem ser adotados métodos alternativos que reduzam os resíduos gerados no beneficiamento mineral. Nesse contexto, a floculação pode ser um processo promissor para desaguamento e consolidação de rejeitos minerais, pois possibilita a redução do volume produzido.

Neste trabalho, foi desenvolvido floculante de base natural para o tratamento de rejeitos de minério de ferro. Os copolímeros de enxerto foram sintetizados por meio da incorporação de cloreto de (2-metacriloiloxietil) trimetil amônio à cadeia principal de amilopectina (AP-g-PMETAC). Para cada polímero, foi alterada a frequência dos enxertos, seu comprimento, proporção de enxerto no produto e o peso molecular. Ao entender como esses parâmetros microestruturais afetam na eficiência de floculação, o polímero pode ser modificado para ter um desempenho melhor do que os floculantes convencionais à base de poliacrilamida. Os polímeros AP-g-PMETAC foram caracterizados por análise termogravimétrica (TGA), espectroscopia de infravermelho por transformada de Fourier (FTIR), espectroscopia de ressonância magnética nuclear (RMN), análise elementar de CHNO e cromatografia de permeação em gel (GPC/SEC). O desempenho de floculação/desidratação foi mensurado por meio da turbidez do sobrenadante, taxa de sedimentação inicial (ISR), tempo de sucção capilar (CST) e teor de sólidos dos sedimentos.

Primeiramente, dois floculantes comerciais de poliacrilamida foram testados para se estabelecer um parâmetro comparativo para a eficiência de floculação do copolímero AP-g-PMETAC. Com relação à clarificação do sobrenadante de rejeitos e taxa de sedimentação dos

flocos formados, o AP-g-PMETAC superou significativamente o desempenho do PAM comercial. Devido ao caráter hidrofóbico da amilopectina, o AP-g-METAC foi capaz de produzir sedimentos treze vezes mais fáceis de serem desaguados do que o PAM comercial. Os AP-g-PMETAC sintetizados com enxertos mais longos e mais distribuídos na cadeia principal da AP, foram melhores em clarificar o sobrenadante com a adição de baixas dosagens do floculante. No entanto, enxertos muito longos devem ser evitados devido ao caráter hidrofílico do PMETAC, que prejudicaria a densificação do sedimento. Além disso, os rejeitos de minério de ferro foram também floculados com dois polímeros desenvolvidos exclusivamente para tratar rejeitos de areia betuminosa: cloreto de poli(vinilbenzil)trimetilamônio (PVB) e poli(metil acrilato) parcialmente hidrolisado enxertado nas cadeias de copolímeros de etileno-propileno-dieno (EPDM-g-HPMA). Apesar de terem sido desenvolvidos para rejeitos completamente diferentes, eles foram capazes de sedimentar as partículas suspensas e produzir um sobrenadante altamente clarificado. No entanto, eles produziram sedimentos com baixo teor de sólidos. Possivelmente, se o peso molecular e a proporção de monômeros hidrofóbicos forem variados, essa restrição pode ser eliminada.

Palavras-chave: floculação, mineração, minério de ferro, rejeitos, polímeros naturais.

ABSTRACT

ZAGO, Gustavo Pereira. **Novel natural-based polymers for dewatering of iron ore tailings**. 2022. 132 p. Thesis (Doctor of Science in Chemical Engineering). - Escola Politécnica, Universidade de São Paulo, São Paulo, 2022.

In response to the growth in demand for mineral products, fine ore tailings continue to be intensively accumulated, but not enough ways exist for them to be processed. Tailings volume and composition depend primarily on the type of ore and the beneficiation processes used. The last few decades have seen extensive exploitation lead to minerals with low metal concentrations and highly complex compositions. These minerals require more water and generate more tailings during beneficiation. Therefore, for the mineral industry to be sustainable, alternative methods must be adopted that reduce waste generated during mineral processing. This context has made flocculation a promising approach to reducing the volume of mineral tailings by dewatering and consolidating them.

In the present work a natural-based graft copolymer was synthesized and used to flocculate and dewater iron ore tailings. The polymers were made by attaching (2-methacryloyloxyethyl) trimethyl ammonium chloride to the amylopectin backbone (AP-g-PMETAC). For each polymer, it was varied the frequency of grafts along the backbone, their length, grafting ratio, and molecular weight. By understanding how these microstructure parameters affect its flocculation performance, the polymer can be tailored to perform better than conventional polyacrylamide-based flocculants, widely used in mineral tailings. The AP-g-PMETAC copolymers were characterized via thermogravimetric analysis (TGA), Fourier transform infrared spectroscopy (FTIR), and nuclear magnetic resonance spectroscopy (^{13}C and ^{1}H NMR), CHNSO elemental analysis, and gel permeation chromatography (GPC). The flocculation/dewatering performance was measured using supernatant turbidity, initial settling rate (ISR), capillary suction time (CST), and solid contents of the sediments.

First, two commercial polyacrylamide flocculants were studied to establish a performance comparison for flocculation of the AP-g-PMETAC copolymer. AP-g-PMETAC outperformed PAM in clarifying tailings supernatant and floc settling rate. Due to its hydrophobic backbone, AP-g-PMETAC produced sediments that were thirteen times easier to dewater than commercial PAM. High flocculation efficiency was achieved by adding small amounts of flocculants (500 ppm) to the graft copolymer with more and longer grafts onto the AP backbone. In addition,

due to the hydrophilicity of PMETAC, the graft length must be tailored carefully to ensure good sediment densification. In addition, we flocculated the iron ore tailings with two polymers designed to treat oil sand tailings: Poly((vinyl benzyl)trimethylammonium chloride) and partially hydrolyzed poly(methyl acrylate) grafted onto ethylene-propylene-diene copolymer backbones. Despite being developed for entirely different tailings, they consistently produced clearer supernatants than commercially available polyacrylamides. Their only disadvantage was that they retained much water in the sediment, in contrast to polyacrylamide (PAM). Nevertheless, if the molecular weight and proportion of hydrophobic monomers are varied, this constraint could be eliminated.

Keywords: Flocculation, mining, iron ore, tailings, natural polymers.

LIST OF TABLES

LIST OF FIGURES

NOMENCLATURE

AP-g- PMETAC	Amylopectin-*graft*-(2-methacryloyloxyethyl) trimethyl ammonium chloride
FTIR	Fourier Transform Infrared Spectroscopy
TGA	Thermogravimetric Analysis
NMR	Nuclear Magnetic Resonance Spectroscopy
CHNO	Carbon-Hydrogen-Nitrogen-Oxygen Elemental Analysis
GPC	Gel Permeation Chromatography
CST	Capillary Suction Time
PMETAC	Poly(2-methacryloyloxyethyl) trimethyl ammonium chloride
PAM	Polyacrylamide
PVB	Poly ((vinyl benzyl) trimethylammonium chloride)
EDM-HPMA	Partially hydrolyzed Poly (methyl acrylate) grafted onto ethylene-propylene-diene copolymer backbones
ISR	Initial Settling Rate
EDL	Electrical Double-Layer
ISP	Isoelectric Point
PAA	Polyacrylic acid
PMA	Poly(methacrylate)
PMMA	Poly(methyl methacrylate)
PDADMAC	Poly(diallyl dimethylammonium chloride)
PEO	Polyethylene oxide
PSD	Particle Size Distribution
AM	Acrylamide
DMA	N, N-dimethyl acrylamide
AA	Acrylic Acid
M_w	Weight Average Molecular Weight

M_n	Number Average Molecular Weight
HMPC	Hydroxypropyl methylcellulose
Chi- g-P(AM-DMDAAC	Chitosan-graft poly(acrylamide-dimethyl diallyl ammonium chloride)
ATR	Attenuated Total Reflection
XRD	X-ray powder diffraction
XRF	X-ray fluorescence
SEM-EDS	Scanning Electron Microscopy coupled with Spectroscopy of Dispersion Energy
TSI	Turbiscan® stability index
TS%	Percentage of light Transmitted
BS%	Percentage of light Backscattered
ICP-OES	Inductively Coupled Plasma - Optical Emission Spectrometry
APS	Ammonium persulphate
KPS	Potassium persulphate
AGU	Anhydroglucose units
N	Average number of graft-chains
L	Average length of graft-chains
$N_{wt.\%}$	Nitrogen content of the copolymer
$M_{w_{(METAC)}}$	Molecular weight of METAC
W_{METAC}	Weight of grafted METAC in the grafted copolymer
W_{AP}	Weight of amylopectin in the grafted copolymer
NTU	Nephelometric Turbidity Units
ppm	parts per million (weight)
Đ	polydispersity index

TABLE OF CONTENTS

Chapter 1

Introduction

1.1 Motivation

Iron ore is one of the world's most exploited raw materials, and Brazil is one of the top three producing countries (69% of global production comes from Australia, Brazil, and China). Due to its importance as the primary raw material for steel manufacture, it was, is, and will remain part of the countries' industrialization process. It is known that iron ore mining impacts the environment in multiple ways, including the consumption of vast amounts of water during the entire beneficiation process, which is then left behind as tailings. The type of ore extracted and its chemical, and mineral composition determines the characteristics of beneficiation processes and tailings generated.

Since the first mines were opened, there has been an increase in demand and, consequently, a need for intensive extraction, which has forced the use of low-grade ore in the processing (Concha, 2014; Edraki et al., 2014). Low-iron ores require additional steps during beneficiation, which increases water usage and produces more tailings that contain ultrafine particles (Adiansyah et al., 2015; Das and Choudhury, 2013; Gunson et al., 2012; Kossoff et al., 2014; Lobato, 2012).

To maximize water recovery from iron ore tailings, they can be dewatered in thickeners, usually through flocculation. Underflow from thickeners is thick slurries that are pumped to tailing dams, where fine particles remain stable with water at the top, whereas coarse particles settle rapidly by gravity. Without treatment, the fine particles remain suspended for decades until the pond area can be reclaimed. As a result of its efficiency in concentrating the solids in the pulp, flocculation has proven to be a more effective strategy for the separation of ultrafine particles from mineral tailings (Cox, 2006; Luz et al., 2010; Mudd, 2008; Peixoto, 2012; Yang et al., 2019; Zuquette, 2015). Most flocculants used to treat mineral tailing are polyacrylamide

or polyacrylamide-based copolymers (Wang et al., 2014). They are widely used because they can form large aggregates easily separable from the mixture. However, polyacrylamide-based polymers and copolymers are strongly hydrophilic, favoring considerable water retention by the flocs and sedimented phase (Asare et al., 2016). In addition, the use of synthetic polymers is controversial due to their usual low biodegradability and potential environmental risk and contamination of water for human consumption.

Recently, polysaccharides with high molecular weight and highly branched structure, such as chitosan, starch, guar gum, and lignin, have been considered promising flocculants. Aside from being biodegradable, these polymers are abundant, cheap, and non-toxic. The problem with these flocculants is that they are ineffective for industrial applications. Therefore, new research has focused on developing new flocculants based on modifications of polysaccharides. There has been increasing use of polysaccharide-based graft copolymeric flocculants due to their ability to bind smaller suspended particles and enhance settling with the formation of larger flocs (Bratskaya et al., 2004; Moran and Soares, 2017; Oliveira, 2017).

In this study, different grades of amylopectin-g-poly[2-(methacryloyloxy)ethyl trimethylammonium] chloride (AP-g-PMETAC) flocculants were synthesized and used to treat iron ore tailings. The METAC monomers were incorporated into the AP backbone by free radical polymerization, and the graft-chain number and length were controlled by varying the ratio between reactants. We compared the flocculation performance of the novel graft copolymer with two commercial PAM-based flocculants. Moreover, two new polymers developed to treat oil sand tailings, which differ chemically and mineralogically from iron ore tailings, were applied. The polymers designed for oil sands application and the novel AP-g-PMETAC copolymers outperformed the conventional polyacrylamide flocculants. These findings suggest that these polymers may be an efficient alternative for the flocculation and dewatering of iron ore tailings.

1.2 Research Objectives

The general purpose of this study is to develop a new class of water-soluble polymers specifically tailored to be applied as flocculants in the dewatering of iron ore tailings. The polymers synthesized in this work will target a high flocculation efficiency, resulting in a solid phase with low water content and a liquid phase clarified enough for disposal in water bodies or, in the best scenario, to be reused in the process.

The specific objectives of this work are:

1. Literature review on technologies for dewatering mineral tailings and the application of natural-based polymers as flocculants.
2. Characterization of the solid and fluid phases in the iron ore tailings regarding its chemical and mineralogical composition, granulometric distribution, particle morphology, the zeta potential of the suspended particles, pH, and natural turbidity.
3. Investigation of the flocculation mechanism and efficiency of iron tailings using commercial polyacrylamide-based flocculants.
4. Flocculation of iron ore tailings using flocculants developed by the Dr. Soares Group and well-established for oil sand tailings.
5. Synthesis and characterization of various amylopectin-based graft copolymers using a cationic monomer ([2-(methacryloyloxy) ethyl] trimethylammonium - METAC).
6. Flocculation of iron ore tailings using the flocculants mentioned above and investigation of underlying flocculating mechanisms.

Chapter 2

Literature review

2.1 Iron ore

Iron (Fe) is the fourth most abundant element on earth and, due to its high capacity to oxidize, is present in more than 400 minerals. The main minerals containing iron are hematite (Fe_2O_3), magnetite (Fe_3O_4), and goethite (FeOOH) (Luz et al., 2010). About 99% of the iron ores are used in steel and cast-iron production.

It is estimated that Brazil has 28.9 billion tons of iron ore, of which 67% is concentrated in Minas Gerais. Of all iron ore available worldwide, the country accounts for 7.2%. (Tonietto, A; Silva, 2011). In 2021, Brazilian mineral production was equivalent to 1,150 million tons. That same year, the iron ore production value was approximately R$ 250 billion, representing 73.7% of the country's total mineral production (IBRAM, 2021).

2.2 Iron ore beneficiation and tailings generation

Mineral beneficiation refers to the physical and chemical separation process where the valuable components of an ore are concentrated to meet market specifications (Zuquette, 2015). These operations generate a large volume of tailings composed of process water, solid particles, and some chemicals (Jones and Boger, 2012; Maurice, N.; Kenneth, 2003). Other terms are used for these operations, such as mineral processing and ore treatment (Luz et al., 2010).

All mining processes have a series of steps in addition to beneficiation, as illustrated in Figure 1.

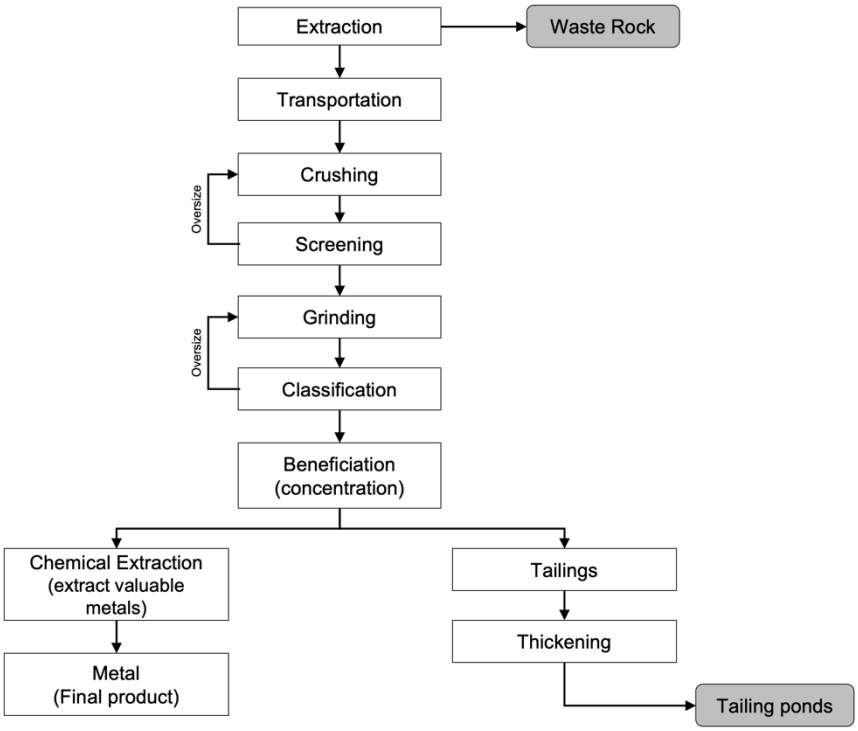

Figure 1 - Typical ore treatment flowchart (adapted from LUZ; SAMPAIO; FRANÇA, 2010)

The tailing's solid phase is composed of particulate material with a size distribution that varies from fine to coarse particles, whose proportion depends on the type and composition of the iron ore processed (Maurice, N.; Kenneth, 2003; Zuquette, 2015). In response to production volumes and market demand, low-grade minerals with highly complex compositions have been extracted and processed. Furthermore, more material must be extracted, and the beneficiation process requires more griding and water, resulting in more waste and fine particles. Consequently, the constant growth in tailings requires more space to store them and has a greater environmental impact (Crowson, 2012; Jones and Boger, 2012; Wang et al., 2014). The mining industry faces significant challenges in becoming more sustainable because of this. Therefore, existing processes must be studied, developed, and modernized to mitigate the impact of this industry (Bowker and Chambers, 2015).

2.3 Iron ore tailings

Due to the intrinsic characteristics of the material extracted from a mine and the processes adopted, the iron ore tailings' physical and geological properties may vary significantly (Araujo, 2006).

Based on the chemical composition of the particles, Fe content is a consequence of the presence of Fe-bearing minerals rejected during the concentration process, and Al content is due to clay minerals composing the slime fraction discharged by size control. The content of SiO_2 is due to the presence of quartz and clay minerals. Wolff (2009) quantified the iron content in tailings from nine Vale S.A. mines, observing concentrations ranging from 44 to 64%. Gomes et al. (2011) characterized the fine fraction of an iron ore tailings pond, finding average contents close to 49 wt.% of Fe_2O_3, 21 wt.% of SiO_2, and three wt.% Al_2O_3. Field Andrade (2014) states that the highest iron oxide content is found in the thinnest ranges, more precisely, below 37 μm. The results indicate the possibility of recycling this material to recover the expressive amount of residual ore. Although this is an up-and-coming alternative, this will not be the focus of this work.

Regarding the average size of the particles, the tailings can be classified as sand, silt, or clay. According to ISO 14688-1, particles with average sizes greater than 63 μm are classified as sands, those in the range from 2 to 63 μm are classified as silts, and finally, with sizes smaller than 2 μm, fit into the classification of clays (ISO, 2017; Wang et al., 2014). Luz, Sampaio e França (2010) reported that the fraction of tailings sent to the ponds is mainly composed of ultrafine particles (1< Ø < 10 μm) and colloids (Ø < 1 μm). Chaturvedi e Patra (2016) report that more than 60% of particles in iron ore tailings are smaller than 20 mm.

In addition, the high exploitation and consequent depletion of mineral resources forced the need for extraction and processing of low-grade materials, which requires process intensification, culminating in the production of tailings with increasingly finer particles and much larger volumes (Crowson, 2012; Jones and Boger, 2012; Rötzer and Schmidt, 2018; Wang et al., 2014). These characteristics of the tailings combined with a complex composition result in a very stable colloidal system, whose treatment is challenging and expensive. If left untreated in the ponds, these tailings take decades to settle, hampering water recovery and reclamation of the significant areas occupied by the tailing's ponds.

When tailings are disposed of in ponds, after some time, there is the formation of a layer on the surface that is free of suspended particles, the clarified layer. As a result of sedimentation, part of the particles settle to the bottom (mainly coarse particles), and the colloidal suspension of fine particles reaches its maximum stability in the central region, between the sedimented particles (at the bottom) and the clarified fraction (on top). To illustrate this formation, a scheme is shown in Figure 2.

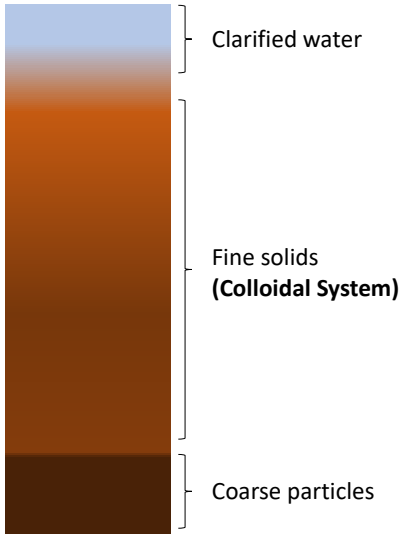

Figure 2 – Cross-sectional view of the tailings pond.

New technologies are needed to recover water from tailings and generate minimal waste. The complex composition of tailings and inefficiency of existing treatment processes have led to many efforts in industry and academia. This motivation is associated with reducing pond rupture risks as well as water recovery, tailings volume reduction, and faster reclamation of the pond (Zuquette, 2015). Over the last few years, the solution to this problem has naturally converged on the concept of 'dewatered' or 'thickened' tailings, motivating numerous studies to develop or improve flocculation and coagulation processes to achieve this goal (Peixoto, 2012).

2.4 Current technologies for the treatment of Mineral Tailings

Grinding intensification has become increasingly important to extract the maximum amount of low-grade minerals. However, this approach generates more tailings containing fine particles. The most effective way of treating mineral tailings with such complexity is to address the main problem that hampers tailings treatment, the presence of fine particles. However, there are still significant knowledge gaps regarding tailings treatment with such characteristic (Das and Choudhury, 2013).

Research on this subject has mainly focused on dewatering processes to dispose of thickened tailings. The close relationship between these processes, the reduction of tailings volume, and the possibility of water recovery make them an attractive alternative. The most common physical methods used to dewater tailings are filtration and centrifugation. Although

these physical processes dewater tailings effectively, they require large equipment and experienced operators, as well as high operational costs (M Dash et al., 2011; Yang et al., 2019).

In chemical treatments, compounds are added that act directly on the stability of the colloidal system formed in a suspension of fine particles. Coagulation and flocculation are the most common processes. During coagulation, inorganic species neutralize the charged particles (mainly negatively charged), reducing electrostatic repulsion, causing the particles to stick together (coagulate) and settle through gravity to the bottom of the pond. Unfortunately, in this process, large amounts of bivalent ions are added to coagulate fine particles, contaminating the treated water. When water reuse is the goal, a downstream separation process may be required (Bolto and Gregory, 2007; Wei et al., 2018). Flocculation, on the other hand, refers to adding polymers that physically attach to the particles. This interaction produces large particles, known as flocs, that are dense enough to settle and densify the sediment (Siah et al., 2014). Coagulants and flocculants are commonly added to the raw tailings in containers called thickeners before disposal in ponds.

2.5 Thickeners

Thickeners consist of a large diameter tank with conical bottom equipped with rotating trussed rake arms to promote movement and help settling the particles. They are used exclusively to recover part of the water and densify the tailings, subsequently transferred to the ponds.

The tailing stream is fed into the thickener's center, where solid phase sedimentation begins. The clarified solution (water) dominates on the top of the thickener, whereas the solids content increases near the bottom. The clarified water exits the thickener through the spillway and the thickener overflow. Finally, the densified solid material (formed at the bottom) is pumped from the thickener underflow into the tailing ponds. (Chaves, 2002). The underflow

stream has a solids content between 40 and 55% (Luz et al., 2010). A typical scheme of a thickener can be seen in Figure 3.

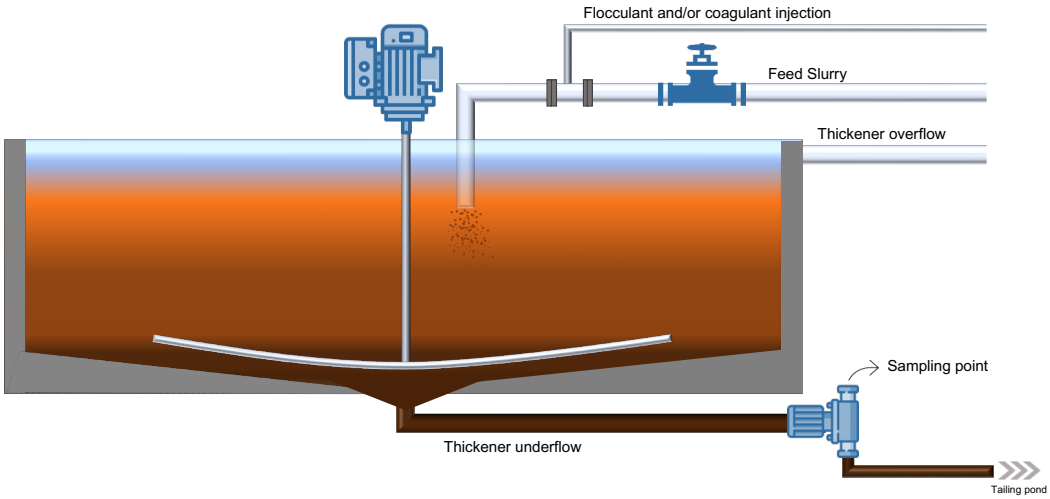

Figure 3 - Thickener scheme

The suspension formed by iron tailings has high stability, making it necessary to add coagulants or flocculants in the thickening process to improve the clarity of the clarified water and dewatering efficiency. Furthermore, these processes reduce thickener dimensions, increase particle settling rate, and enable the treatment of tailings with high fine particle content. The amount of flocculant or coagulant used is determined by considering the tailings composition, especially the fines content (Rodrigues, 2017).

Comparable to filters and centrifuges, thickeners are easier to operate and are widely used in the mineral industry. There are, however, some disadvantages to consider: it still requires experienced operators; it requires large equipment, and it may be necessary to stock the treated water through new containment structures (Arjmand et al., 2019; Luz et al., 2010).

2.6 Stability of colloidal systems

Fine particles suspended in tailings become electrically charged when dispersed in a polar environment, such as an aqueous medium. Different mechanisms can form these charges, such as ionization or dissociation of surface groups, adsorption of specific ions, or substituting surface ions. These characteristics play a significant role in the suspension's properties, such as colloidal stability, viscosity, shear strain, and compression stresses. In addition, the charge and

electrical potential of the particles depend on the solution's pH and the presence of foreign ions (Birdi, 2008).

In colloidal systems, the same signal particles repel each other, thus promoting stability and inhibiting particle aggregation. Tailings with such characteristics may require many years before they settle without treatment. Adding flocculants and coagulants to the mixture can destabilize it, accelerating particle settling. It may seem simple, but repulsion between particles is just one aspect of the mechanism behind colloidal systems. Understanding this behavior and how coagulants and flocculants destabilize the suspension requires kno`wledge of both colloidal and surface chemistry (Israelachvili, 2011; Lawrence, 1951; Ng, 2018).

In colloidal chemistry, the Derjaguin-Landau-Verwey-Overbeek (DLVO) theory discusses colloidal stability in terms of the balance between attractive van der Waals forces and repellent electrical double-layer (EDL) interactions. To favor and promote colloidal instability, it is essential to understand how colloidal particles interact based on these theoretical concepts (Cornell and Schwertmann, 2003; Napper, 1983).

2.6.1 The van der Waals force

A van der Waals force results from the attraction and/or repulsion between atoms, molecules, and/or particles. It can be either attractive or repulsive, depending on the system composition and particle properties. Furthermore, van der Waals forces are weaker than other forces, such as hydrogen bonding and coulombic interactions, and decay as the distance between particles grows (Israelachvili, 2011).

Fine particles in iron ore tailings are attracted to each other by van der Waals forces (Ho and Lee, 1998; Leong, 2021). Having only this interaction force in the bulk would result in an unstable system, which would lead to aggregation, and settling of the particles. Fine particles suspended in iron ore tailings at alkaline media, however, carry a negative charge, resulting in a much stronger repulsive force caused by the electrical double-layer effect.

2.7 Electrical double layer

A region composed of inhomogeneous cations and anions surrounds the charged colloidal particles in an aqueous environment. Because it is formed by charged species and consists of two distinct parts, this region is known as an Electrical Double Layer (EDL). Electric fields and Coulombic forces are created by the particle's and ions' electric charge to determine the distribution of ions between the particle surface and interstitial solid solution, making the individual layers. The schematic of the double-layer structure for a negatively charged particle is shown in Figure 4, and it's explained below.

To explain the formation of the EDL, we will consider the iron ore tailings scenario, where the particles are negatively charged. In solution, oppositely charged ions (counterions) are attracted and adsorbed onto the particle surface, forming an organized, fixed layer. This layer is called the stationary or Stern layer. The proximity from the negatively charged surface of the particle determines the ion distribution in this layer. As a result of Coulombic forces, cations are attracted to negatively charged particles, resulting in a higher concentration of cations in this region. This concentration decreases as the distance from the particle surface increases. Similarly, anions are repelled by particle surfaces, so their concentrations are lowest close to the surface and increase with distance. Poisson-Boltzmann equation typically governs the ion distribution in diffuse layers (see Equation 1).

$$\frac{d^2\psi}{dx^2} = -\frac{ze\rho}{\varepsilon_0\varepsilon} = -\frac{ze\rho_0}{\varepsilon_0\varepsilon} e^{-\frac{ze\psi}{kT}} \quad (1)$$

Where ψ is the electrostatic potential, z is the valence of the ion, e is the charge of an electron, x is the thickness of the stern layer, ρ is the counter ions density. ε_0 and ε are the vacuum permittivity and dielectric constant, respectively, k is the Boltzmann constant, and T is the absolute temperature (Gregory & O'Melia, 1989).

Combined, the stationary stern and diffuse layers form the so-called EDL. The stern and diffuse layers boundary is called the shear plane, where the Stern potential is defined. Immediately after the Stern layer, there is a region where cations are most concentrated and are strongly bound to the particle surface, forming an immobile region that moves simultaneously with the particle. The plane where this stationary effect ends is called the Shear plane, and the electrical potential at this point is called the Zeta potential.

The electric potential along the EDL is inversely proportional to the distance from the particle's surface. To understand this effect, consider a negatively charged particle carrying a hundred elemental charges and a single negatively charged unit distant from it. To bring the remote negative unit close to the particle, energy must be provided as a repulsion force emerges. This is the electrical potential energy expressed in volts (V). Therefore, the electrical potential refers to how much energy is required for a charged unit to move within a bulk solution. The higher the energy, the greater the repulsion force between the charged species. As a result of the presence of only negative elemental charges on the surface of the particles and the EDL around them, the starting potential is the highest on the surface of the particles. Afterward, oppositely charged ions cover the surface, causing the electrical potential along with the Stern layer. Due to ion distribution and the polarity of the solution, the electrical potential continues to decay in the diffuse layer. Shear plane potentials can be instrumentally measured and are referred to as zeta potentials. Although the surface potential (ψ_0) cannot be measured, the zeta potential is used to study the surface potential properties.

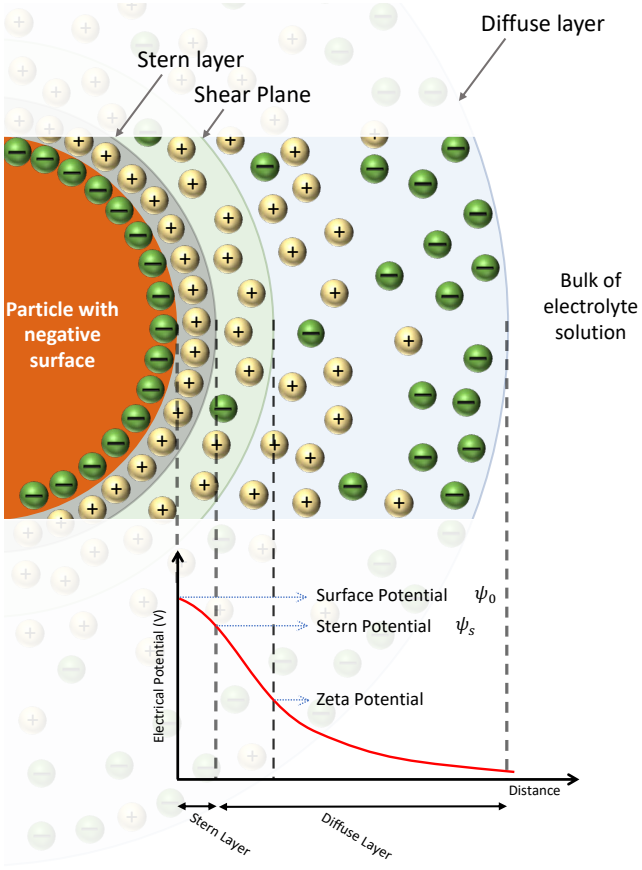

Figure 4 - Schematic of the Electrical Double Layer structure of negatively charged particle surface (adapted from Abbasi Moud, 2022; Cornell and Schwertmann, 2003; Lawrence, 1951).

2.8 The DLVO theory

When two colloidal particles approach each other, the diffuse layers overlap, inducing the emergence of a repulsive force, the so-called electrostatic double-layer force. The balance between the van der Waals forces and the electrical double-layer force will define the system's stability. The relationship between these forces was first explained by Derjaguin, Landau, Verwey, and Overbeek, who proposed the DLVO theory (Concha, 2014; Hiemenz and Rajagopalan, 1997; Pattanaik, 2021).

The attractive force (4^{th} quadrant - negative) and the repulsive force (1^{st} quadrant – positive) are shown in Figure 5 as a function of the distance between two particles. If the net forces are attractive, the system lacks stability, and the particles will aggregate. On the other hand, if the net forces are repulsive, the system stability arises, hampering aggregation. In the last case, the colloidal system is formed.

Considering most systems formed by fine particles, the attractive van der Waals force is weaker than the repulsive electrical double layer force, even at greater distances (above 10 nm) where the van der Waals force is practically zero. Therefore, a resultant repulsive force arises, promoting the formation of the colloidal system (Hiemenz and Rajagopalan, 1997; Jacob H. Masliyah, 2011; Lawrence, 1951). The resultant force reaches a maximum, which is the energy barrier related to the system stability (illustrated as point A in Figure 5)

Before the energy barrier, repulsion is predominant, and the particles repel each other, stabilizing the suspension. However, if the kinetic energy of the particles is greater than the energy barrier, they can continue to approach each other until the energy barrier is overcome. At this stage, the van der Waals forces of attraction become predominant, and the particles aggregate (Concha, 2014; Vajihinejad et al., 2019a). Therefore, to overcome the system's stability, it is necessary to reduce the energy barrier by suppressing EDL forces (with coagulation) or providing energy to overcome the energy barrier through a bridge between the particles (with flocculation).

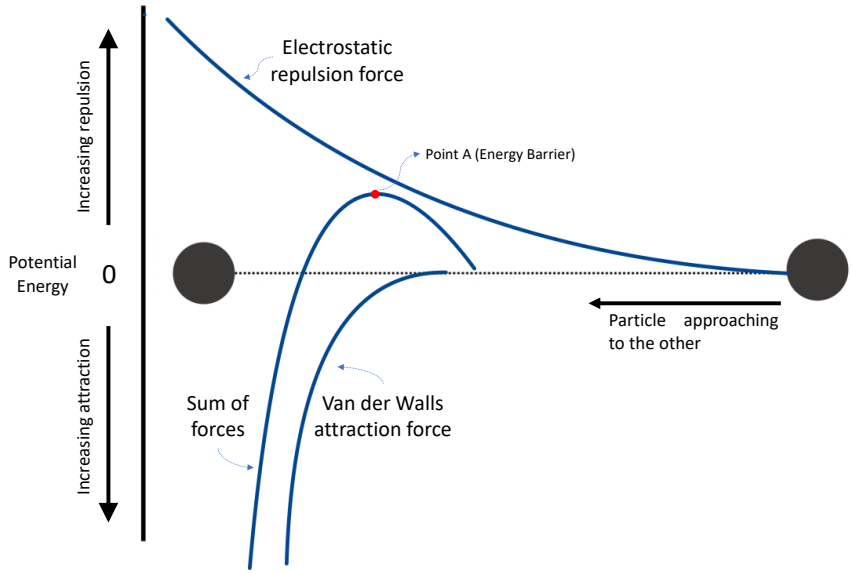

Figure 5 - The balance between van der Waals attraction and electrical double layer repulsion *(adapted from Lawrence, 1951; Grasso* et al., 2002)*.

As a result, the DLVO is essential for understanding the relationship between the forces within the system and for determining methodologies for overcoming the energy barrier and enabling tailings dewatering. A theoretical background is provided here to assist in the development of polymers that can be used as flocculants.

2.9 Destabilization of the colloidal system and particles aggregation

Overcoming the barrier necessary for aggregating colloidal particles in a stable system requires energy. This energy can be provided by physical methods such as centrifugation or raising the temperature to increase particle kinetic energy. Another way is by lowering the energy barrier that hampers particle aggregation. Coagulation and flocculation are two different methods used for this purpose. Flocculation requires the addition of an organic polymer to "bridge" the particles forming large aggregates. In contrast, coagulation involves adding inorganic chemicals (salts composed of multivalent ions) to reduce repulsive forces between particles (Wang et al., 2014; Water, 2011).

2.9.1 Coagulation

Adding inorganic salts to colloidal suspension promotes total or partial neutralization of surface charges and/or EDL compression. Both significantly reduce the energy barrier necessary for the attractive van der Walls forces to aggregate the particles and promote solid-liquid separation. The most common coagulants used in colloidal systems stabilized by negative particles are salts composed of multivalent cations, such as aluminum, calcium, and iron (Besra and Prasad, 2007; Siah et al., 2014).

The added cations increase the ions concentration of the solution and, consequently, raise the medium's ionic strength. This effect leads to the migration of counterions from the bulk solution to the particle's surface, increasing the concentration of these species in the diffuse layer. This disturbance on the charge balance of the diffuse layer causes the EDL compression, suppressing repulsive forces and enabling governance by attractive van der Walls forces. Thus, the particles will tend to approach each other, forming aggregates that settle at the bottom of the pond (Osborn, 2015).

The surface charge neutralization mechanism will dominate the coagulation process if there is an affinity between the added ions and the particle surface. In this case, ions will adsorb to the surface structure, reducing its original electrostatic charge until the zeta potential approaches zero (Osborn, 2015).

For both mechanisms, surface neutralization or EDL compression, the added salt dosage is proportional to the concentration and electrical potential of the particles. Since, in most cases, these parameters are considerably high, the dosage of coagulants follows the same trend.

It is essential to consider that, although inorganic coagulants are very effective in treating most mineral tailings, the high dosages have detrimental effects on the treated product and can cause corrosion in metallurgy equipment. Moreover, it is widespread that the clarified water obtained by coagulation does not have the minimum specification to be reused or even released into water bodies. In the last decade, the solution to this problem has converted to paste technologies by adding a polymer flocculant as a chemical additive (flocculation) to aggregate particles (Nanda and Mandre, 2019; Osborn, 2015; Yang et al., 2019).

2.9.2 Flocculation

Flocculation is a method of aggregating suspended particles by adding small amounts of long-chain polymers. For the polymer-particle interaction to occur, chemical affinity must exist between them. However, this affinity does not necessarily need to be strong, as several adsorption points will form along the long polymer chain. The binding mechanism of polymer segments and particle sites was proposed by Napper (1983). It is illustrated in Figure 6. In this model, the polymers segment is attached in trains, leaving polymer "tails" free in the solution, and forming loops (regions without interaction) between "trains."

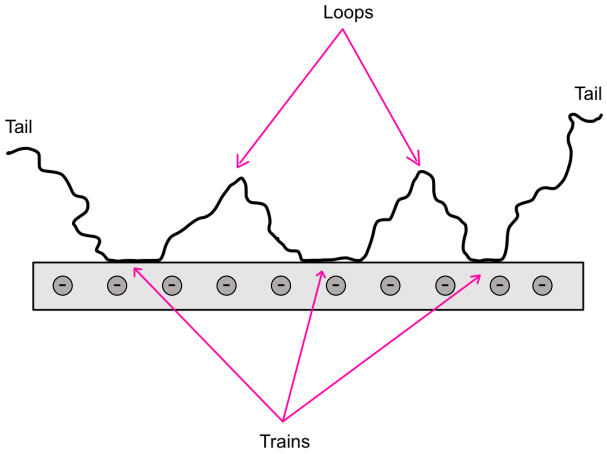

Figure 6 – Polymer-particle adsorption model (Napper, 1983).

The adsorption between polymers and particles occurs mainly due to three intermolecular bonding (Bolto and Gregory, 2007; Nanda and Mandre, 2019; Siah et al., 2014):

Electrostatic interaction: Polymers with charged functional groups adsorb oppositely charged particles through attraction forces that arise between them. In this case, it is common for polymers with lower molecular weight to be able to neutralize the particles completely and promote aggregation. The ions in the solution can negatively influence flocculation under these conditions. An example of electrostatic interaction is the use of cationic polymers in colloidal systems formed by negative particles, such as iron ore tailings.

Hydrogen bonding: Non-ionic polymers can bind to particle surfaces when both have chemical groups that enable H-bonding. The bonds between the amide groups of PAM and the hydroxyl groups present in some oxides, such as silica exemplify the H-bonding mechanism.

Ion binding: In some cases, anionic polymers mixed with divalent cation salts (such as Ca^{2+}) are used to flocculate colloidal systems formed by negatively charged particles. A possible explanation for this application is the role of cations as bridges between the charged functional group of the polymer and the particle's surface charge (Botha et al., 2017).

After the adsorption of a particle by the long-chain polymer, new particles and other polymer-particle species will be "bridged," forming big particulate units called flocs. This phenomenon is called the "bridging mechanism." The "bridging mechanism" is the most important mechanism to explain the particle aggregation, the formation of the flocs. High flocculation efficiency can be achieved when the long chains have functional groups capable of adsorbing the suspended particles. A single macromolecule can bind several other particles by "bridging" them together. Furthermore, a high density of functional groups of interest is desired, so the simultaneous bridging with many particles is achieved concomitantly with small polymer dosages. Under ideal conditions, a fast-settling rate and clear supernatant are obtained (Hogg, 2000).

Polymer adsorption and parameters that affect flocculation

A polymer's flocculation efficiency depends on the amount of polymer adsorbed at equilibrium, the suspension pH, the salt concentration, and the amount of polymer covering the particle surfaces. To study how adsorption conditions affect colloidal suspension stabilization, it is necessary to understand how polymers and particles interact.

Polymer dosage

Particles' settling rate and water clarification (turbidity of the liquid phase after settling) are frequently considered to evaluate the flocculation efficiency. The bridging flocculation will always have an optimal concentration in which both parameters are ideal. Above and below this concentration, the flocculation is compromised. Figure 7 illustrates the relationship between the flocs settling rate and the flocculant dosage.

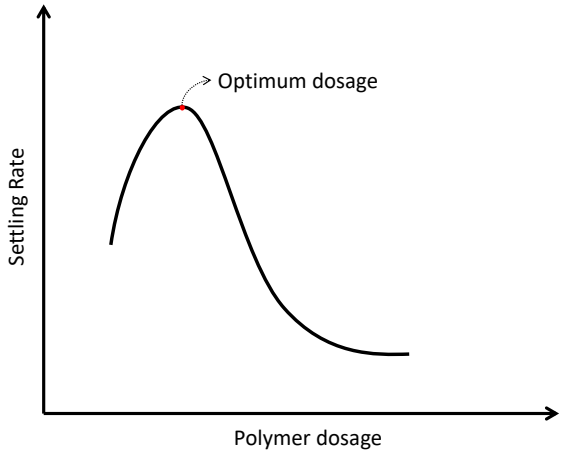

Figure 7 - Settling rate versus polymer dosage (Nittala, 2017; Vedoy and Soares, 2015).

There are some factors to consider regarding the relationship between polymer dosage effect and flocculation efficiency. Low polymer dosage results in insufficient bridging sites with particles, leading to small flocs. Thus, most of it does not settle, and the supernatant stays contaminated by small flocs and particles. On the other hand, polymer excess covers the entire surface of the particles, hampering the "bridging effect" and leading to small flocs. The total coverage of the particle's surface will result in a steric repulsion effect, where the attached brushes repel one another when the particles approach. Thus, the emergence of repulsive forces drives the recovery of the system's stabilization. These effects suggest an optimal polymer dosage where the particles are not entirely covered, and the bridging effect is maximum, allowing the formation of large flocs and the clarification of the supernatant (Nittala, 2017; Osborn, 2015; Wang, 2014). It has been proposed that this optimum dosage is achieved when less than half of the surface of the particles is covered (Bolto and Gregory, 2007)

Mixing conditions

Besides polymer dosage, mixing parameters also influence flocculation efficiency. If excessively applied, the mixing variables, such as speed, impeller, and time, have an adverse effect on flocculation. Among these variables, stirring speed is undoubtedly the most critical, followed by mixing time. After a specific time, the energy transferred to the system by agitation causes floc breakage and the formation of smaller units. This triggers a series of undesirable effects on flocculation, such as low settling rate, particle stabilization, and insufficient supernatant clarification.

Molecular weight and charge density

Cationic or anionic polymers' molecular weight and charge density also play a significant role in the flocculation process. Generally, larger polymers with high charge density can adsorb more particles, forming more "bridges" and, consequently, are more efficient. But it is worth mentioning that polymers with high charge density and lower molecular weight may be able to completely neutralize the particles and promote the destabilization of the system. In this case, other factors such as zeta potential and the ionic strength of the medium must also be considered (Guo et al., 2020; Nasser and James, 2006).

pH and zeta potential

As the stability of colloidal systems is related to the zeta potential, any change in this variable can considerably influence the flocculation efficiency. The pH of the solution affects the degree of ionization of the polymers and the surface charge of the particles, changing their zeta potential. H^+ and OH^- ions are potential determiners for oxi-minerals and can, therefore, modify the surface charge of these particles, altering the stability of the systems (ARINGHIERI and PARDINI, 1983; Keng, 1974). This effect on the zeta potential dictates the system stability and the required polymer dosage for effective flocculation. At a certain pH, the zeta potential is zero, called isoelectric point (ISP). At this condition, the particles can easily aggregate and settle.

Vidyadhar et al. (2014) studied the effect of pH on synthetic colloidal suspensions of hematite and Quartz prepared in 10^{-3} M KNO_3 solutions. The studied pH range was 2-9, varied by HCl or NaOH dosages. The isoelectric point (ISP) hematite was about pH 6.7. Quartz has negative zeta-potentials at all pH values, which tends to zero (increase) as pH increases. Lakshmipathiraj et al., (2006) reported a similar study using a synthetic goethite colloidal system in a 0.2 M Na_2CO_3 solution. The zeta potential varied significantly with minor changes in pH, with an ISP around pH 6.7. Shrimali et al., (2016) studied the surface chemistry of hematite and goethite colloidal particles in 10^{-3} M KCl solution. An ISP of approximately pH 6.2 for hematite and around pH 5 for goethite was found. Ouachtak et al., (2018) dispersed goethite in 0.02 M NaCl and found an ISP of pH 8.85. In 0.03 M NaCl, the ISP for hematite was at pH~6.5 (Pan et al., 2004). It can be observed that the ionic strength of the medium alters the zeta potential dependence profile with pH. At larger ionic forces, electrostatic interactions will be screened, decreasing zeta potential and electrostatic interaction. It is worth mentioning that when there are no potential determining ions, changing the

ionic strength by adding indifferent electrolytes will not affect the ISP. This discussion is shown in Figure 8.

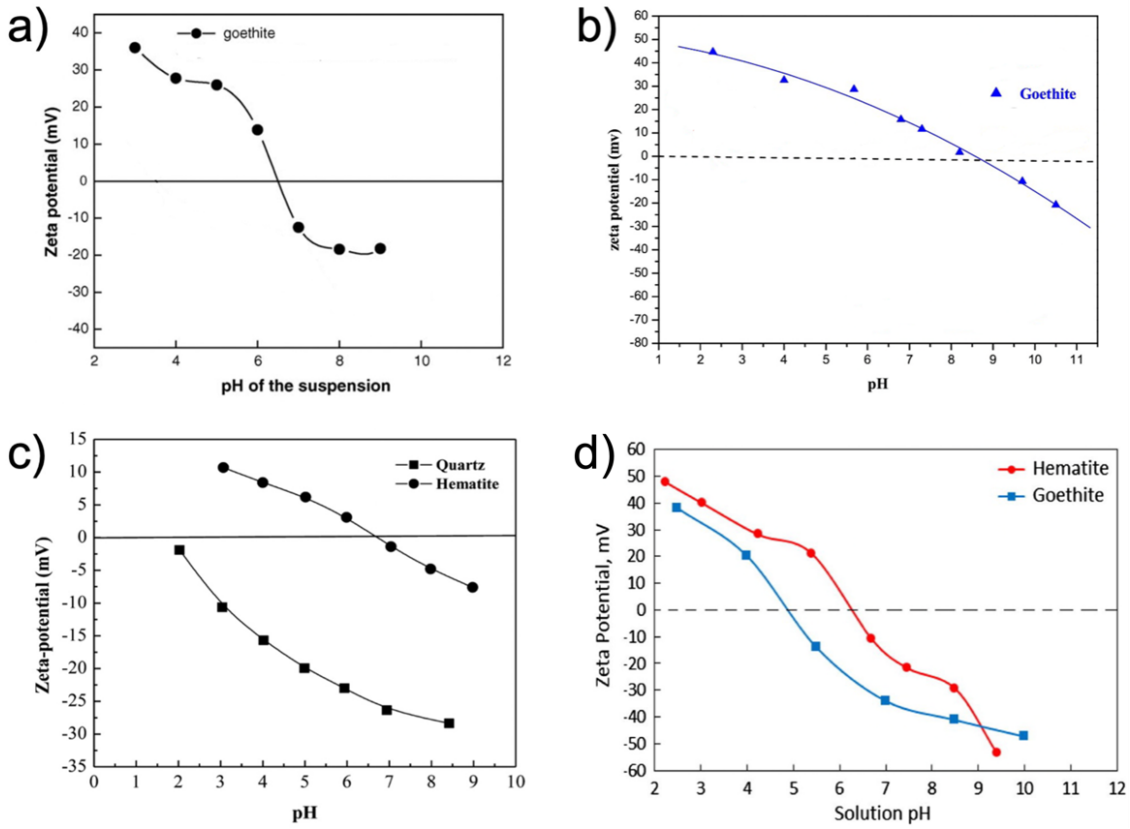

Figure 8 – Zeta potential variation of Hematite, Goethite, and Quartz under different solutions and reported by other authors: (a) adapted from Lakshmipathiraj et al. (2006) (b) adapted from Ouachtak et al. (2018) (c) A. Vidyadhar, (2014) and (d) Shrimali et al. (2016).

The Zeta potential of the particles of tailings from mineral beneficiation plants is generally not correlated with those collected from synthetic experiments performed in a laboratory because the particles in tailings are composed of mixed mineral phases. Besides the considerable influence of the medium ionic strength, each mineral phase has its ISP, and the result will be a consequence of this complex system. Eisele et al., (2005) studied the effect of pH on the zeta potential of a concentrate collected from an iron ore processing plant in Houghton, Michigan, USA. It was found that an ISP between pH 3.0 and 3.5. Quast (2012) studied the zeta potential of several samples from an iron ore mine in South Africa as a function of pH and found an ISP of approximately pH 2.6. Arjmand et al., (2019) reported a similar value (ISP at pH 2.7) for an iron ore tailing pond in northeast Iran. These values are significantly lower than previously published in the literature and those mentioned above. In addition, an ISP of about pH 6.2 from a sample collected in an iron dam in Minas Gerais (Brazil) was reported

by Grilo et al., (2020). Similarly, M. Dash et al., (2011) found an ISP of pH 6.4 for a tailing dam in Odisha, India. Interestingly, these last two reported result is close to the ones found in synthetic colloidal suspensions.

The results above prove that it is impossible to generalize the dependence of the zeta potential with pH for all existing iron ore mining plants. pH is dependent not only on the complex mineralogy of the particles, but also on the ion concentration at interfaces, surface morphology, and other chemicals (such as surfactants). As these characteristics will depend on the extracted mineral composition and mineral processing, the effect on zeta potential is an intrinsic parameter for each tailing.

Polymer structure

Flocculation processes usually produce larger and stronger flocs, but generally, the structure formed is not compact enough and retains a significant volume of water. In the case of polyacrylamide-based flocculants, due to their high hydrophilicity, the flocs are poorly compacted, keeping considerable water content. In this context, although flocculation is a promising method for treating mineral tailings, such characteristics hinder the dewatering, and that’s why it's essential to understand them.

Polymers interact with solid surfaces based on their chemical structure relative to the surface. For instance, polar groups will bond favorably with a hydrophilic surface, while nonpolar groups will bond favorably with a hydrophobic surface. In polymers with charged groups, electrostatic interactions govern the adsorption process, which is now affected by the pH and ions concentrations of the solution. On the other hand, H bonds and solvation control adsorption when the polymer has no charged groups (A. Vidyadhar, 2014; Lee and Somasundaranh, 1989).

2.10 Previous Studies on Flocculation of Iron ore Tailings

The use of polymers in the solid-liquid separation of colloidal systems, such as those formed in mineral tailings, has already been discussed. Among the polymers that have the potential to be applied as flocculants, the most widely used are polyacrylamide (PAM),

polyacrylic acid (PAA), poly(methacrylate) (PMA), poly(methyl methacrylate) (PMMA), poly(diallyl dimethylammonium chloride) (PDADMAC) and polyethylene oxide (PEO) (Bazoubandi, 2018; Vajihinejad et al., 2019a).

The performance of a polymer applied as a flocculant is evaluated by the capacity of obtaining densified solids (with very low water content) and water that has a required quality to be reused in mineral processing. In addition, several parameters of the solid (PSD, mineralogy, and surface charge density) and liquid phases (pH, electrical conductivity, and electrolyte concentration) must be considered to determine the polymer to be used as flocculants in the tailings (Azam and Imran, 2008; Peixoto, 2012).

Undoubtedly, PAM is the most widely used polymer in the mining industry. They can be non-ionic, anionic, or cationic. Anionics are generally synthesized by hydrolysis non-ionic polyacrylamide or by copolymerizing acrylamide with acrylic acid. Cationic polyacrylamide is synthesized by copolymerization of acrylamide with cationic comonomers. The molecular structure of each type is shown in Figure 9.

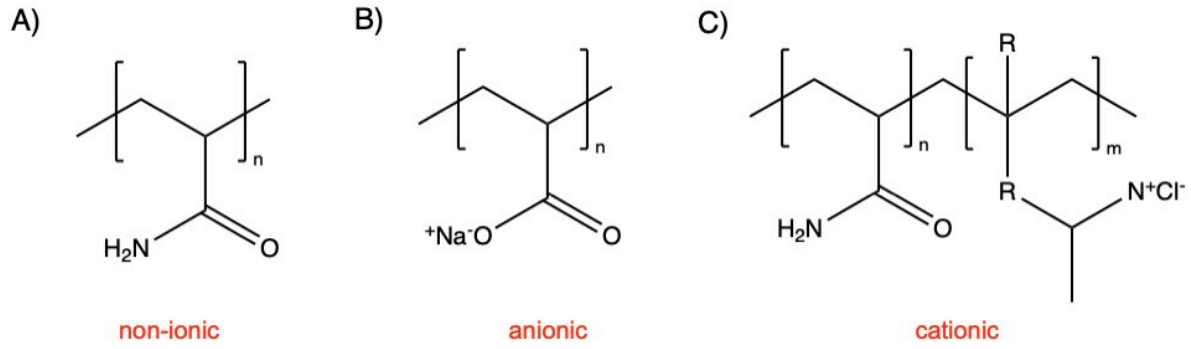

Figure 9 – Chemical structure of the different types of PAM: non-ionic (a), anionic (b) and cationic (c) (McGuire et al., 2006).

Many studies on the application of polyacrylamide in the flocculation of tailings can be found in the literature. Dash et al. (2011) studied the characteristics and adsorption mechanisms of non-ionic and anionic polyacrylamide as a flocculant applied to dewatering iron ore tailings. The study was carried out based on adsorption isotherms using the Langmuir and Freundlich models. The authors concluded that the Freundlich model best described the adsorption of the polyacrylamide-based flocculant in iron ore tailings. The non-ionic polyacrylamide presented the best sedimentation efficiency when compared with anionic polyacrylamide.

Lu et al. (2016), using two oppositely charged polymers (anionic polyacrylamide and cationic chitosan), proposed a new flocculation process that significantly improves yield and maintains a higher settling rate compared to the isolated addition of the polymers. In another work, Fan, Turro e Somasundaran (2000) studied the effect of the combination of an anionic polyacrylic acid (PAA) and a high molecular weight cationic copolymer of acrylamide and quaternary acrylate salt (Percol) on the flocculation of fine alumina waste (red mud). They found an appropriate ratio of both oppositely charged polymers that can significantly improve flocculation as the primary flocs serve as anchors for the adsorption of the second polymer.

Yang et al. (2019) studied the flocculation of iron ore tailings in an alkaline medium and carried it out in two stages. All polymers used were commercial polyacrylamides, differing mainly in electrical charge. The authors initially added an anionic or non-ionic PAM for the primary flocculation, and later, an anionic flocculant was added. Compared with the conventional one-step flocculation process, the two-step flocculation resulted in more concentrated sediment, indicating a more significant recovery of the water contained in the tailings. In addition, the secondary flocculant dosage had an optimal value for a maximum rate of total water recovery.

Arjmand et al., (2019) studied the flocculation efficiency of a commercial anionic PAM, varying the flocculant dosage (5 -20 g/t solid), the suspension concentration (3-12%), pH (4-12), and the concentration of the polymer stock solution. The performance parameters measured were settling rate, turbidity, and sediment volume. The solid-liquid separation efficiency improved from laboratory-scale tests at higher pH and flocculant dosages and in suspensions with lower solids contents. Similar results were observed on an industrial scale.

Yang et al., (2019) proposed a new flocculation method in an alkaline medium, in which two polymers with different characteristics were added in two steps to the tailings. They used an anionic or non-ionic flocculant as the primary flocculant, followed by adding a cationic flocculant. After the end of the primary flocculation, the system was shaken again, and the second polymer was added. The results showed that solid-liquid separation was more efficient in two-step flocculation than single-step flocculation commonly used in the industry. The secondary polymer (cationic) allowed the re-aggregation of the flakes broken by the shear disruption by agitation. Furthermore, he could flocculate residual particles from the first part of the process.

Despite some results showing polyacrylamide to be a suitable flocculant of mineral tailings, sediments retain significant water due to the hydrophilic nature of this class of polymers. To increase the solid's content, these sediments can be further processed through separation operations such as centrifugation and filtration, which makes the treatment process more expensive and complicated. In addition, studies have shown that acrylamide, the monomer used to manufacture polyacrylamide, has carcinogenic and toxic properties (Leite and Reis, 2020; Wei et al., 2018). Thus, new polymers capable of dewatering mineral tailings have been extensively studied in recent decades (Leite and Reis, 2020; Siah et al., 2014; Wang et al., 2014). Several works have focused on developing new flocculants or modifying existing ones, seeking a more efficient solid-liquid separation (dewatering) and more environment-friendly chemicals. Every day it becomes more evident that conventional industrial processes must be improved to be minimally harmful to the environment. In this context, most studies on mineral flocculation have converged on developing natural-based flocculants with minimal or zero environmental impact.

Chitosan is one of the most studied biopolymers due to the presence of primary amine groups, which give the molecule a high cationic charge density. This biopolymer is a linear copolymer of D-glucosamine and N-acetyl-D-glucosamine obtained by the alkaline deacetylation of chitin, a biopolymer extracted mainly from mollusks. It is insoluble in water or organic solvents and soluble in dilute organic acids such as acetic acid. At pH less than 5, chitosan becomes a soluble cationic polymer with a high charge density. Thus, its application in tailings flocculation is conditioned to the low pH, which induces the solubility and protonation of amine groups, allowing the electrostatic interaction with the particles in the suspension. (Oliveira, 2017; Siah et al., 2014). Lu et al., (2016b) studied the flocculation of mineral tailings using a combination of chitosan with anionic PAM, concluding that the association of these two polymers provided a better separation than when used separately.

Starch-based flocculants are also widely used. In terms of its chemical structure, starch is a homopolysaccharide composed of two macromolecules, amylose, and amylopectin. Amylose has a linear chain where α-1,4 glycosidic bonds join the glucose monomer units. Amylopectin has a branched structure, where the glucose units are connected by α-1,4 and α-1,6 glycosidic bonds. The second bond forms the connection between the main chain and the branches. In terms of composition, amylopectin predominates with composition ranging from 80 to 95%, depending on the starch source. The other portion of the starch corresponds to amylose. The chemical structure of both polymers is shown in Figure 10

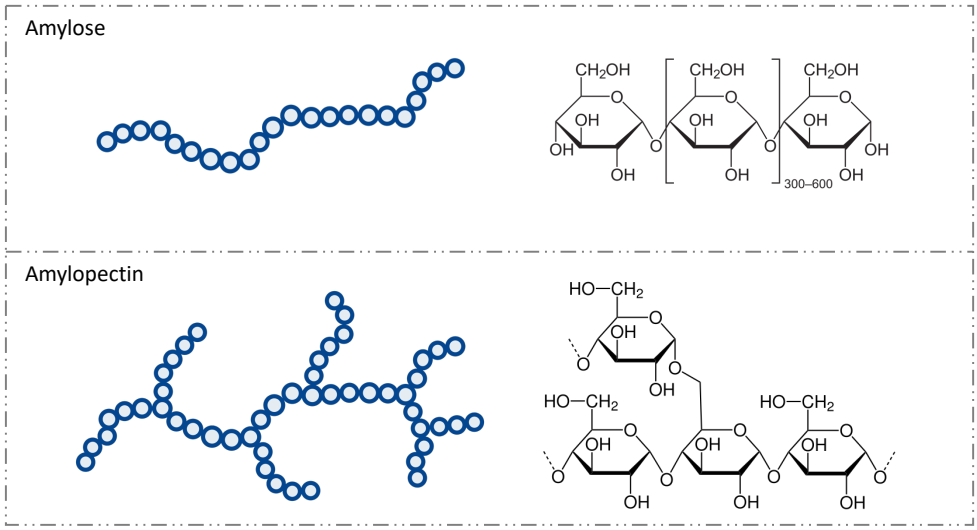

Figure 10 - Structural molecule of Amylose and Amylopectin

For starch to have a good flocculation efficiency, cationic or anionic polymers are grafted onto the natural polymer backbone, leading to better hydrophilicity and charge density. In addition, PAM-grafted starch has a higher molecular weight, enhancing the bridging formation. Mishra et al. (2011) synthesized a starch grafted with varying amounts of polyacrylamide in the flocculation of a kaolinite suspension. All graft grades tested showed better flocculation efficiency compared to pure starch. Such efficiency was attributed to the greater hydrodynamic volume of the grafted polymer.

Furthermore, for all synthesized polymers, there is an optimal dosage at which flocculation efficiency is maximum (measured to a minimum turbidity value of the supernatant). Above this dosage, the flocculation efficiency decreases due to the destabilization of the flocs formed by the excess flocculant. Yang et al. (2014) synthesized a grafted copolymer based on starch and with an amphoteric character. This polymer can be used as flocculants in suspensions containing both positively and negatively charged particles by cations and anions in its structure.

Kolya et al., (2017) explored the efficiency of several polymers synthesized from the grafting of different monomers (acrylamide (AM), N, N-dimethyl acrylamide (DMA), and a mixture of N, N-dimethyl acrylamide, and acrylic acid (AA)) onto starch. The tests were carried out in iron ore suspensions (0.25 wt. % iron ore slime) and other industrial effluents. The polymer's performance was compared with some commonly applied commercial flocculants. Among all synthesized graft copolymers, HES-based copolymers showed the best flocculation

performance. This result was attributed to the presence of polar hydroxyethyl groups and their more branch structure.

Kumari et al., (2019) studied the flocculation for selective metal recovery of tailings from the Barsua mines in India, using natural (Starch) and synthetic polymers (PAM). According to the chemical and mineralogical characterization, the sample contains 52.6% Fe, 3.8% SiO_2, 7.4% Al_2O_3, and 6.7% others. The major iron-bearing minerals were hematite and goethite. PAM with high M_w showed the highest efficiency in alkaline media (pH 9). Lower pH hampered most of the flocculation parameters because PAM's structure is alkaline due to its presence of the amide group, which donates electrons to its more electronegative nitrogen atom. Long-chain molecules and amide groups enhance the bridging point, leading to better performance. In addition, the selective flocculation provided by PAM made it possible to obtain an iron content of 65.4% and a recovery of 91%.

Leite & Reis (2020) used two commercial cationic starch (cross-linked and pregelatinized) to flocculate samples from a treatment plant in the Iron Quadrangle region in the State of Minas Gerais, Brazil. The authors concluded that the pre-gelatinized cationic starch presented the best flocculation performance. Although flocculation occurred satisfactorily under the conditions evaluated, the minimum turbidity reached was 65 NTU, evidencing that the polymer could not wholly clarify the supernatant.

Cellulose is one of the most abundant natural polysaccharides and has shown great potential as a flocculant. Hydroxypropyl methylcellulose (HPMC) is a modified form of cellulose and is widely used as a pharmaceutical incipient. Das et al. (2013) synthesized HPMC grafted with polyacrylamide chains and studied the flocculation efficiency in suspensions containing kaolinite and iron ore. According to the authors, the grafted polymers increased the aggregation rate and greater separation efficiency than the primary polymers used separately.

Although natural polymers have promising efficiency and their use in treating some types of tailings has increased, their application has many limitations that need to be better understood. As can be seen in the studies presented above, to overcome the limitations, many studies have addressed the modification of the chain of synthetic polymers by the addition of natural polymers (or vice-versa), combining the attractive properties of both classes of polymers in a single molecule (Bazoubandi, 2018; Pal et al., 2011; Siah et al., 2014; Vajihinejad et al., 2019a).

Chapter 3

Why is polyacrylamide still one of the most used polymers for iron ore tailings treatment?

3.1 Introduction

The mineral extraction and ore processing industry has grown significantly over the last several years, raising concerns regarding its impact on the environment (Laskowski and Ralston, 2015). Tailings generated during mineral extraction are mainly made of water and fine particles that form a stable colloidal system and cause water recycling challenging (Nanda and Mandre, 2019). Even though the submicron particles in these colloidal suspensions may sediment by gravity, the process may take several years (Pattanaik, 2021; Wang et al., 2014).

The growth in demand for mineral products is making the mining and processing of lower-grade ores inevitable, requiring more energy and resources. In this case, ore grinding and classification must be intensified to obtain the metal of interest, which generates more water and fine particles to be disposed of in the tailings pond (Edraki et al., 2014; Kinnunen et al., 2018; Li et al., 2008; Liang et al., 2021; Wills and Napier-Munn, 2005).

A chemical compound, such as a polymer flocculant, is often added to mineral tailings before they are pumped into tailings ponds. Polymers ease the solid-liquid separation by bridging, neutralizing charges, or forming electrostatic patches with suspended particles (Hogg, 2000).

Most mineral tailings are treated with polyacrylamide (PAM), which can be anionic, cationic, or non-ionic. Despite producing large flocs that settle rapidly, PAM has many disadvantages as a dewatering agent: 1) their hydrophilicity causes them to form hydrogen bonds with water molecules, making sediment that expands and retains water (Bratskaya et al., 2004; Rooney et al., 2016); 2) because of their high molecular weights, they are difficult to

disperse in tailings with high solid content (Vajihinejad et al., 2019a); 3) PAM degrades slowly in water (Levitt et al., 2011; Yi et al., 2013); 4) divalent cations that enhance particle-polymer bonding are often added to help flocculation, but cause problems when the water is recycled to the extraction process (Abbasi Moud, 2022; Gumfekar et al., 2019; Nasser and James, 2007); 5) acrylamide can be carcinogenic and have other toxic properties (Galeša et al., 2008; Vajihinejad et al., 2019a). These disadvantages have increased the interest in replacing PAM with other more environmentally friendly flocculants.

The performance of polymer flocculants is strongly correlated with the chemical and mineral composition of tailings: polymers engineered to flocculate one tailing type may not work equally well with other types. Many studies have pointed out the drawbacks of PAM and the system-specific application characteristics of new flocculants, so they can be modified or substituted to reduce their disadvantages and risks. However, there is still a surprising lack of publications on dewatering iron ore tailings. Xu et al. (2022) used an anionic PAM in combination with chitosan-graft poly(acrylamide-dimethyl diallyl ammonium chloride) (Chi-g-P(AM-DMDAAC)) to flocculate a kaolinite suspension. The positively charged Chi-g-P(AM-DMDAAC) adsorbed on the suspended particles, easing the adsorption of anionic PAM, and accelerating the flocculation. Dubey et al., (2021) investigated the settling behavior of iron tailings with a binary graft copolymer flocculant of starch (St), polyacrylamide (pAAm), and poly(sodium p-styrene sulfonate) (pSS) (St-g-(pAAm-co-pSS)). They compared it with four commercial flocculants, mainly composed of acrylamide and acrylate. The novel polymers had faster-settled rates than commercial flocculants and produced clearer supernatants.

The flocculation and dewatering of a 5 wt.% iron ore suspension were studied using two commercial PAMs with high and low molecular weights. Our main objective was to understand why PAM continues to be widely used to treat iron ore and other mineral tailings. We also tested two new polymers developed to treat oil sand tailings, which are chemically and mineralogically distinct from iron ore tailings. The flocculation/dewatering performance was measured using multiple light scattering, initial settling rate (ISR), supernatant turbidity, capillary suction time (CST), and solid contents of the sediments. The higher molecular weight PAM performed slightly better than the low molecular weight PAM, but neither could clarify the tailings supernatant. The polymers developed for oil sands application did unquestionably better than polyacrylamide. These findings show that polymers other than PAM are viable alternatives for flocculation and dewatering iron ore tailings.

3.2 Experimental

3.2.1 Materials

The tailings samples were collected in the thickener underflow stream immediately before being disposed into the Vargem Grande pond (Nova Lima, Minas Gerais, Brazil), as shown in Figure 3. Two commercial non-ionic polyacrylamides were used as flocculants: 1) PAM1 (Sigma Aldrich) is widely used in laboratory-scale flocculation, and 2) PAM2 (Kemira Chemicals) is commonly used to treat industrial mineral tailings. Poly((vinyl benzyl)trimethylammonium chloride) (PVB) and a partially hydrolyzed poly (methyl acrylate) grafted onto ethylene-propylene-diene copolymer backbones (EPDM-g-HPMA) were also used as flocculants. The synthesis and characterization of these polymers were reported in our group's previous work on oil sand tailing flocculation (Nguyen and Soares, 2022; Rostami Najafabadi and Soares, 2021).

3.2.2 Handling and drying the tailing samples

We dried the tailings samples (to make them easier to store and transport) according to the procedure: 1) drying in an oven at 60 ºC for 72 hours; 2) sieving in a Tyler series granulometric sieve (28 mesh) to break the clods formed during drying; 3) homogenizing the dried tailings (using the long pile quartering method) by spreading the dry clods back and forth on a clean surface, making a triangular cross-section pile of about 5 m in length (Figure 11); 4) removing the less homogeneous ends of the pile and spreading them over the pile, and 5) fractionating the pile into 600 g samples. Later, we used these dried samples to prepare colloidal suspensions for the flocculation studies.

Figure 11 – Dried sample spread following the long pile method.

3.2.3 Suspension preparation for flocculation tests

We prepared suspensions for the flocculation tests by mixing the dry tailings with distilled water to make a slurry with 60 wt.% solids, similar to the concentration in the thickener underflow stream. First, we added water to the solids and stirred the mixture for 60 minutes at 300 rpm. During mixing, we adjusted the pH to 10 by adding 0.5 M NaOH. By adjusting the pH to 10, we aim to reproduce the natural pH of the tailings. Next, we allowed the mixture to rest for 2 hours to allow the coarse particles to settle, leaving a supernatant colloidal suspension of fine particles. Then, we carefully transferred the supernatant to another recipient who was stirred at 300 rpm and adjusted its pH to 10 using the same NaOH solution. Finally, we diluted the solids content using DI water to 5 wt.%. We calculated the amount of water that needed to be added to obtain the 5 wt.% colloidal suspensions after determining the solid contents of the supernatant by placing 1 mL aliquots in an MB45 moisture analyzer (in triplicate). A schematic for preparing the flocculation suspension from the dried tailings is shown in Figure 12.

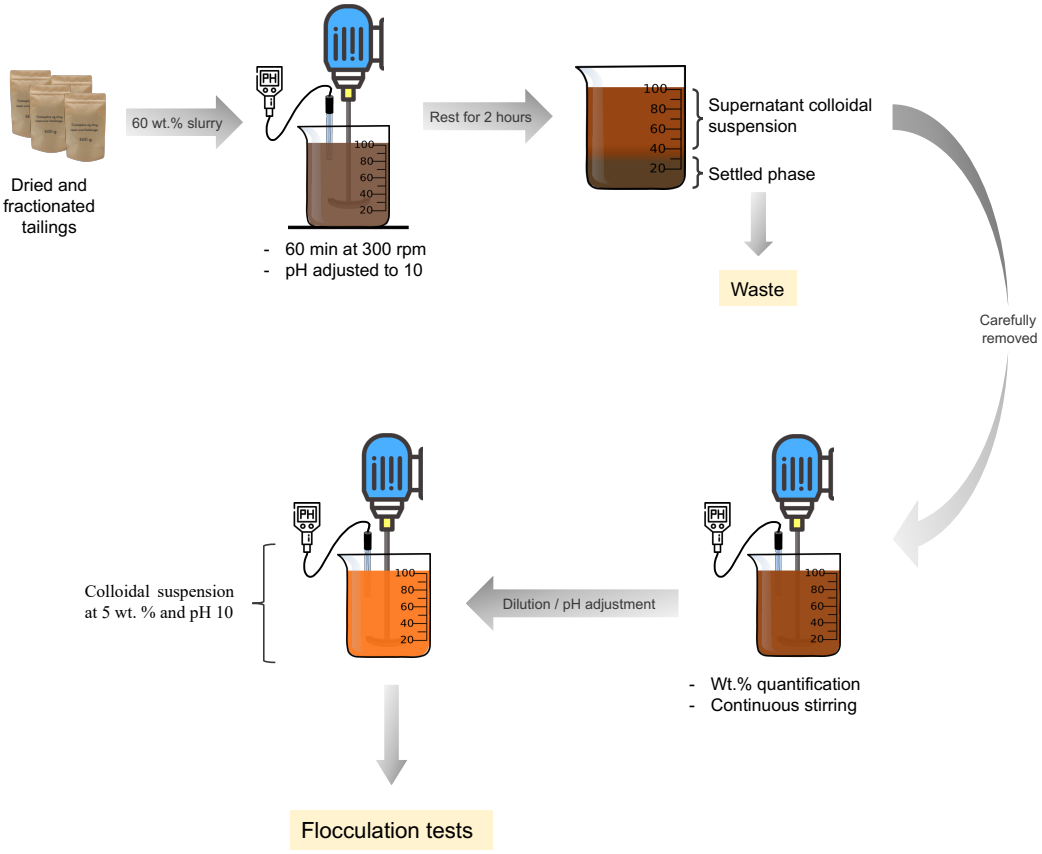

Figure 12 – Schematic of flocculation media 5 wt. % preparation.

3.2.4 Polymer Characterization

Fourier transform infrared spectroscopy (FTIR) was used to confirm the presence of the characteristic groups of the non-ionic PAM by attenuated total reflection (ATR) using an Agilent Cary 600 FTIR spectrometer. The data were collected in the range from 400 to 4000 cm^{-1}. The weighted average molecular weight (M_w) of all polymers was characterized by gel permeation chromatography (GPC) (1260 Infinity Multi-Detector GPC/SEC System, Agilent Technologies) coupled with three detectors: viscosity, refractive index, and light scattering. Two columns (PL aquagel-OH MIXED-H 8 µm, 300 x 7.5 mm) connected in series were used to obtain a better resolution and increase the instrument's detection range. Water containing 0.15 M $NaSO_4$ and 0.05 M acetic acid was used as a mobile phase for the analysis. The characterization of PVB and EPDM-g-HPMA were reported in our group's previous work on oil sand tailing flocculation (Nguyen and Soares, 2022; Rostami Najafabadi and Soares, 2021).

3.2.5 Tailings characterization

The solid's content was determined gravimetrically by heating approximately 1 g of the sample at 105ºC until all liquid was evaporated and a constant weight was obtained. The difference between the initial and final masses was used to calculate the solid's content. All samples were analyzed in triplicate. The particle size distribution (PSD) was obtained by laser diffraction using a Mastersizer X particle size analyzer (Malvern Panalytical) in a range from 1 to 600 μm. The PSD was determined for the tailing as received and after being dried and quartered, to validate the methodology and identify any effects on particle sizes after drying. Because the Mastersizer X cannot analyze particles with sizes in the colloidal spectrum, a Zetasizer Nano ZS90 (Malvern Instruments, UK) was used to determine the PSD of the colloidal suspensions. All samples were diluted to 1:100 using DI water, and the pH was adjusted to 10 by adding a 0.5 M NaOH solution.

X-ray powder diffraction (XRD) (Rigaku - Miniflex®) and X-ray fluorescence (XRF) **(**Malvern Panalytical-Zetium) were used to characterize the mineral phase and chemical composition, respectively, of the settled and colloidal phases from the 60 wt.% slurries. The XRD patterns were collected using Cu Kα radiation (45kV, 40mA and λ = 1,5418 Å) at a scanning angle (2θ) from 2.5° to 80° and a time per step of 200s. The XRD patterns were analyzed with the X'Pert HighScore software. For the XRF analysis, the loss to fire (LF) was performed at 1,020 °C for 2 hours, using samples melted with lithium tetraborate. The morphology and chemical composition of a single particle of the tailing samples was studied by scanning electron microscopy coupled with spectroscopy of dispersion energy (SEM-EDS) (JEOL JSM-7401F).

The ion composition of the aqueous phase of 5 wt.% colloidal suspensions was determined by inductively coupled plasma atomic emission spectrometry (SPECTRO ARCOS ICP-OES analyzer). The ions analyzed were Al, Ca, Fe, K, Mg, Mn, Na, Ni, Ti, and Zn. The aqueous phase was separated from the suspended solids using a 0.45 μm PTFE syringe filter. To ensure maximum reproducibility of the natural tailing conditions, we assumed that the chemical composition of the processing water (provided by the mining company) was the same as in the tailing pond.

3.2.6 Settling tests

We varied the PAM dosage from 500 to 5000 ppm (grams of polymer per ton of suspended solids) to better demonstrate the economic viability of the flocculant. We also tested two new polymers designed for treating oil sand tailings, poly(vinyl benzyl)trimethylammonium chloride (PVB) and partially hydrolyzed poly(methyl acrylate) grafted onto ethylene-propylene-diene copolymer backbones (EPDM-g-HPMA), to find out whether polymers designed to treat different tailings could be viable alternatives to PAM.

Multiple light scattering

The settling behavior and dewatering efficiency with different polyacrylamide concentrations were studied using an optical analyzer (Turbiscan Lab - Formulation, Toulouse, France) that relies on the multiple scattering behavior of light. A pulsed infrared laser (850 nm wavelength) moves vertically (up and down) along with a flat-bottomed cylindrical glass cell containing the fluctuating sample. The percentage of light transmitted (TS%) and backscattered (BS%) can both be measured using two detectors. Transmission and backscattering data acquisition are performed every 40 μm along the sample (Kokhanovsky and Weichert, 2001; Mengual et al., 1999; Olatunji et al., 2016).

Each test was performed by placing 22 g of the flocculation suspension into the sample vial and adding the desired volume of the stock polymer solution. The mixture was stirred for precisely 30 seconds at 300 rpm using a Vortex mixer (Stuart, SA8) and then fitted to the equipment, standing the readings. Data acquisition was set for every 5 seconds for 24 hours.

The Turbiscan® stability index (TSI) was calculated from the backscattering data with TurbiSoft software. The TSI is a dimensionless parameter proposed by the equipment manufacturer to study the effects on suspension stability over time. It is calculated based on the sum of all variations in TS% and BS% that are directly related to the destabilization of the suspension, as shown in Equation (2). Therefore, the larger the TSI value, the lower the stability of the medium (Formulaction, 2019).

$$TSI(t) = \frac{1}{N_h} \sum_{t_i=1}^{t_{max}} \sum_{z_i=z_{min}}^{z_{max}} |BS\%\,(t_i, z_i) - BS\%\,(t_{i-1}, z_i)| \quad (2)$$

In Equation (1), t_{max} is the measurement point corresponding to the time t at which the TSI is calculated, z_{min} and z_{max} are the lower and upper selected height limits, $N_h = (z_{max} - z_{min})/\Delta h$ is the number of height positions in the designated zone of the scan, and BS% is the considered signal (BS% if I < 0.2%, TS% otherwise).

Naked eye visualization is commonly used in flocculation studies. The visual appearance generally varies considerably with high flocculant dosages, and it cannot be detected at lower concentrations. A correlation between TSI and visual observation was recently proposed by Formulaction (2019) using the reference scale shown in Figure 13. At the lowest values, A+ means that the TSI does not represent significant destabilization, and the suspension is visually stable. At the highest value, D represents a stage in which the destabilization occurs and can be seen by the naked eye, such as the formation of large flocs.

Figure 13 - TSI scale used as stability criteria and correlation to visual observation (Formulaction, 2019).

Initial Settling Rate (ISR)

A sample of 100 g of the prepared tailing suspension (5% by mass) was placed in a Becker and allowed to mix for 1 min at 500 rpm with a mechanical stirrer coupled with a 3-bladed propeller stirrer (IKA - R-1388). Then, the polymer solution was added (always in the same spot) and stirred for another 1 minute and 500 rpm, followed by 2 minutes at 280 rpm. Finally, the mixture was rapidly transferred to a 100 ml graduated cylinder, where the mudline height was recorded as a function of time for 10 minutes. ISR was calculated from the slope of the h/H versus time plot, where h is the mudline height, and H is the total suspension height at the start of flocculation. The slope was determined for the first 2 minutes of flocculation.

Capillary Suction Time (CST)

Capillary suction time (CST) measures the time required for water to travel between two electrodes in a cellulose filter paper. The rate at which solvent flows through the porous surface is proportional to the suspension dewaterability. All readings were done by pouring 3 mL of the sedimented phase (24 hours after adding the flocculant) in an open cylinder in contact with the CST filter paper 7x9cm (Triton Electronics) and using a Type 319 Multi-Purpose CST apparatus (Triton Electronics). Two electrodes, placed 0.5 cm from each other, measured the time taken by the water to travel radially between them.

Zeta potential

The zeta potential of colloidal suspensions without flocculant and after 24-hour flocculant addition was determined by electrophoretic light scattering using a Zetasizer Nano ZS90 (Malvern Instruments, UK). Samples were diluted to 1:100 using Milli-Q® water at pH 10, adjusted with a 0.1 M NaOH solution. The temperature was set at 25 °C for all runs. The effect of pH ranges from 2 to 10 on the zeta potential of the 5 wt. % colloidal suspensions were also studied. The pH adjustment was made by adding 0.1 M NaOH or 0.1 M HCl solutions.

3.3 Results and Discussion

3.3.1 Polymer Characterization

Figure 14 compares the FTIR spectra of the commercial polyacrylamide samples PAM1 and PAM2. The double peak in the 3100 and 3400 cm^{-1} range confirms the presence of NH_2 groups, while the peak at 1650 cm^{-1} is related to the C=O bonds and amide groups. The peaks at about 2900 cm^{-1} and 1400 cm^{-1} are due to the presence of C-H and C-H_2 groups, respectively (Lin-Vien et al., 1991).

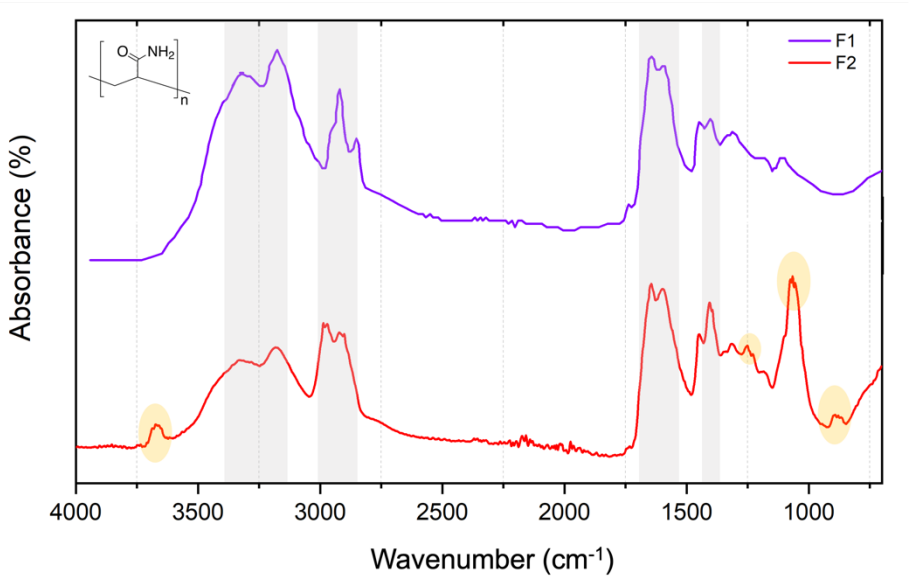

Figure 14 – FTIR spectra of polyacrylamide samples PAM1 and PAM2. Grey regions indicate peaks common to both spectra, whereas orange oval marks indicate peaks not detected in PAM1.

The characteristic wavelengths of the functional groups expected for polyacrylamide are listed in Table 1.

Table 1 -Characteristic wavelengths for the functional groups of PAM (Lin-Vien et al., 1991).

Functional group	Wavenumber (cm^{-1})
C-H	3000-2850
Methylene (–CH_2–)	~1465 (bending)
Amide (N–H)	1640-1550 (bending)
Amide (C=O)	1680-1630 (stretch)
Primary amide (–NH_2)	3350 and 3180 (stretch)

The FTIR spectra of sample PAM2 also detected a few peaks that were absent from the spectra of sample PAM1 (orange oval marks in Figure 14). Sample PAM1 is made only for research purposes but sample PAM2 is a commercial flocculant developed for the mining industry. Therefore, the extra peaks in sample PAM2 are probably related to additives—which are considered intellectual property and not disclosed by the manufacturer—which may explain its better performance, as we will discuss below. Other works also reported similar considerations about commercial polymers for industrial flocculation purposes (Cobbledick et al., 2017; Dentel et al., 2000; LaRue et al., 2016).

The weight average molecular weights, M_w, and dispersities, $Đ$, of samples PAM1 and PAM2 were measured by GPC and are listed in Table 2.

Table 2 - GPC results for samples PAM1 and PAM2.

Flocculant	Mw (MDa)	$Đ$
PAM1	5.95	1.11
PAM2	12.49	1.81

The M_w measured for sample PAM1 falls within the range reported by the manufacturer (M_w = 5 – 6 MDa), but no data was reported for $Đ$. The low $Đ$ value indicates that the polymer is likely made by controlled free-radical polymerization under uniform synthesis conditions. The M_w value measured for sample PAM2 was also included within the broad range provided in manufacturer's datasheet (M_w = 1 – 20 MD) for this brand of flocculants. Abu-Zreig et al. (2007) reported M_w = 12 – 15 MDa for PAM samples from the same family.

3.3.2 Tailing characterization

Solid content

The solids content of the settled phase of the tailings sample (as received) was 87.3 ± 0.4 wt.%. This value was higher than in the thickener underflow stream (about 60 %), which is the most concentrated fraction of the thickening stage (Torquato and Luz, 2011). The solids content of our sample was higher because the tailings sample settled for a few weeks and part of the supernatant water (clarified phase) was removed to reduce its volume. However, the

higher solids content had no impact on this work because the concentration was adjusted to 5 wt.% for all tests.

A sample of the supernatant of the received tailings was reserved to determine its solid content. Then, we dried the tailings samples and used it to prepare the flocculation media by mixing it with water to form a 60 wt.% slurry and adjusting its pH to 10 to reproduce the thickener underflow concentration. After the slurry settled for 2 hours, two phases were formed: a coarse particle layer at the bottom and a colloidal suspension at the top. We separated both phases and measured their solids content. We diluted the colloidal suspension to 5 wt.% and adjusted its pH again to 10 to match the value in the tailings pond. The concentration of 5 wt.% is commonly adopted in the literature (M. Dash et al., 2011; Gumfekar et al., 2017; Osborn, 2015; Wang, 2011) to investigate polymer flocculants.

The solids contents of the tailing supernatant (as received) and of the coarse particle and the colloidal phase from the prepared slurry at 60 wt.% are shown in Table 3.

Table 3 – Solid content of this suspension from the received tailings, of the sedimented and suspended phase from the prepared slurry at 60 wt.%.

Phase	Solid content (wt.%)
Suspension of the received tailings	11.8 ± 1.40
Sedimented phase of the prepared slurry at 60 wt.%	76.8 ± 0.86
Suspension of the prepared slurry at 60 wt.%	17.2 ± 1.25

The solid content of the coarse particles phase of the 60 wt.% slurry was slightly smaller, compared to the same phase of the received material (87.3 ± 0.4 wt.%). This result was unexpected, as the prepared 60 wt.% slurry aims to reproduce the tailings samples collected in the thickener's underflow. This difference was attributed to the shorter settling time (2 hours) and no removal of the clarified phase for the prepared suspension. A low solid content means large volumes of unrecovered water and low shear strength and susceptibility to liquefaction of the material. Such geotechnical factors are critical for the structural stability of the pond (Espósito, 2000).

Regarding the supernatant colloidal phases, the solid content was smaller for the received tailings because they were stored in the laboratory for several weeks before use, leading more particles to settle naturally.

Particle Size Distribution

Figure 15 shows that the volume-based cumulative particle size distributions of the received and dried tailings are nearly the same, proving that the drying procedure did not change the particle sizes of the tailings sample. About 40 % of the particles are smaller than 10 µm. These results agree with Guimarães (2011), who reported a range of 35 to 60 wt.% for particles smaller than 10 µm. Luz et al. (2010) classified this size range as ultrafine. In addition, as also reported by Chaturvedi and Patra (2016), more than 60 wt.% of the particles have average sizes lower than 20 µm.

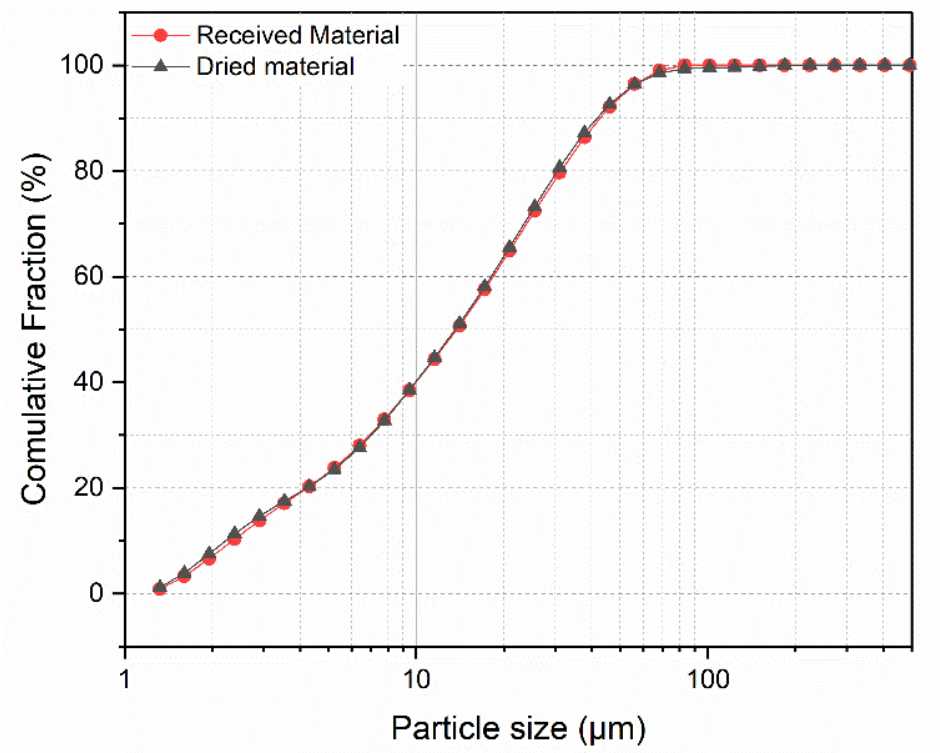

Figure 15 – Volume-based cumulative PSD of the received (red curve) and dried (blue curve) tailings.

The MasterSize equipment used in this work can only measure particle sizes ranging from 1 to 600 µm. Figure 16 shows that the colloidal suspension particle size distribution encompasses particles with a lower average size obtained in the Zetasizer (particle size range of 0.3 µm to 10 µm). More than 90% is composed of particles smaller than 1 µm, consistent with the size of particles that can form a colloidal suspension.

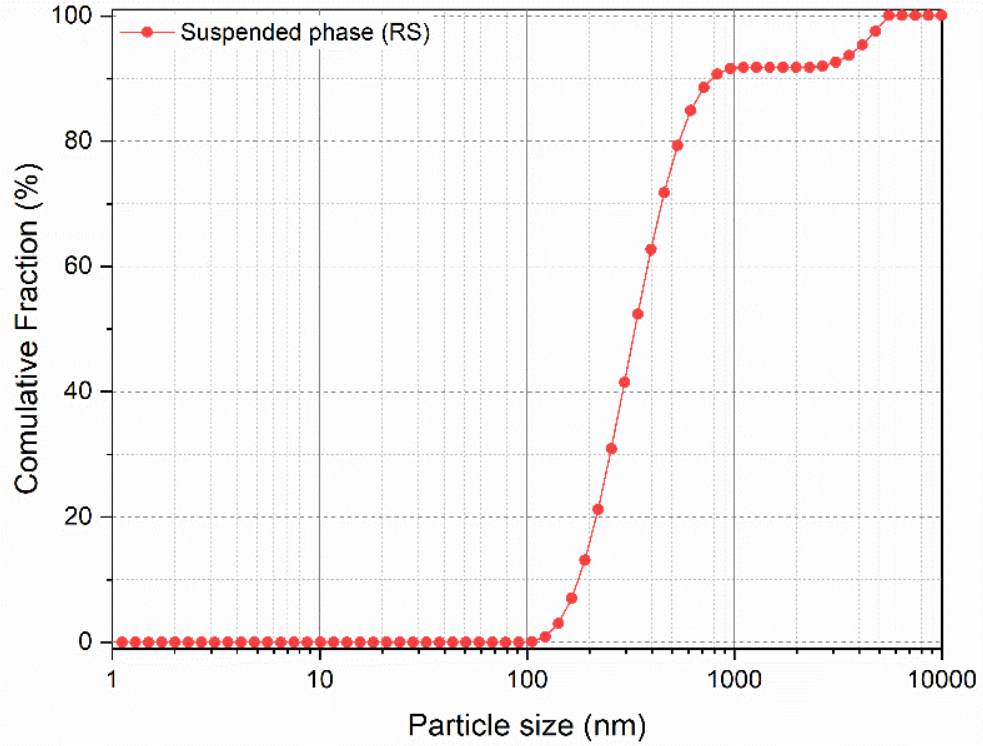

Figure 16 - Volume-based cumulative PSD of the suspended colloidal phase (supernatant) from the prepared 60 wt.% slurry.

Chemical and mineralogical composition

The chemical composition (measured by XRF) and mineral phase identification (measured by XRD) for both phases formed in the 60 wt% slurries, are shown in Table 4 and Figure 17, respectively.

The suspended and sedimented phases were mainly composed of iron oxides, SiO_2 and Al_2O_3. Iron was the predominant element, followed by SiO_2 and Al_2O_3 in the sediment and Al_2O_3 and SiO_2 in the colloidal suspension. Comparing the sediment with the colloidal suspension phase, SiO_2 decreased by 88%, and Al_2O_3 increased by 207%. These elements correspond to hematite (α–Fe_2O_3), quartz (SiO_2), goethite (α–$Fe^{3+}O(OH)$), kaolinite ($Al_2Si_2O_5(OH)_4$), gibbsite ($Al(OH)_3$). Titanium oxide (TiO_2) was only identified in colloidal suspension. Hematite and quartz were the most abundant minerals in the sedimented coarse particles, while Goethite and hematite represented the colloidal suspension. These findings were consistent with comparable studies reported elsewhere (Andrade, 2014; Gomes et al., 2011; Nanda and Mandre, 2022; Wolff, 2009). The lower SiO_2 concentration in the colloidal supernatant suggests that SiO_2 particles are more significant and, therefore, prominent in the

sediment. In addition, Gomes (2011) also observed higher Al_2O_3 content in the fine fractions of iron ore tailings and concluded that they were associated with the silt-clay portion of the tailings. According to Andrade (2014), the concentration of Al_2O_3 in iron ore tailings is determined by the geology of the extraction region, which may be rich in phyllites with aluminosilicates.

Table 4. - Chemical composition of the sediment and colloidal suspension from 60 wt.% slurries.

Compound	Composition (wt.%)	
	Sediment	Colloidal Suspension
Fe	44.34	47.7
SiO_2	29.72	3.54
Al_2O_3	2.58	7.94
P	0.06	0.345
Mn	0.11	0.7
TiO_2	0.11	0.48
CaO	<0.10	<0.10
MgO	<0.10	<0.10
Na_2O	<0.10	1.96
K_2O	<0.10	<0.10
Cr_2O_3	<0.10	<0.10
LOI	2.74	15.3

LOI = Lost on ignition

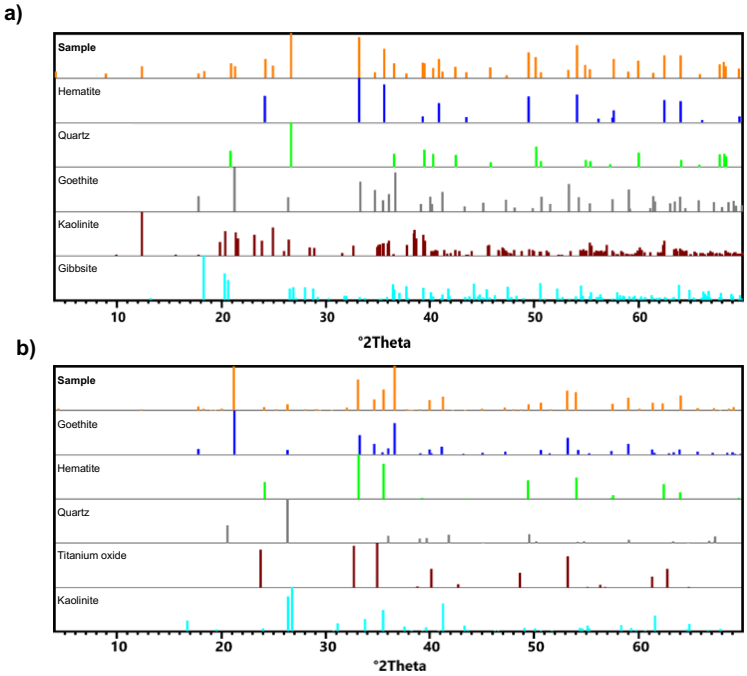

Figure 17 - XRD patterns of the sediment (a) and colloidal suspension (b) from the 60 wt.% slurry.

Scanning Electron Microscopy

The surface morphology of the dried tailings was studied by scanning electron microscopy (SEM), as shown in Figure 18. The tailings were polydisperse, with the predominance of angular and granular particles. The polydispersity is consistent with the PSD of the material (see Figure 15 and Figure 16). A powdery material adhered to the particles, which is characteristic of clay minerals (Andrade, 2014).

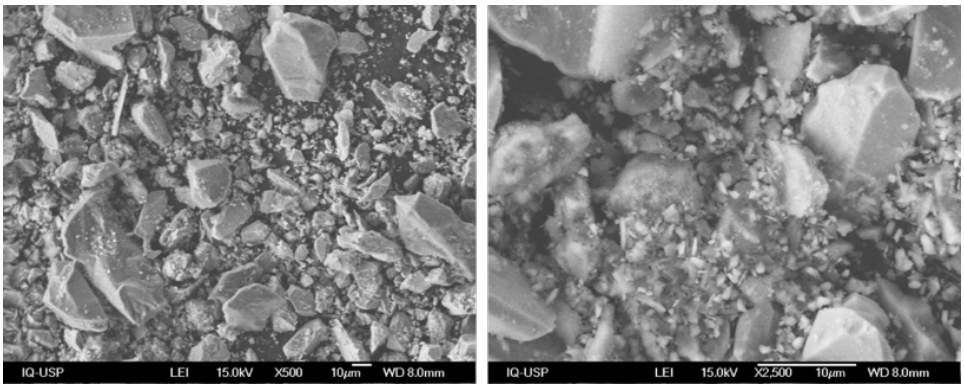

Figure 18 - SEM images of the received tailings

The elemental mapping of a single particle surface of the dry tailing was done by energy dispersive spectroscopy (EDS), as shown in Figure 19. The color density of the images is proportional to the amount of the element found on the particle surface. Fe, Si, and Al were detected along the particle surface. These findings are consistent with the chemical and mineralogical results. The presence of different elements in a single particle implies that the extracted rocks consist of aggregates of different minerals, segregated into distinct phases. Among the detected elements, iron comes from hematite and goethite iron-containing minerals, silicon was found in quartz and kaolinite, while aluminum was seen from the kaolinite and gibbsite mineral phases.

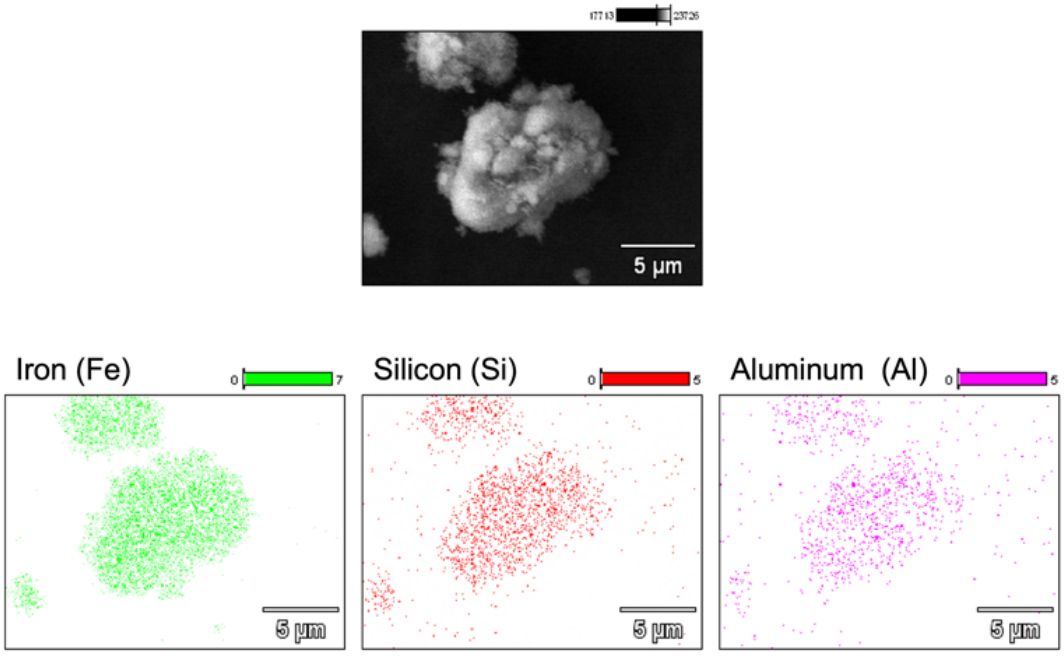

Figure 19 - EDS elemental mapping of a single particle of the dry tailings.

Chemical composition of the aqueous phase

The chemical composition of the aqueous phase of the 5 wt.% colloidal suspensions was determined by ICP-OES. As zeta potential and colloidal stability are determined by system composition, prepared flocculation media must be as tailings-like as possible (Addai-Mensah and Ralston, 2004; Konduri and Fatehi, 2017). Processing water composition (provided by the tailings supplier) was assumed to be the same as tailing pond composition because tailing composition varies considerably along the tailing pond. The processing water concentration was converted to a 5 wt.% suspension (same as the suspension used in the flocculation tests), by assuming the solids content of the tailings pond was the same as for the 60 wt.% slurries. The chemical compositions are shown in Figure 20.

Sodium, potassium, and calcium were more abundant in the 5 wt.% colloidal suspensions. Grilo et al., (2020) studied the effect of the concentration of different salts on the zeta potential of iron mining tailings from the Fundão dam in Minas Gerais (Brazil). According to the authors, by increasing 20 times (from 0.5 to 1.0 mM) the concentration of NaCl, KCl and $CaCl_2$the magnitude of the potential decreases by 5, 4, and 46%, respectively. Monovalent ions, like sodium and potassium, were expected to not affect the zeta potential. However, the opposite is observed for divalent cations. Higher the ion valency, the higher the neutralization and compression effect on the EDL, favoring particles' destabilization. We decided not to change

the calcium concentration since a higher content of this cation enhances the flocculation process, which is the objective of this work. In addition, the concentration was considered slightly different if the experimental error was considered.

According to the experimental errors, iron and aluminum concentration was considered the same for both. Aluminum was the less abundant among all analyzed elements for the 5 wt.% colloidal suspensions. This is related to the solubility of the mineral phase, aluminosilicates. This result is consistent with the chemical quantification of the solid colloidal phase, where Al_2O_3 had the second-highest concentration. Because manganese was detected only in the processing water, it was added (with $MnSO_4$) to the prepared suspension to compensate for the possible effects of this polyvalent ion on the system's zeta potential.

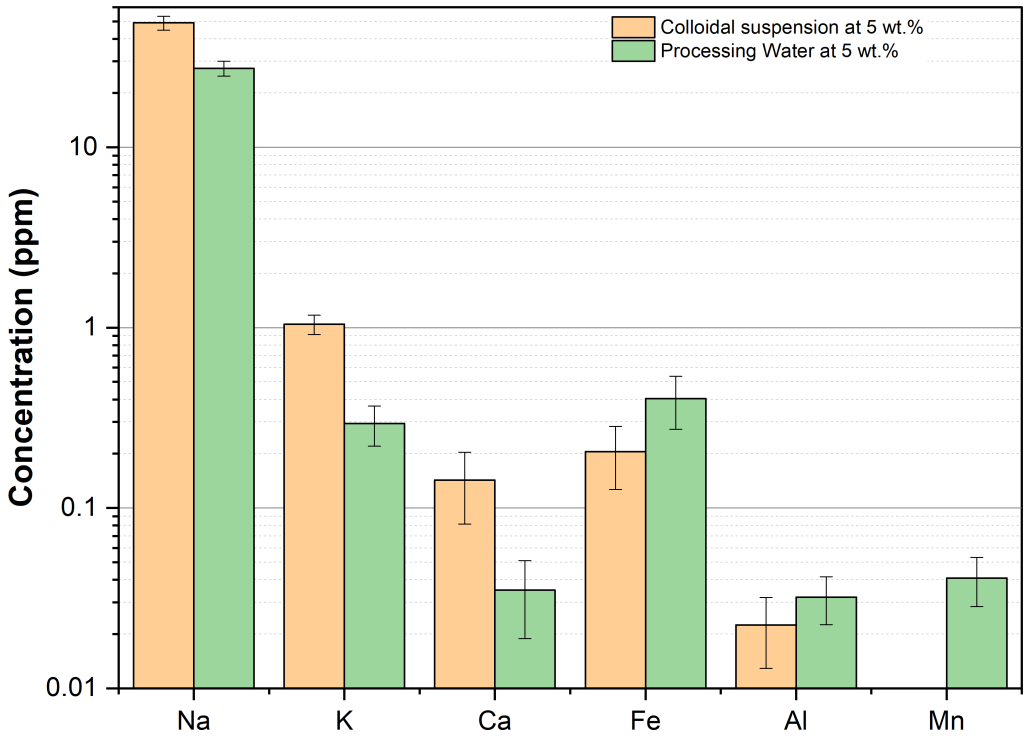

Figure 20 - Chemical composition of the aqueous phase of the prepared flocculation media and the processing water at 5 wt.%.

Zeta potential

The effect of pH ranging from 2 to 10 on the zeta potential of the 5 wt.% colloidal suspensions was studied by adding 0.1 M NaOH or 0.1 M HCl solution. The results are shown in the graph in Figure 21.

The isoelectric point (ISP) was found to be pH 5.5. This value is close to similar tailings reported elsewhere (Carlson and Kawatra, 2013; M. Dash et al., 2011; Grilo et al., 2020; Mamghaderi et al., 2021). Since each mineral phase of the tailings has its ISP (ranging from 1.8 to 9.5), the ISP of 5.5 seems reasonable if the proportion among them is taken into account (Kosmulski, 2021; Lakshmipathiraj et al., 2006; Pan et al., 2004; Shrimali et al., 2016; Vidyadhar et al., 2014). Furthermore, the mineral particle surface protonates at low pH levels (below the ISP), which produces a positive zeta potential. In the same way, mineral particle surfaces are deprotonated at high pH (above the ISP) (Bahmani-Ghaedi et al., 2022).

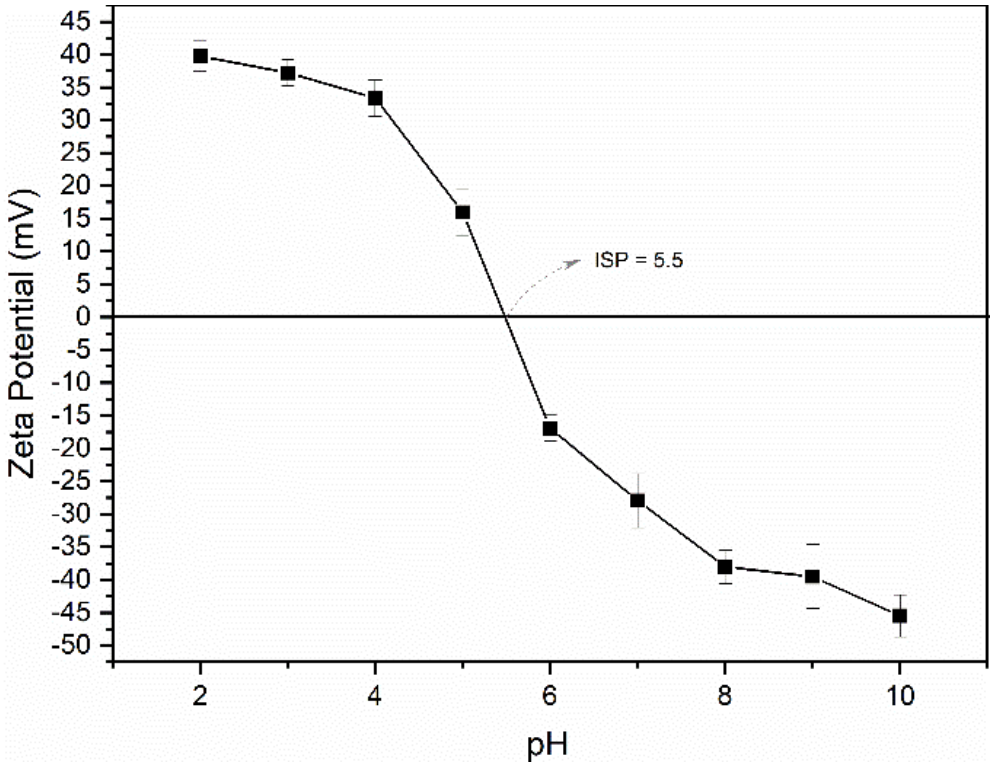

Figure 21 - Zeta potential measurements at different pH (2 to 10).

3.3.3 Flocculation tests

We flocculated 5 wt.% iron ore tailing suspensions using two commercial non-ionic polyacrylamides, PAM1 and PAM2, investigating the effect of dosages from 500 to 5000 ppm. Flocculant performance was investigated by multiple light scattering, solid contents, zeta potential; initial sedimentation rate (ISR); and capillary suction time (CST).

Effect on Initial Settling Rate (ISR)

Figure 22 shows the initial settling rate (ISR) for flocculation with PAM1 and PAM2 at different dosages.

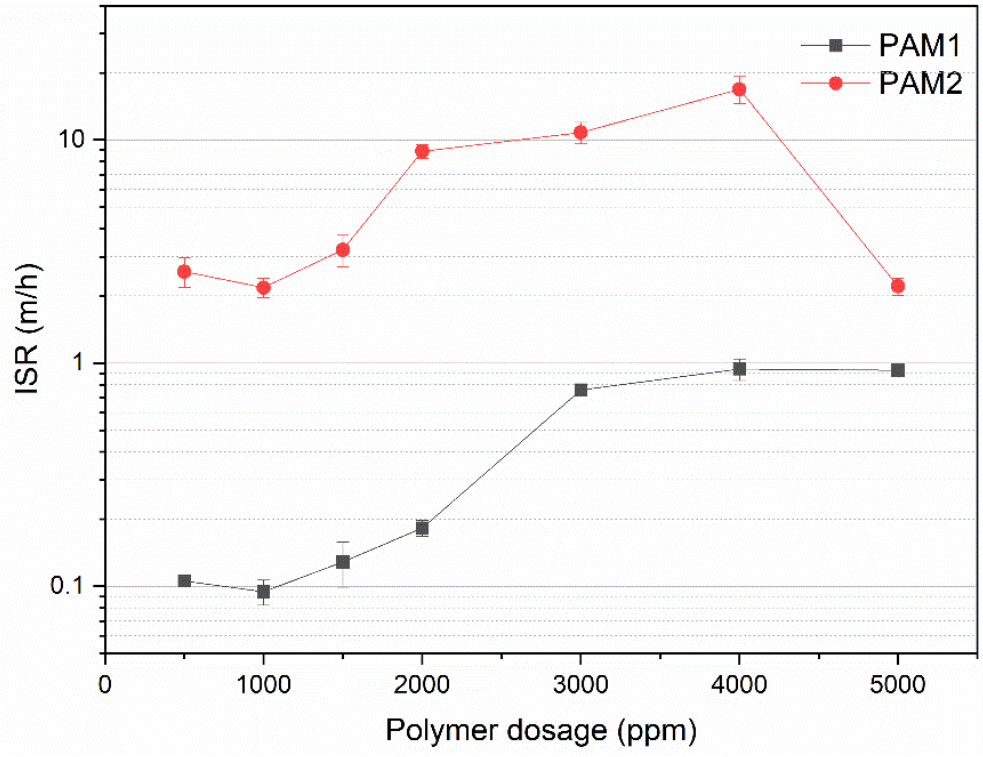

Figure 22 - Initial settling rate for flocculation with PAM1 and PAM2 at different polymer dosages

For conventional thickeners, the settling rate is considered low when ISR < 5 m/h and high when ISR ≥ 20 m/h (Pearse, 2003; Witham et al., 2012). For PAM2, the ISR exhibited the typical behavior of polymer flocculants, increasing with dosage until reaching a maximum value and decreasing for higher dosages. This effect is explained by the increase in polymer-particle bridges that leads to bigger flocs that settle faster. After an optimal dosage, typically covering 50% of the particle surface, the polymer molecules start hindering bridge formation (overdosing), which results in smaller flocs that settle more slowly. In addition, steric repulsions between polymer chains may stabilize of the suspension (Bolto and Gregory, 2007; Nittala, 2017; Osborn, 2015; Wang, 2014).

A similar effect was observed for PAM1, where ISR increased up to 3000 ppm but unlike PAM1, reached a plateau. Since PAM1 has a lower M_w and a much narrower molecular weight distribution, it is not surprising that the maximum ISR occurs at a different polymer dosage. Moreover, for the exact dosage of both polymers, the ISR for PAM2 was always higher,

which may also be attributed to the higher M_w of PAM2. Increasing M_w is a strategy for improving flocculation efficiency, especially in the case of non-ionic polymers, in which there is no charge in the polymer chains (Gumfekar and Soares, 2018; Vajihinejad et al., 2019a).

Effect on transmission (%) and backscattering (%).

The floc formation and settling profile was investigated by multiple light scattering. After polymer addition, the solids concentration decreases from top to bottom, forming a clarification zone at the top and a thickening zone at the bottom. The change in light backscattering percentage in the clarification zone was used to evaluate the flocculation dynamics and tells how fast the polymers form flocs that settle to the bottom of the vial. Figure 23 compares the dynamic backscattering values for PAM1 and PAM2 at several dosages. Because no significant change in backscattering was observed after 2 hours, only this time range was considered. This analysis will not consider results for 500 ppm, as they were not reproducible due to high turbidity.

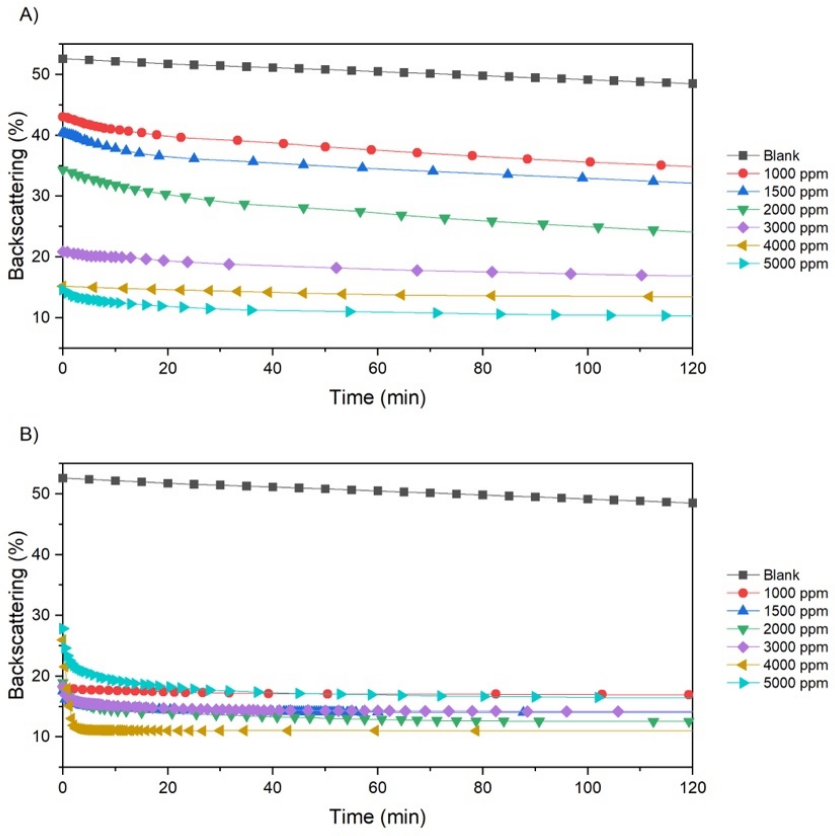

Figure 23 - Backscattering as a function of time in the clarification zone for PAM1 (a) and PAM2 (b) at different dosages.

All BS% values decreased with increasing PAM1 dosage, reaching a minimum of 11% at 5000 ppm. At this concentration, at about 2 hours of flocculation, BS% tends to approach a steady-state. For the blank suspension (without flocculant), it took about 60 days to reach the same conditions (Figure 49 - Appendix A). Although a significant reduction was obtained, 2 hours still seems industrially impractical. Furthermore, as shown below, a BS of 11% represents inferior clarification efficiency.

PAM2 had a smaller BS% for all dosages. BS% approach a steady-state at 50, 50, 47, 40, 6, and 50 minutes for 1000, 1500, 2000, 3000, 4000, and 5000 ppm, respectively. At 4000 ppm, the system quickly tends to the steady-state and a minimum BS% of approximately 11%. By increasing the dosage to 5000 ppm, the BS% values increased and reached a minimum of 16%. This result seems to be caused by polymer overdosing, forming smaller flocs that suffer steric repulsion. The higher M_w of PAM2 and the possible presence of additives are likely responsible for improving the separation efficiency.

Ideally, BS% should approach zero at a steady state, indicating that no particles remain suspended in the supernatant. However, among all conditions we tested, the minimum BS% of 11% was insufficient to clarify the supernatant. This conclusion is supported by the pictures shown in Figure 24.

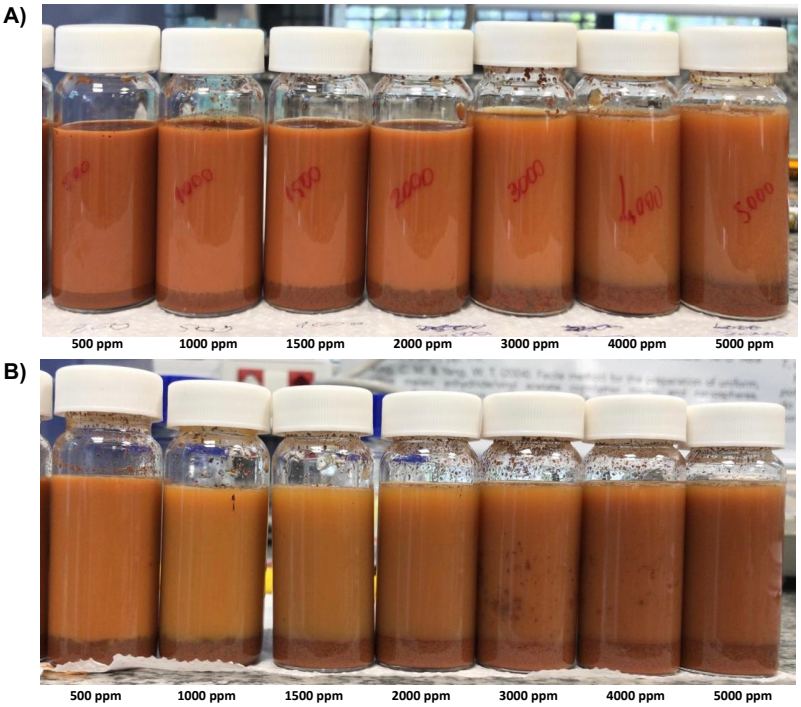

Figure 24 - Flocculation samples after adding different dosages of PAM1(a) and PAM 2(b).

The turbiscan stability indices (TSI), calculated with the TurbiSoft software, are compared in Figure 25. We also used the TSI scale, proposed by the manufacturer, to discuss the system stability based on the correlation of the TSI values with visual methods (Formulaction, 2019).

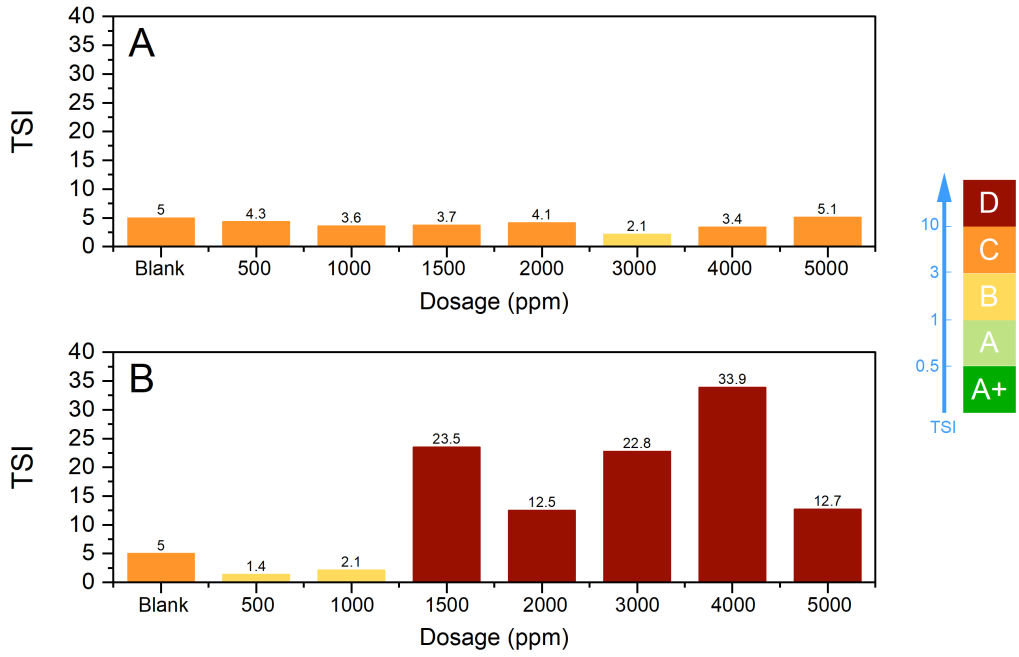

Figure 25 – TSI of the whole sample with PAM1(A) and PAM2 (B) as flocculants and different dosages.

The lower the TSI, the more stable the suspension. The TSI for PAM1 varied from 2.1. to 5.1. According to the TSI scale, from 3 to 10, the TSI falls into group C, in which there is a certain degree of destabilization detected experimentally and with a naked eye. At this stage, the flocs may be formed with a broad particle size distribution and sediment poorly. Both phenomena were visualized during the experiment, even at the beginning of flocculation (as shown in Figure 25a).

As expected, PAM2 performed better than PAM1. Above 1500 ppm dosages, all TSI's belong to group D, which corresponds to considerable medium destabilization, significant sedimentation, phase separation, and widespread change in particle size or color. After 4000 ppm, there is a reduction in TSI, indicating the suspension stabilization is being restored. This result corroborates to the steric repulsion effect due to the polymer excess.

Solid content

The solids contents of the supernatant and sedimented phase after 24 hours of flocculation are shown in Figure 26.

Higher dosages of PAM1 and PAM2 reduced the solids content of the supernatant (shown in Figure 26a). For all dosages, the values were higher for PAM1. This finding agrees with our previous observation that PAM1 is less efficient than PAM2: the lower the M_w, the more particles are left suspended in the supernatant. In addition, a slight increase in the solids content of the supernatant was observed when the dosage of PAM was 5000 ppm. This result is consistent with the BS% discussion, where an increase of this parameter was observed at 5000 ppm.

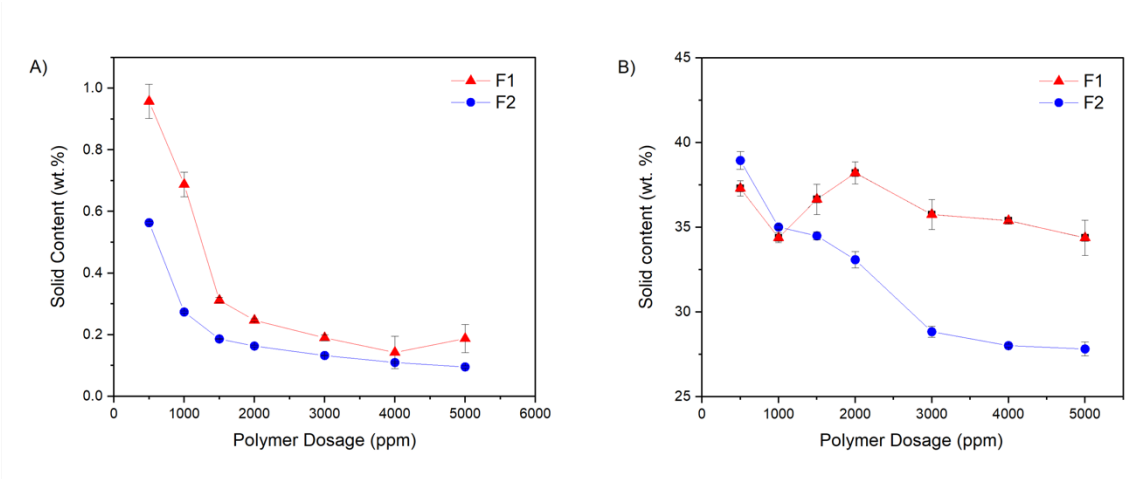

Figure 26 – Solid content of the supernatant (A) and sedimented phase (B) after 24-hour flocculation with PAM1 and PAM2.

Regarding the supernatant, PAM1 performed slightly worse than PAM2. On the other hand, for the sediment, the opposite was observed. This was attributed to the higher hydrophilicity and Mw of PAM2, which promotes a better settling of the suspended fine particles and retains more water in the floc's interstices due to the predominance of h-bonding.

Capillary Suction Time (CST)

Figure 27 shows the CST of the sediments formed after 24 hours of flocculation under different dosages of PAM1 and PAM2.

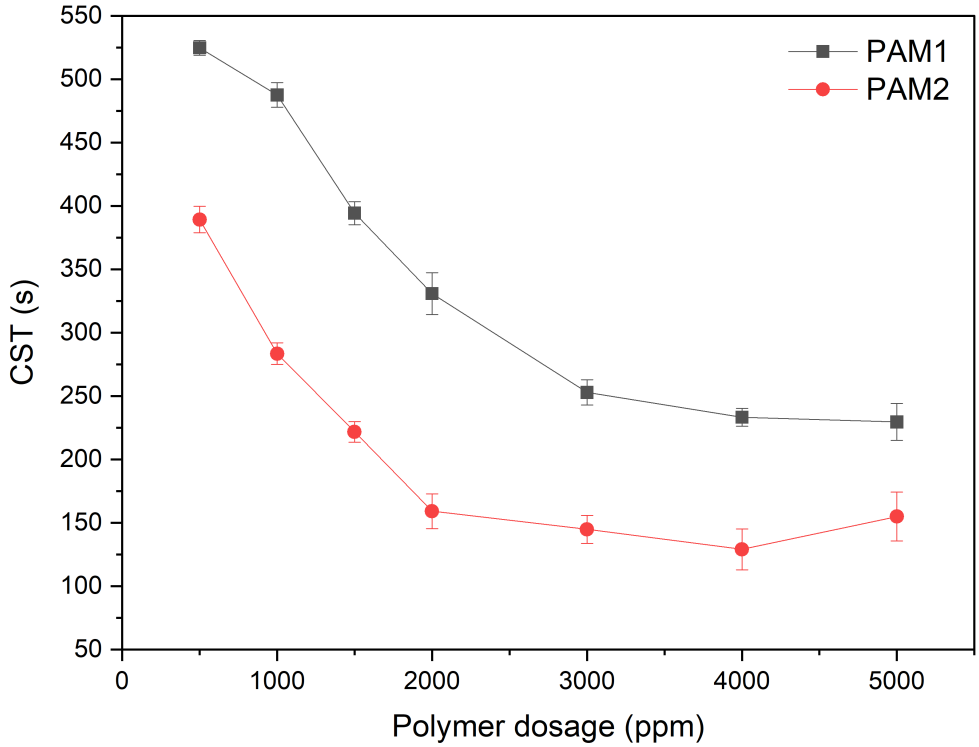

Figure 27 – CST for PAM1 and PAM1 at different dosages.

Although most relevant studies with CST focus on oil sand tailings, this parameter was useful to predict the dewaterability of the iron ore tailings under flocculation with PAM. As a reference, we used the protocol proposed by the Oil Sands Tailings Consortium (OSTC), where the sediment has good dewaterability if the CST is less than 100 s. CST decreased with increasing dosage for PAM1 and PAM2. As molecular weight increases, aggregates are expected to be larger and more compact, retaining less water, and resulting in lower CSTs. This decrease in CST is reversed when polymer overdosing is reached (visible by the increase for PAM2 after 4000 ppm). This polymer excess effect was explained based on the hydrophilic character of PAM (Botha et al., 2017). After a specific concentration, water retention is favored by intermolecular interactions, both inside the formed floc and residual polymer. In other words, water tends to flow slowly due to the dominance of stronger interactions with the water molecule from the hydrogen bonds formed with the polymer's amide group (Botha and Soares, 2015; Lee and Liu, 2001). For PAM1, this trend was very subtle according to the experimental error. This result corroborates previous discussions in which, for lower Mw, higher dosages are necessary to achieve saturation. Similar results were observed by Lee & Liu, (2001), where higher molecular weight resulted in optimal CST at lower dosages. The lowest CST among all tested conditions was 129 s (for PAM2 at 4000 ppm), which was not in the range adopted as a parameter for good dewatering efficiency.

Zeta potential

Zeta potentials of the supernatant after 24-hour flocculation with different dosages of PAM1 and PAM2 were determined and are shown in Figure 28.

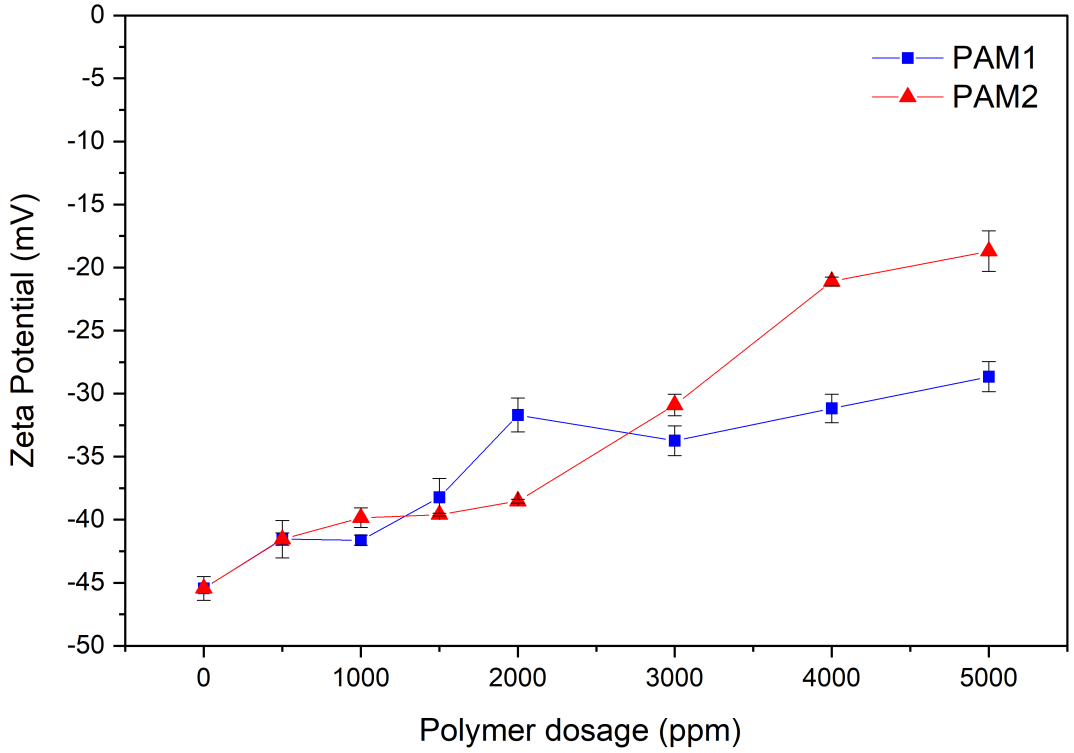

Figure 28 – Zeta potential of the supernatant at different flocculant dosages of PAM1 and PAM2 and after flocculating for 24 hours.

The zeta potential for the colloidal suspension (blank) was -45.45 mV. The zeta potential converged to neutrality with increasing polymer dosage, with a more subtle trend for PAM1. The maximum increase was -18.70 and -28.65 at 5000 pm of PAM2 and PAM1, respectively.

H-bonding is believed to be the primary adsorption mechanism between electronegative sites of mineral particles and PAM's amide and carbonyl groups (Botha et al., 2017; M. Dash et al., 2011; Lee and Somasundaranh, 1989; McGuire et al., 2006; Mpofu, 2003). The electronegative C=O group of the amide forms an H-bonding with the oxide/hydroxyl groups of the mineral phases present in the iron ore tailings (determined by XRD). In addition, not only the undissolved hydroxyl metals (MOH) are present in the tailings, but also charged groups (MOH_2^+ or MO^-) formed by H^+ adsorption or desorption by the hydroxyl groups of the mineral surface. The negative sites MO^- are more suitable to interact with the amide group (Lee and Somasundaranh, 1989; McGuire et al., 2006). The inability of PAM to completely neutralize

the zeta potential has been attributed to two factors: the steric stabilization effect when H-bonding governs the bridging interactions; and the hydrolyzation that can occur during PAM synthesis which gives them some anionic character (Kanungo, 2005). The more subtle effects of PAM1 on potential zeta increase were due to its lower M_w, leading to less H-bonding interaction, hydrolyzation, and steric stabilization, if compared to PAM2 (higher molecular weight) (Kanungo's (2005). The charged group formation and the H-bonding mechanism are shown in Figure 29.

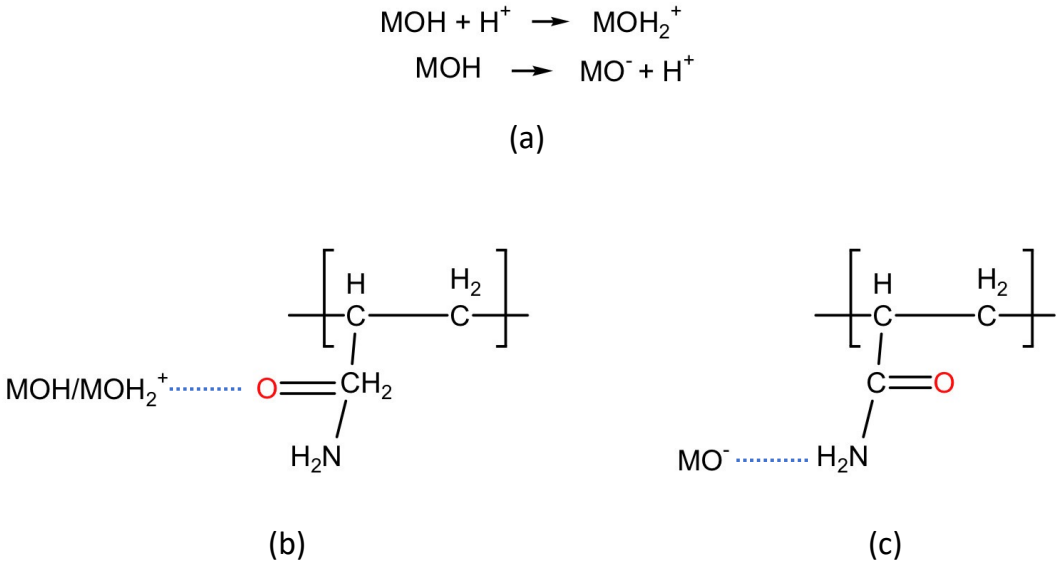

Figure 29 - Charging mechanism (a) and H-bonding between PAM groups (b-c) (Lee and Somasundaran, 1989).

3.3.4 A comparison with different polymer flocculants

We studied the flocculation performance of a 5 wt.% iron ore tailing suspension using two different polymers developed for oil sands tailings. These polymers have been extensively studied to treat oil sand tailings and have already been reported in our previous publications. Poly((vinyl benzyl)trimethylammonium chloride) (PVB) (Nguyen & Soares, 2022) is a linear, cationic, and partially hydrophobic polymer because of its pendant benzene rings. Polymer chains with polar groups interact strongly with positive charges and negative suspended particles. This creates sediment with high solid content. The polymer had a high molecular weight (2.9×10^6 g/mol) and narrow dispersity ($Đ = 1.19$). Partially hydrolyzed poly(methyl acrylate) grafted onto ethylene-propylene-diene copolymer backbones (EPDM-g-HPMA) (Rostami Najafabadi & Soares, 2021) is a graft copolymer designed to have a certain degree of

hydrophobicity provided by the EPDM backbone and negatively-charged functional groups provided by the partially hydrolyzed poly(methyl acrylate) (HPMA). These polymers were synthesized by varying the molecular weight of the EPDM backbone and HPMA grafts. We used a polymer with a molecular weight of 2.1×10^5 and 1.5×10^5 for the backbone and graft, respectively. The chemical structure of the monomers of both polymers is shown in Figure 30.

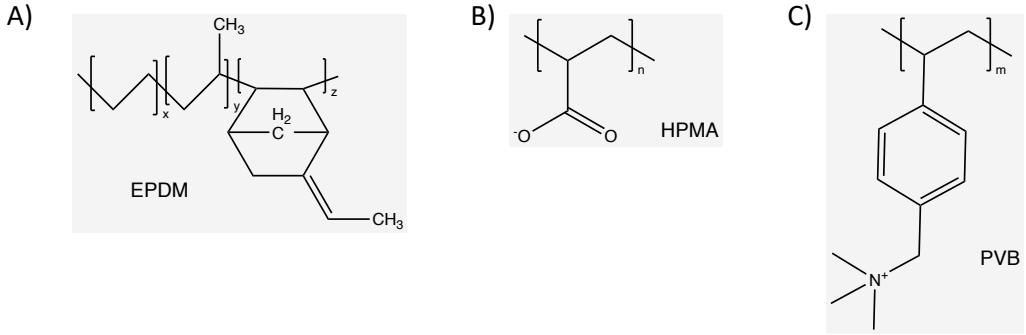

Figure 30 - Chemical structure of EPDM (A), HPMA (B), and PVB (C).

Figure 31 shows the solids content, turbidity, and CST determined for all tests using the exact dosage of 1000 ppm. PVB produced supernatants with lower turbidity (Figure 31A), slightly lower solids content (Figure 31B), and higher CST (Figure 31C). Figure 32 shows that either of the two new polymers clarified the water better than PAM. The positive charges of PVB helped the adsorption of the suspended negative particles, resulting in their destabilization and settling. The higher molecular weight of PVB also boosted the flocculation, resulting in more bridging with fine particles. EPDM-g-HPMA made supernatants with higher turbidity, likely because of their negative charges. Anionic polymers require divalent cations salts to promote bridging between their charged functional groups and the clay's negatively charged surface.

Figure 31B showed that neither new polymers could outperform PAM for solids content of the sediment. Surprisingly, the partial hydrophobicity of PVB did not improve the densification of the sediments. Similar results were observed by Nguyen & Soares (2022) for oil sands tailings flocculation. Regarding EPDM-g-HPMA, the low solid content was likely because of the low molecular weight of the grafts and backbone. Similar results were observed by Rostami Najafabadi & Soares, 2021), in which the highest solids content was observed for polymers with the highest molecular weights of the grafts and backbone. Figure 31C also shows that the sediments obtained with EPDM-g-HPMA were easier to dewater (lower CST), possibly because of the hydrophobicity of the backbone.

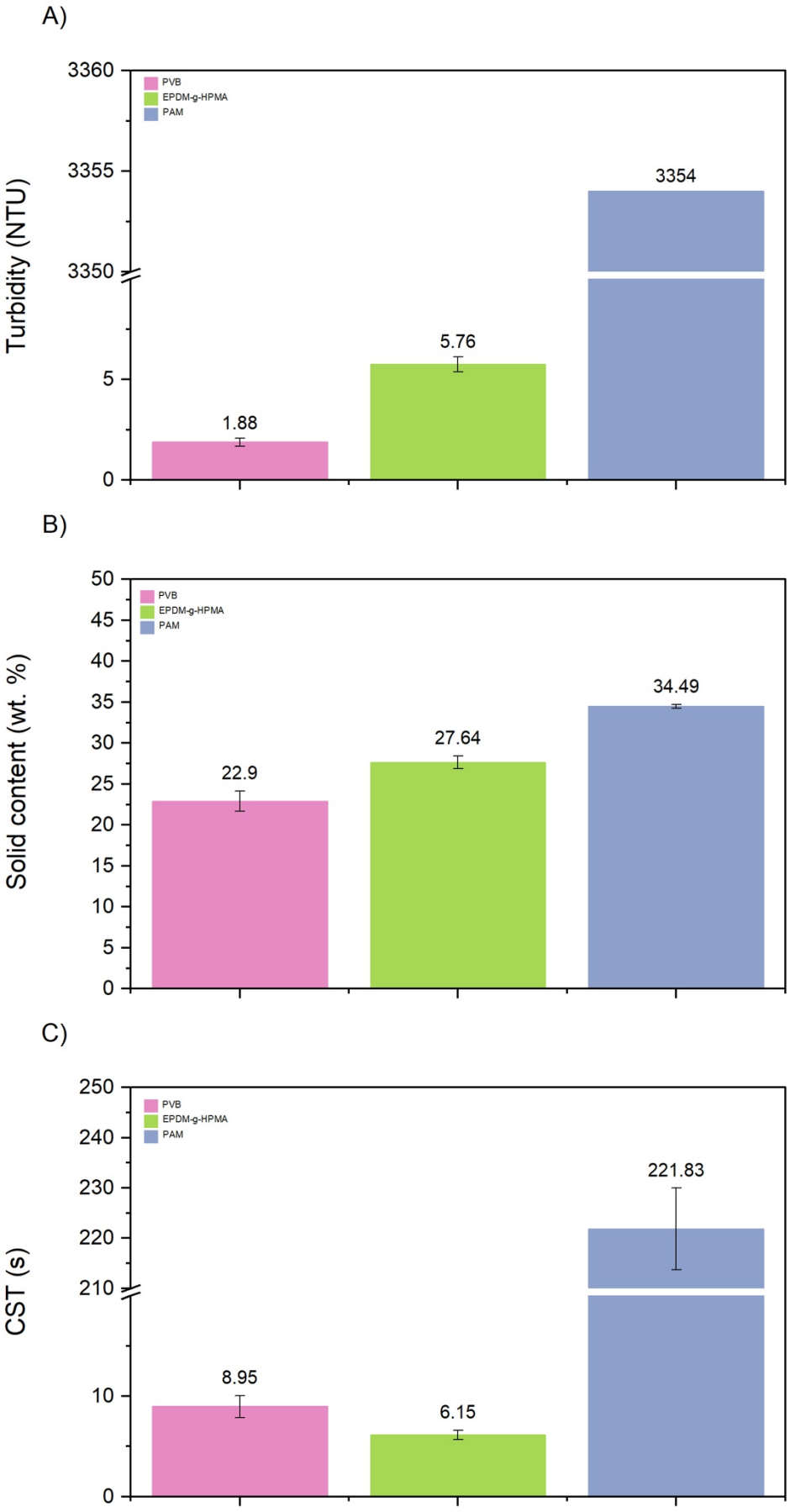

Figure 31 -Turbidity, solid content, and CST for a 5 wt. % iron ore tailing treated with PVB and EPDM-g-HPMA)

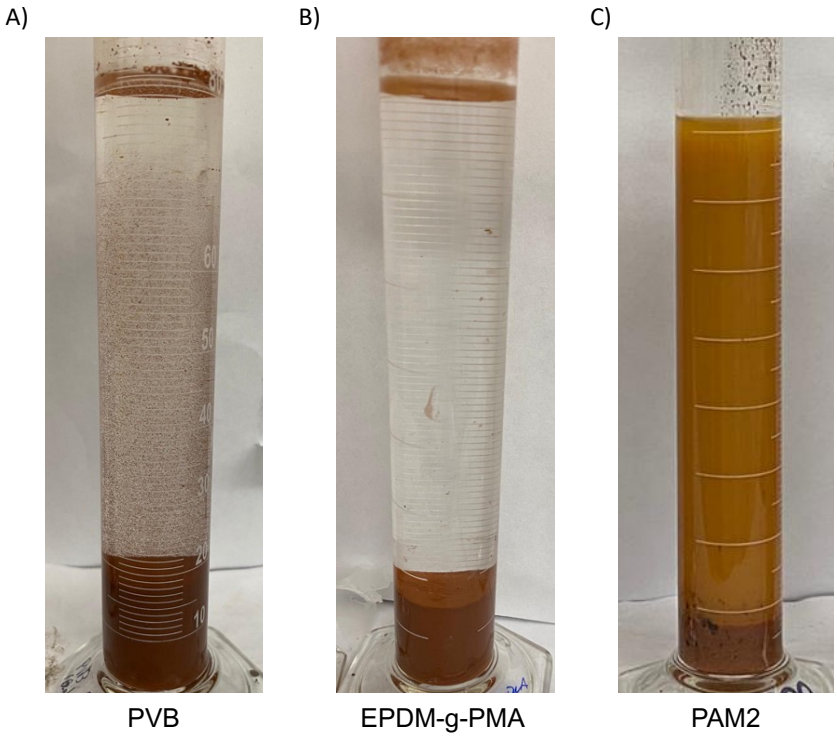

Figure 32 - Flocculation performance of 5 wt.% iron ore tailings with different polymers: PVD (A), EPDM-g-PMA (B) and PAM2 (C).

3.4 Conclusions

We studied the flocculation and dewatering efficiency of two commercial polyacrylamides, PAM1 and PAM2, using tailings from the Vargem Grande pond (Nova Lima, Minas Gerais, Brazil).

The industrial mineral tailings polyacrylamide (PAM2) has a higher molecular weight than laboratory-scale flocculation polyacrylamide (PAM1), which explains PAM2's better performance. For both PAM flocculants, the dosage correlated with better separation efficiency. For PAM2, 4000 ppm was found to be the optimal dosage. PAM2 at 2000 ppm produced sediments with the highest solid content (35 wt.%) among all conditions. Because of PAM's high hydrophilicity, this polymer still retains a large amount of water in the sediments.

Despite PAM2's superior flocculation performance, none of the dosages tested could overcome colloidal stability and clarify the supernatant. Also, sediments with a high-water content are less able to resist shear forces, increasing the risk of pond failures. While PAM did remove some fine suspended solids, its maximum efficiency was significantly low, making it ineffective at flocculating and dewatering iron ore tailings.

Poly((vinyl benzyl)trimethylammonium chloride) (PVB) and partially hydrolyzed poly (methyl acrylate) grafted onto ethylene-propylene-diene copolymer backbones (EPDM-g-HPMA) were considerably superior to commercially available high molecular weight polyacrylamides. They consistently produced clearer supernatants, despite being developed for entirely different tailings. Compared with PAM, these polymers had the only disadvantage of retaining high amounts of water in the sediment. We may speculate, however, that this constraint could be overcome by increasing the molecular weight of the hydrophobic monomers and varying their proportions.

Chapter 4

Cationic amylopectin graft copolymers for flocculation and dewatering of iron ore tailings.

4.1 Introduction

Various factors contribute to the depletion of high-grade iron ores worldwide, such as increased mining and processing activities and increased steel consumption in multiple sectors. Due to this scenario, low-grade minerals with complex metal compositions need to be exploited and processed, making iron ore beneficiation water- and grid-intensive, with fine-particle tailings being extensively produced. By 2030, it is estimated that iron ore mining will produce 1 million tons of waste per day (Das and Choudhury, 2013; Ihle and Kracht, 2018; Pearse, 2003; Wang et al., 2014).

Although the disposal of dewatered tailings is a promising alternative, fine particles, which are difficult to separate from water, pose a challenge for implementing and developing such processes. In a stable suspension, the energy barrier that keeps the particles suspended may be overcome by adding polymer flocculants that cause the particles to aggregate (Ji, 2013; Kolya et al., 2017; Leite and Reis, 2020; Wang et al., 2018). Ideally, the polymer chains adsorb on the suspended particles forming large flocs that settle down by gravity, producing dense sediment and a clear supernatant that can be reused as process water. Ideally is the keyword in the previous sentence since it is easier said than done.

Acrylamide-based polymers such as polyacrylamide (PAM) are the most used flocculants for mining tailings. However, these polymers are strongly hydrophilic and form poorly packaged flocs that retain large amounts of water (Bahmani-Ghaedi et al., 2022; Vajihinejad et al., 2019b). Often, they also produce turbid supernatants that are not well-suited to recycled process water. One of the reasons for this poor performance is that developed initially to treat municipal water but never specifically designed to remediate different mineral

tailings with distinct demands. Given this motivation and the still incipient use of natural polymers on the flocculation of mineral tailings, it is unquestionable that we need to study and develop novel polymers with molecular structures optimized to treat different mineral tailings types (Vajihinejad et al., 2019b).

Polysaccharide-based polymers have been extensively studied to be used as flocculant for the dewatering of tailings from various industrial processes. Among many natural polymers with potential for this kind of application, starch is undoubtedly one of the most studied. This polysaccharide is composed of a mixture of two polymers, amylose, and amylopectin, with a composition of approximately 20 and 80%, respectively. Amylose is a linear amorphous polymer of repeating glucose units connected by α-1,4 glycosidic linkages. Otherwise, amylopectin is a crystalline and branched polymer formed by glucose units linked by both α-1,4 glycosidic bonds and α-1,6 glycosidic linkages. The second is found to create the starting point of the branches and occurs approximately after every 28-30 glucose units (Guo et al., 2017; Kalia and Sabaa, 2013).

As the application of pure natural polymers as flocculants has numerous limitations, the solution to this problem has converged to the chemical modification where a synthetic monomer is attached to the natural polymer's main chain. This type of reaction is called grafting polymerization. Amylopectin-graft-copolymers are synthesized by polymerization of the monomers in the presence of a free radical initiator and have been extensively studied in the past years.

The performance of natural graft copolymer-based flocculants relies on their molecular structure, including charge density, grafting ratio, functional group substitution, distribution, and length of the grafts (Flory, 1953). Nonetheless, because various environmental factors affect the initiation and graft copolymerization efficiency, it is challenging to determine the precise distribution and length of grafts in natural polymer backbones using current characterization methods. Hence, they have usually been estimated in theory-based assumptions. Huang et al., (2017) proposed two equations assuming that: all initiated free radicals propagate graft chains efficiently; the number of dissociated initiators can be calculated from their half-lives, and each initiator (APS or KPS) can generate two free radicals after initiation. By simplifying these equations, we determined that the average grafting length is proportional to the square root of the initiator concentration, and that the average grafting number was proportional to the ratio of the initiator concentration to the natural polymer

concentration (Bazoubandi and Soares, 2020; Davey and Soares, 2021; Vajihinejad et al., 2019b).

Davey and Soares, (2022) synthesized a variety of amylopectin-graft-hydrolyzed-poly (methyl acrylate) (AP- g-H-PMA) copolymers and studied their performance in treating oil sands tailings. They found that polymers with longer grafts and lower graft density mainly enhanced flocculation performance. According to the authors, grafting hydrophilic synthetic chains onto hydrophobic natural substrates was a viable way to synthesize tailorable flocculants for oil sands tailings. Bazoubandi and Soares, (2020) synthesized various amylopectin-graft-polyacrylamides with different molecular structures for flocculating and dewatering oil sands tailings. These graft copolymers exhibited higher solids content than commercial polyacrylamides, suggesting they are a valuable alternative to commercial polyacrylamides. Hu et al., (2021) studied the performance of cationic flocculants with distinct structural characteristics by grafting (2-methacryloyloxyethyl) trimethyl ammonium chloride and acrylamide onto cationic starch (St) to dewater sewage sludge. The flocculants with the highest charge density, long graft chains, and less distributed grafts exhibited superior sludge dewaterability due to their improved charge neutralization and bridging flocculation effects.

In this work, the flocculation of iron ore tailings suspensions was studied using various synthesized graft polymer flocculants with distinct graft-chain numbers, lengths, and grafting ratios. The polymer was made through graft copolymerization of [(2-methacryloyloxyethyl) trimethyl ammonium chloride] onto the amylopectin backbone (AP-g-PMETAC). We divided the graft copolymers into four groups, each with a different graft-chain length (20, 40, 60, 80) and a constant graft-chain number (1, 2, 3). Various concentrations of amylopectin, monomers, and initiators were used to control the structural parameter. We characterized the polymers by thermogravimetric analysis (TGA), Fourier transform infrared spectroscopy (FTIR), nuclear magnetic resonance spectroscopy (NMR), CHNO elemental analysis, and gel permeation chromatography (GPC). Different dosages of AP-g-PMETAC were used in the settling tests, and the flocculation/dewatering performance was measured by turbidity, sediment solids content, ISR, and capillary suction time. AP-g-PMETAC outperformed conventional polyacrylamide flocculants, even at lower dosages, compared to two commercial polyacrylamides (PAM) studied in Chapter 3. AP-g-PMETAC flocculants might become promising candidates for treating iron ore tailings in the future, based on these results.

4.2 Materials and methods

4.2.1 Materials

We collected the tailings in the thickener underflow stream before they were disposed into the Vargem Grande pond (Nova Lima, Minas Gerais, Brazil). Amylopectin from maize (AP), potassium persulfate (≥99.0%), [2-(methacryloyloxy) ethyl] trimethylammonium chloride (METAC) (75 wt. % in H_2O), deuterium oxide (D_2O), dimethyl sulfoxide-d6 (DMSO-d6), sodium sulfate (Na_2SO_4), acetic acid and ethanol anhydrous were purchased from Sigma-Aldrich. The tailings were dried and stored according to the protocol described in Chapter 3. (See section 3.2.2).

4.2.2 Synthesis and purification of AP-g-PMETAC

Different grades of AP-g-PMETAC were synthesized as follows: A three-neck round-bottom flask of 100 mL coupled with nitrogen and reflux was used for the grafting reaction. For gelatinization, a mixture of amylopectin and water at 90°C was heated for 1 hour at 90°C (Davey and Soares, 2021; Huang et al., 2017; Liu et al., 2017). Then, the temperature was decreased to 70°C under continuous mixing (300 rpm) and an N_2 atmosphere. KPS initiator was then dissolved in 1 mL of deoxygenated DI water and injected into the reaction media. The solution was stirred for 15 minutes, allowing the free radicals to attack the AP backbone forming the radicals' sites, where the grafting polymerization takes place. After this, a deoxygenized METAC solution was added to the reaction, and the grafting polymerization was carried out for 5 hours at 70 ^oC, 300 rpm, and N_2. The reaction was cessed by adding 2.7 mg of hydroquinone, and the product was precipitated in ethanol 80% and mixed for 24 hours. The precipitate was then dried in a freeze dryer for 24 hours. Then, a 3 g sample of the dried product was purified with a Soxhlet extractor for 48 hours with ethanol as solvent to ensure total removal of the homopolymer. This purification process was validated for our polymers, and the results are shown in Figure 50 of the supplementary information (see Appendix B). The schematic of the experimental setup is shown in Figure 33.

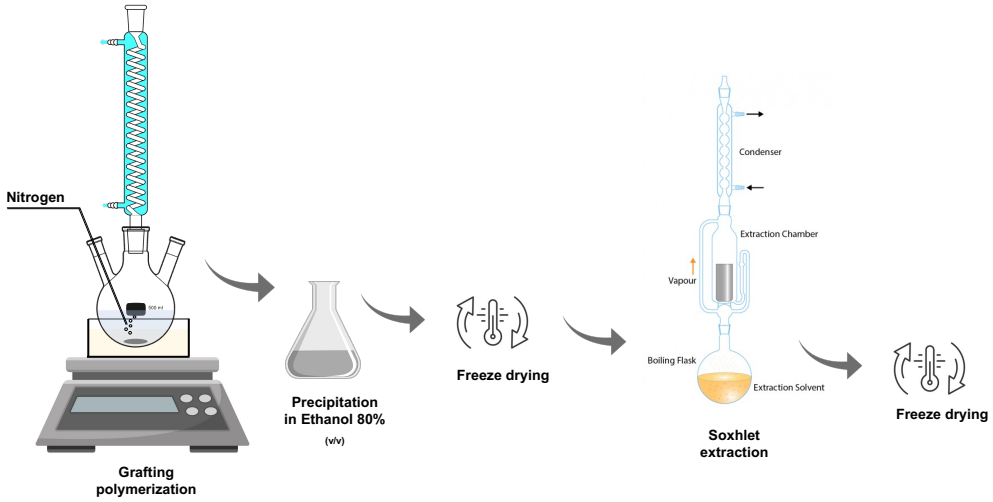

Figure 33 – Scheme of the experimental polymerization and purification setup for AP-g-PMETAC.

4.2.3 Synthesis and purification of PMETAC

Synthesis of PMETAC homopolymer was carried out by free radical polymerization. A 100-ml round-bottom flask reactor with three necks was first filled with monomer METAC (1 M) and water. The mixture was heated to 70 °C and stirred (300 rpm) for 1 hour under an N_2 atmosphere. Then, we added to the reactor 68 mg of KPS (2.5×10^{-4} M) dissolved in 2 ml of deoxygenated water. The homopolymerization was conducted for 3 hours at 70°C, 300 rpm, and N_2. After this, 2.7 mg of hydroquinone was used to stop the free-radical polymerization reaction. We removed the unreacted monomers from the synthesized polymer utilizing a dialysis membrane for four days, changing the water every 12 hours. After purification, the product was dried in a freeze dryer for 24 hours.

4.2.4 Experimental details

The different AP-g-PMETACs were synthesized by varying the concentrations of AP, METAC, and KPS. We determined the ratio between reactants based on two compositional parameters: the average number of chains (N) and the average length of chains (L). The graft-chain number represents the number of Anhydroglucose units (AGU) containing grafted METAC chains, while the graft-chain length measures the length of the chains. L was calculated by dividing the AP concentration (based on its monomeric unit, anhydroglucose, 162.15 g/mol) by the initiator concentration. N was calculated by the ratio between the monomer concentration

and the square root of the initiator concentration ([M]/√I) (Bazoubandi and Soares, 2020; Vajihinejad et al., 2019a).

We grouped AP-g-PMETAC polymers into four groups based on their graft lengths (L) and graft numbers (N) to correlate polymer microstructure with their characterization and flocculation efficiency. The synthesis details, group name, and structural parameters are shown in Table 5. The name of the synthesized polymers was chosen based on their graft-chain number and length. For example, the first grafted copolymer (N1L40) has N equal to 1 and L equal to 40.

Table 5 – Structure and synthesis details of various AP-g-PMETAC polymers

Grafted Copolymer	Group	Mass Ratio AP:METAC:KPS	Graft-Chain number (N)[a]	Graft-Chain length (L)
N1L40	N1	2:8:0.003	1	40
N1L80		2:17:0.003	1	80
N2L40	N2	1:8:0.003	2	40
N2L80		1:17:0.003	2	80
N3L20	N3	2:8:0.011	3	20
N3L40		2:17:0.011	3	40
N3L60		1.5:12:0.007	3	60
N6L20	N6	1:8:0.011	6	20
N6L40		1:17:0.011	6	40

[a] value per 1000 AGU units

4.2.5 Polymer characterization

The polymers were qualitatively analyzed using FTIR, 1H-NMR, and 13C-NMR. Solid samples were analyzed using Agilent Cary 600 FTIR spectrometers in the range of 4000–400 cm^{-1}. The NMR spectra were collected at 25 °C using a three-channel Agilent / Varian Inova 400 MHz spectrometer. Graft-copolymers and pure amylopectin were dissolved in D_2O and DMSO-d6, respectively. Synthesized polymers were evaluated for nitrogen content with a CHNS elemental analyzer (Thermo Flash 2000). The grafting ratio of METAC onto AP was calculated by using the nitrogen content of the copolymer ($N_{wt.\%}$) and the molecular weight of

METAC ($M_{w_{(METAC)}}$), as shown in Equation 3. W_{METAC} and W_{AP} is the weight of grafted METAC and AP in the copolymer, respectively.(Fang et al., 2009; S. Wang et al., 2015).

$$\%grafting\ ratio = \frac{W_{METAC}}{W_{AP}} \times 100 = \frac{\frac{N_{wt.\%}}{14} \times M_{w_{(METAC)}}}{100 - \frac{N_{wt.\%}}{14} \times M_{w_{(METAC)}}} \times 100 \quad (3)$$

Thermogravimetric analysis of the polymers was conducted using a TGA analyzer (TGA/DSC 3+ METTLER TOLEDO) at a temperature of 25 to 600 °C under an N_2 atmosphere and a heating rate of 10 °C.min^{-1}. Gel permeation chromatography (GPC, Agilent 1260 Infinity) equipped with two TKS gel G6000PW XL-CP columns was used to determine the grafted copolymers' molecular weights (Mw). 0.30 M $NaSO_4$ and 0.15 M acetic acid were used for the mobile phase. We used the exact solution to dissolve the polymers at approximately 3 mg/ml. GPC flow rate was 1.0 ml/min with an injection volume of 100 µL. We kept the injection volume and flow rate constant for all samples. The reproducibility of the results was ensured by performing the characterizations at least twice and often in triplicate. These replicate experiments are represented by error bars in each figure.

4.2.6 Tailing characterization and flocculation media preparation

We characterized the tailings samples used for the flocculation tests to determine their particle size distribution (PSD), particle morphology, solid content, and chemical/mineralogical composition. A detailed description of the methodologies and results was done in Chapter 3.

Briefly, gravimetry was used to determine solid content. In contrast, X-ray diffraction was used to determine the mineralogy of sedimented and colloidal phases (Philips - X'PERT-MPD - copper tube, 45-40 kV/mA, 2θ from 2.5° to 80° and time per step equal to 200 s). X-ray fluorescence spectroscopy (XRF) was used to analyze the chemical composition (Zetium - Malvern Panalytical). An ICP-OES (SPECTRO ARCOS ICP-OES) was used to chemically quantify the aqueous phase of the colloidal suspension prepared at 5 wt.%. Flocculation tests were conducted with the same colloidal suspension prepared at 5 wt.% at pH 10 (0.4 M NaOH added for adjustment). The flocculation media was prepared as follows: 1) from dry tailings, a

60 wt.% slurry with pH 10 was prepared; 2) following 2 hour resting period, two distinct phases formed: a sedimented phase and a supernatant colloidal suspension; 3) they were carefully separated, and their solid content determined gravimetrically; 4) the sediment was discharged, and the supernatant was combined with water to produce the 5 wt.% colloidal suspensions at pH 10.

4.2.7 Flocculation tests

In this experiment, different dosages of the AP-g-PMETAC copolymers were used to flocculate 100 mL of a 5 wt.% tailing suspension. Figure 34 shows the schematic of the flocculation tests. The desired dosages were calculated based on the suspension's solids and expressed in ppm (mg of polymer per kg of tailings solids). The prepared tailing suspension was stirred continuously (300 rpm), and pH was monitored. We transferred an aliquot of 100 g of the suspension to a 200 mL beaker and stirred it at 500 rpm for 3 minutes. The polymer was pipped from a stock solution (2 mg/ml) and then added to the mixture in a single pulse at the same spot (approximately 0.5 cm away from the stirrer rod). After adding the flocculant, the sample was stirred for two minutes at 500 rpm, followed by three minutes at 280 rpm. Immediately after mixing, the suspension was transferred to a 100 mL graduated cylinder, and the mudline height (h) (solid-liquid interface) was recorded for one hour. We calculated the ISR from the slope of the graph of mudline height normalized by total height (h/H) over time.

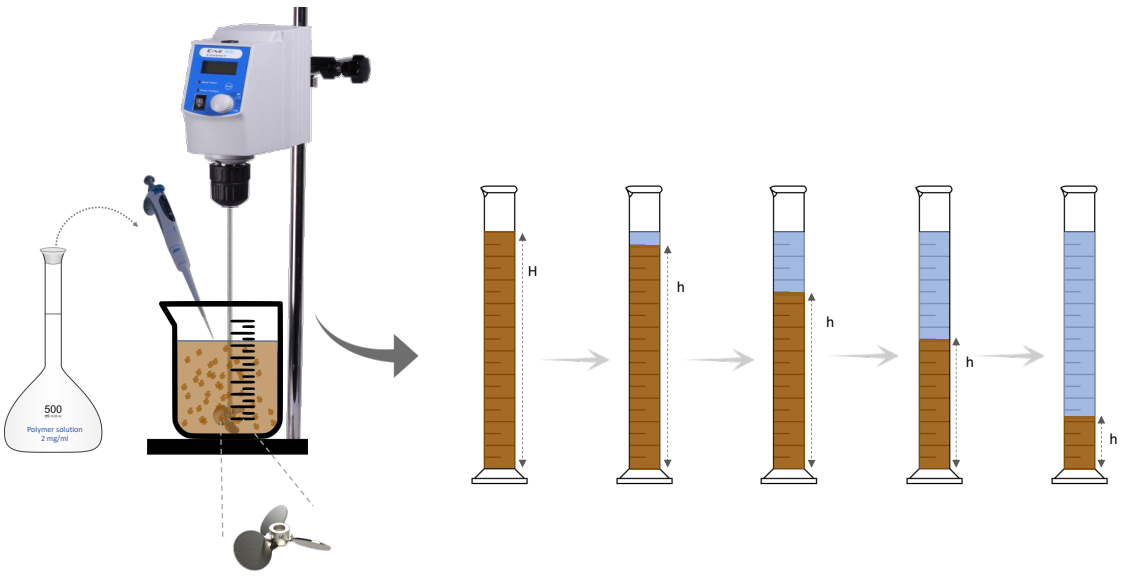

Figure 34 - Schematic of the flocculation and ISR procedure.

Following 24 hours of settling in the cylinder, sediment and supernatant were separated and characterized. To measure the CST of the sediment, we homogenized it and poured 3 ml of it into a capillary suction time unit (Triton Electronics Type 319 Multi-CST). We measured the solid content of the sediment by pouring a known mass of the sediment into an aluminum weighing dish and letting it dry at 65 ºC for 24 hours or until all water had been completely removed from it. Using a Hach 2100AN turbidimeter, the turbidity of the supernatant was measured and expressed as NTU (Nephelometric Turbidity Units).

4.3 Results and discussion

4.3.1 Synthesis of AP-g-PMETAC and grafting copolymerization mechanism

METAC monomers were grafted onto the amylopectin backbone through free-radical polymerization with KPS, which occurred in three steps: initiation, propagation, and termination. During polymerization, various reactions occur concomitantly, and some may result in undesired by-products. A graft copolymerization mechanism for AP-g-PMETAC is shown in Figure 35. The thermally decomposed radicals attack the AP backbone to create active sites by hydrogen transfer on the hydroxyl group of the monomeric glucose unit's primary carbon. Many authors have used the mechanism illustrated in Figure 35 (Chen et al., 2016; Kalia and Sabaa, 2013; Pal and Pal, 2012; Salehizadeh et al., 2018; Sarkar et al., 2013; Wang et al., 2013), but recent studies have proposed a different one in which the hydrogen transfer can occur at all glucose hydroxyl groups (Das et al., 2019; Czarnecka and Nowaczyk, 2020). As discussed below, the ^{1}H NMR spectrum of the AP-g-PMETAC suggested this mechanism might happen, but it couldn't be confirmed conclusively.

In the propagation step, the active sites along the AP backbone react with the vinylic double bond of METAC to form the graft chains. The propagation process also produced PMETAC by homopolymerization, which must be removed in a downstream purification step. Finally, the chain ends are paired or deprotonated to terminate the polymerization reaction.

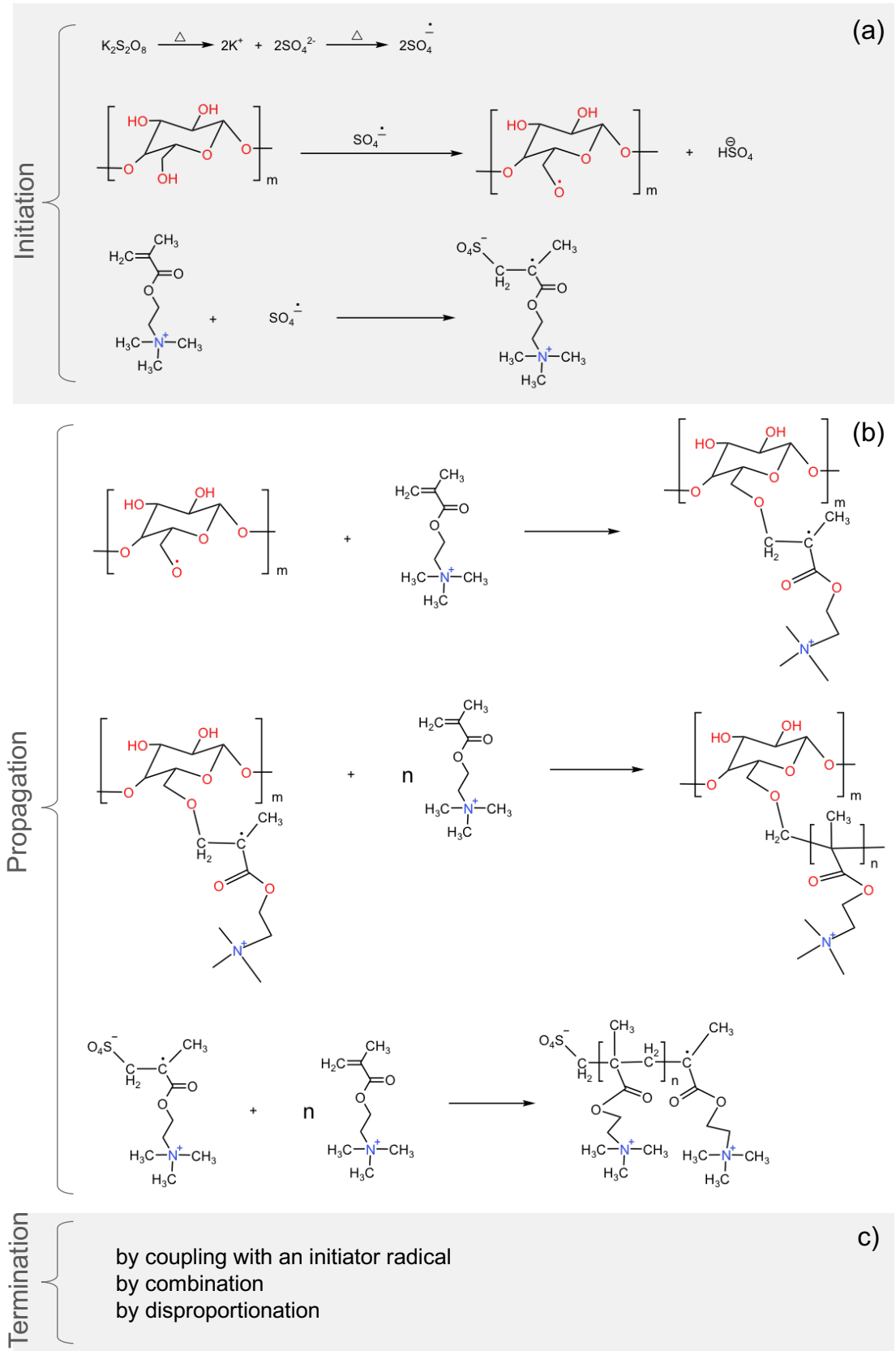

Figure 35 – Proposed mechanism of METAC graft copolymerization onto Amylopectin.

4.3.2 Polymer Characterization

For most of the characterizations, N3L20 was chosen as representative of all AP-g-PMETAC samples.

Thermogravimetric Analysis (TGA)

Thermogravimetry studied the thermal stability and decomposition properties of AP-g-PMETAC and AP after gelatinization. Figure 36 shows the samples' weight loss as a temperature function.

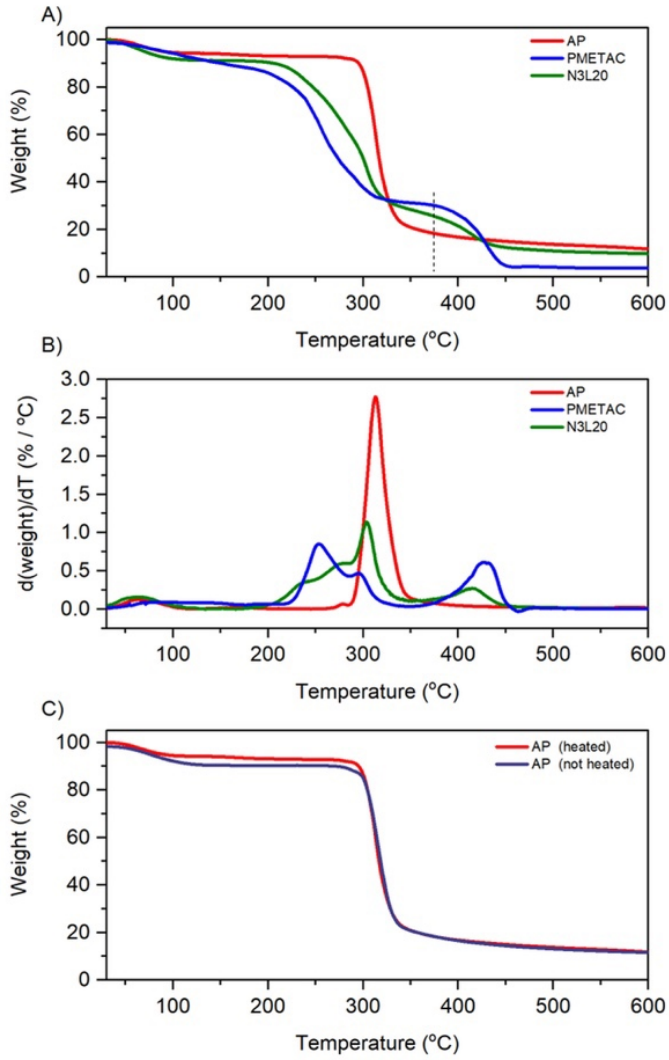

Figure 36 - Thermogravimetric analysis of: A) AP, PMETAC, AP-g-PMETAC (sample N3L20); B) weight loss rate of AP, PMETAC, and N3L20; C) AP before and after heating for gelatinization.

In Figure 36A, the first weight loss (below 200 ºC) was attributed to the evaporation of adsorbed water. At 375 ºC, the weight loss reached 81.2 % for AP, 69.5% for PMETAC and 74.1 % for AP-g-PMETAC. In summary, AP-g-PMETAC polymers were less stable than PMETAC and more stable than AP up to 375 ºC. At about 460ºC, all weight losses reached a plateau of approximately 85%, 89 %, and 95% for AP, AP-g-PMETAC, and PMETAC, respectively.

In Figure 36B, PMETAC shows two peaks at 250 and 420°C, whereas AP had only one peak at 312°C. The literature has reported that at 250°C, the peak results from the decomposition of quaternary ammonium groups in METAC. In comparison, at 420 °C, it results from PMETAC main chain decomposition (Wang et al., 2018). The decomposition of the AP main chain and quaternary ammonium groups of METAC produced a broad peak between 250 and 312°C for AP-g-PMETAC. The peak for PMETAC main chain decomposition was also observed at 420°C.

Figure 36C shows that the gelatinization step (90 ºC for 1 hour) did not affect the thermal stability of the molecular structure of AP. In addition, the weight loss caused by water evaporation was lower for AP subjected to gelatinization because the sample was freeze-dried after gelatinization.

Fourier Transform Infrared Spectroscopy (FTIR)

In Figure 37, the characteristic bands in the FTIR spectra of amylopectin, PMETAC, and a mixture of both (AP + PMETAC, 1:5 wt.%) were compared to the AP-g-PMETAC copolymer.

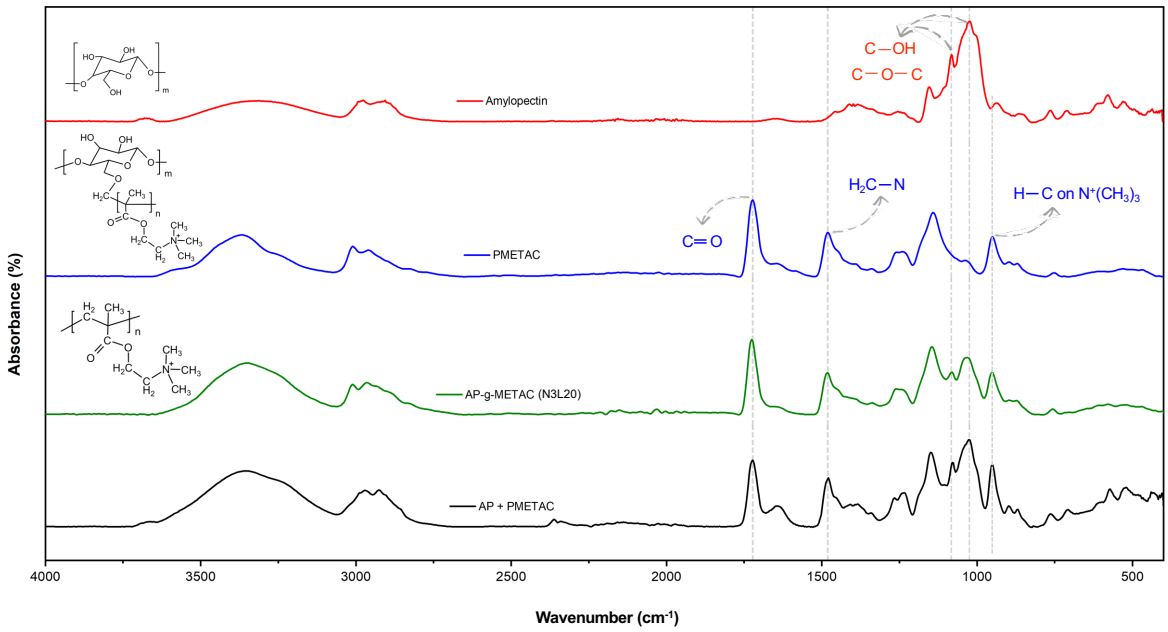

Figure 37 - FTIR spectra of amylopectin (AP), homopolymer (PMETAC), AP-g-PMETAC (N3L20) and mixture of AP and PMETAC (AP + PMETAC).

In all spectra, the stretching band observed at 3900-3000 cm^{-1} was attributed to the O-H bonds of adsorbed water and hydroxyl groups of amylopectin. All analyzed structures showed banded peaks at 3000-2800 cm^{-1}, indicating an aliphatic C-H (Hu et al., 2020; Huang et al., 2017; Kalia and Sabaa, 2013; Velásquez-Barreto et al., 2021; Wang et al., 2013). The peaks observed in the amylopectin spectrum at 1080 and 1024 cm^{-1} may correspond to stretching vibrations of the glycosidic bonds (Lanthong et al., 2006; Salehizadeh et al., 2018; Velásquez-Barreto et al., 2021) and C-O-H groups (Velásquez-Barreto et al., 2021). Compared to AP, three new characteristic peaks at 1720, 1482, and 952 cm-1 were found in the spectra of PMETAC. Carbonyl (C=O) is the peak at 1720 cm-1 of the ester group. The other two peaks, at 1482 and 952 cm-1, are the methylene (H_2C-N) and methyl (C-H) groups of quaternary ammonium, respectively (Abdollahi et al., 2011; Chen et al., 2018; Hu et al., 2020; Huang et al., 2017; Liu et al., 2017; M. and S., 2016a; Wang et al., 2013, 2007).

In the AP-g-METEC graft copolymer, the intrinsic characteristic peaks of AP and PMETAC were also observed. Furthermore, the spectra of the AP + PMETAC mixture and AP-g-PMETAC were almost identical. Both observations indicate that METAC was effectively grafted onto amylopectin.

NMR spectral analysis

Figure 38 shows the ^{1}H NMR signals obtained for AP, PMETAC, and AP-g-PMETAC (N3L20) and the hydrogen positions on the chemical structure based on the signals.

The ^{1}H NMR for AP is shown in Figure 38A, and it is consistent with literature (Abdollahi et al., 2011; Das et al., 2019; Dragunski and Pawlicka, 2001; Fan et al., 2019; Nilsson et al., 1996; Tizzotti et al., 2011; L. Wang et al., 2015). The peaks H-1 (5.1 ppm) and H-1' (4.9 ppm) were associated with the hydrogen atoms of the α-1,4 and α-1,6 links, respectively (Gidley, 1985; Petronilho et al., 2021). The adsorbed water of DMSO-d6 (highly hydrophilic) produced a prominent peak at about 3.3 ppm. The same peak was found in the PMETAC and AP-g-PMETAC spectra, possibly because the samples were not dried before the analysis (Tizzotti et al., 2011). The presence of adsorbed water is consistent with the TGA analysis. AP and PMETAC were dissolved in D_2O, and its corresponding peak appeared at 4.8 ppm. The hydrogens of the C-H groups and CH_2 (H2, H4, H6, H7, and H8) were found to be in a superposition of peaks between 3.6 and 3.4 ppm.

PMETAC's 1H NMR was also consistent with the literature and is shown Figure 38B (Das et al., 2019; Fan et al., 2019; Kim et al., 2019; M. and S., 2016b; Ozturk et al., 2018; Sánchez et al., 2017; Sponchioni et al., 2019; Sweedman et al., 2013). The absence of the METAC vinylic proton signal at 6.5 ppm in the PMETAC and AP-g-PMETAC spectrum evidenced the lack of residual monomer. It verified the efficiency of the purification methods. The hydrogens of the methyl groups, H-11 and H-14, correspond to the peaks at 2.0 and 3.3, respectively.

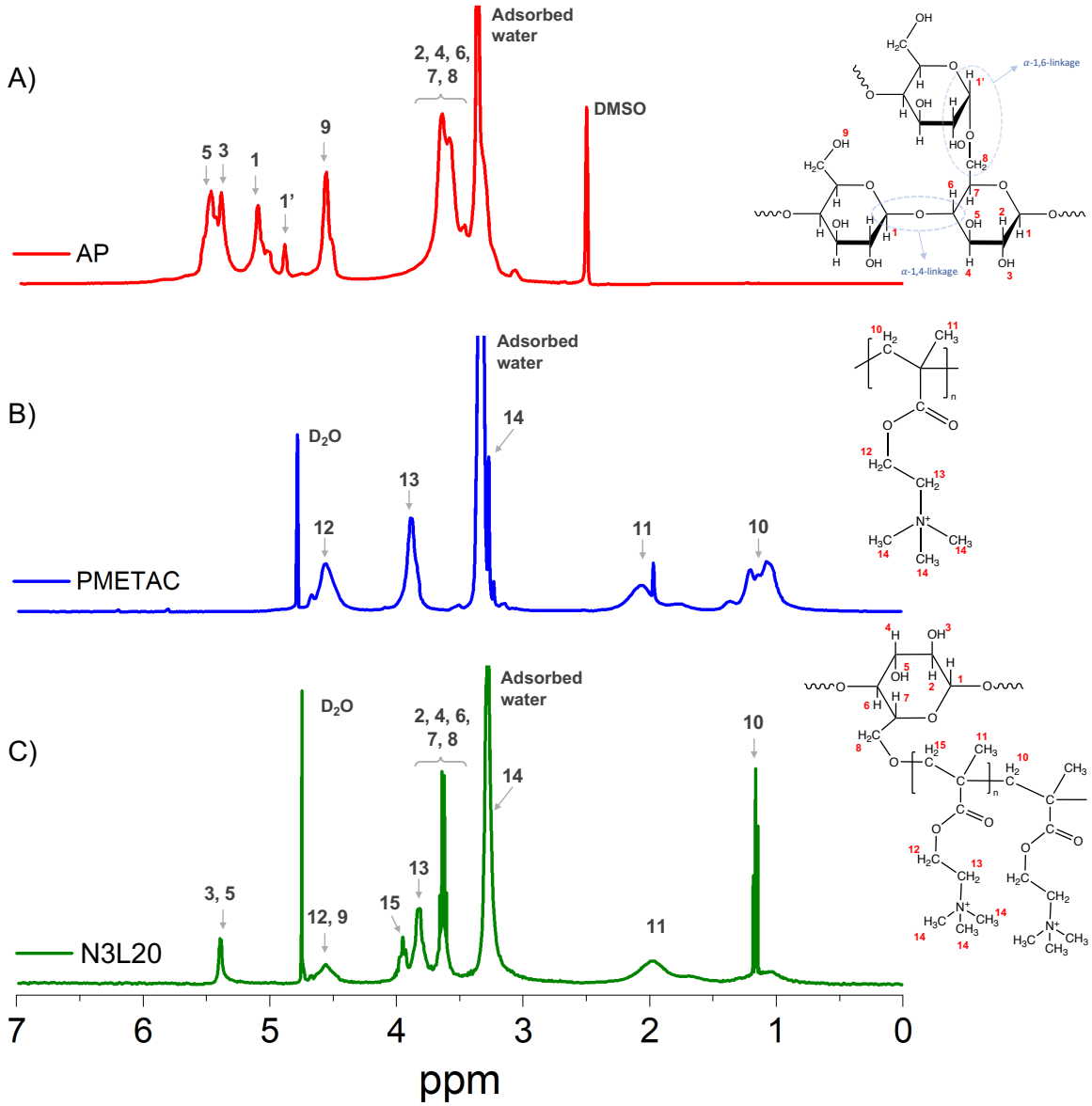

Figure 38 - H NMR spectra of AP (a), PMETAC (b), and AP-g-PMETAC (N3L20) (c).

The spectrum of AP-g-PMETAC (N3L20) showed the characteristic peaks of AP and PMETAC, indicating that METAC was successfully grafted onto the AP backbone. According to the AP spectrum, hydrogens from hydroxyl groups H-3, H-5, and H-9 were detected at chemical shifts 5.4, 5.5, and 4.6, respectively. Unexpectedly, a reduction in the chemical shift intensity of these peaks was observed in the AP-g-PMETAC spectrum, which suggested that all hydroxyl groups probably attacked the radicals to form grafting sites. Also, the AP-g-PMETAC spectrum was absent of the AP chemical shifts of H-1 (at 5.1 ppm) and H-1' (at 4.9 ppm), indicating a possible breakage of these bonds during the polymerization. Unfortunately, more data would be needed to support this hypothesis, which will be addressed in future contributions. It is worth mentioning that variations in the characteristic peaks of the backbone

in grafted copolymers have already been reported elsewhere (Kolya and Tripathy, 2013; Lv et al., 2013; Siyamak et al., 2020). The immobilizing effect of intramolecular interactions that are formed after grafting is one of the causes related to variations in intensity and frequencies of NMR spectrums (Siyamak et al., 2020). In addition, the ratio between the reactants also changes the product's spectrum characteristics compared to reactants in their pure form. According to Moad (2011), because the grafted copolymer is more soluble in water (compared to AP), H-bonding is favored, acting as a shield to the protons, which results in different chemical shifts.

Figure 39 shows the ^{13}C NMR spectra of AP, PMETAC, and AP-g-PMETAC. In each polymer, the carbon atoms were assigned the corresponding chemical shift value and agreed with previous works (Chang et al., 2021; Kobayashi et al., 2010; M. and S., 2016a; Mandal et al., 2017; Sarkar et al., 2013; Singh et al., 2013; Siyamak et al., 2020; Sun et al., 2009; Wang et al., 2022). All resonance peaks in AP were within 60 to 105 ppm, which match the characteristic peaks of carbons C1 to C6 in the AGU unit (Figure 39a). The high-intensity peak at 38 ppm was attributed to DMSO-d6, used as the solvent. Similarly, the characteristic peaks of PMETAC were observed in its spectrum (Figure 39b). Among the ligands of the quaternary ammonium, the methyl ($-CH_3$) and methylene ($-H_2C-N$) groups were observed at 178 and 64 ppm, respectively. The peak observed at 19 ppm was assigned to the methyl group attached to the quaternary carbon. The other carbon atoms had signals between 60 and 45 ppm. All characteristic peaks of AP and PMETAC were observed in the ^{13}C NMR spectrum of the grafted copolymer, confirming the grafting reaction.

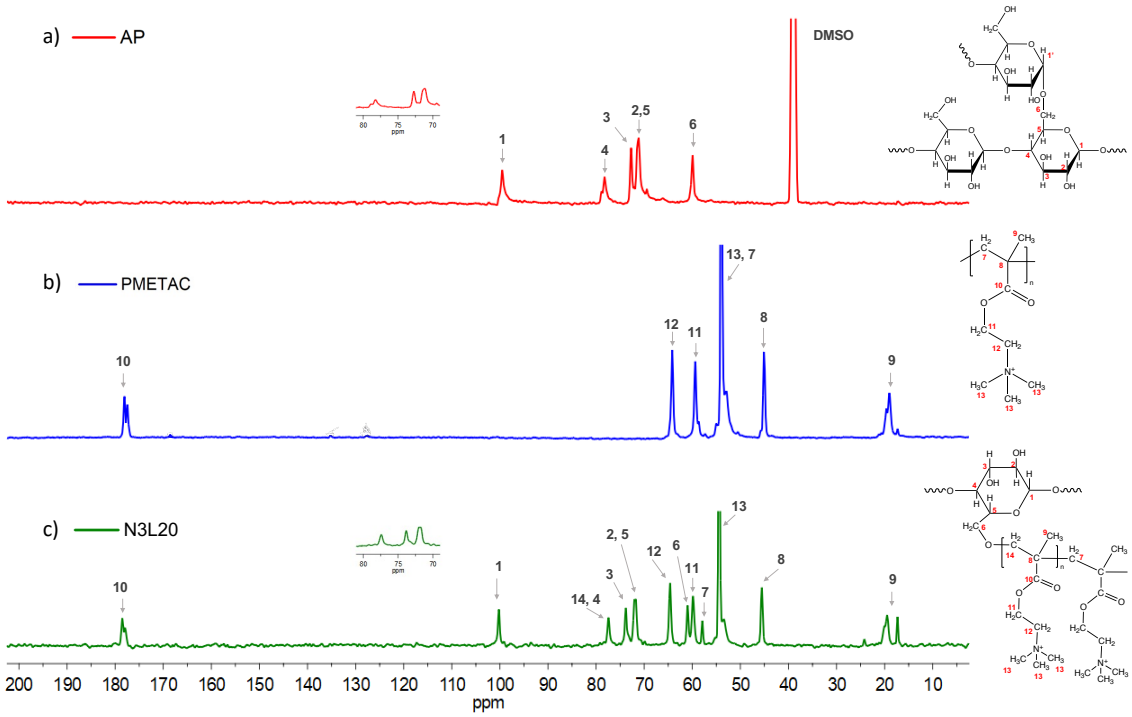

Figure 39 - ^{13}C NMR spectra of AP (a), PMETAC (b) and AP-g-PMETAC (N3L20) (c).

Elemental Analysis

Because amylopectin is a nitrogen-free chemical, the %grafting ratio of METAC was calculated by quantifying the nitrogen content of the AP-g-PMETAC copolymer (according to Equation (3). The nitrogen quantification was also interpreted as proof of the grafting reaction.

Figure 40A shows that %grafting ratios varied with increasing the graft-chain length in each grafted copolymer group. Figure 40B confirmed that the %grafting ratio increased not only with the length of the chains (L) but also with the number of graft chains (N). This result was expected because longer and denser graft chains mean more METAC are incorporated onto the AP backbone.

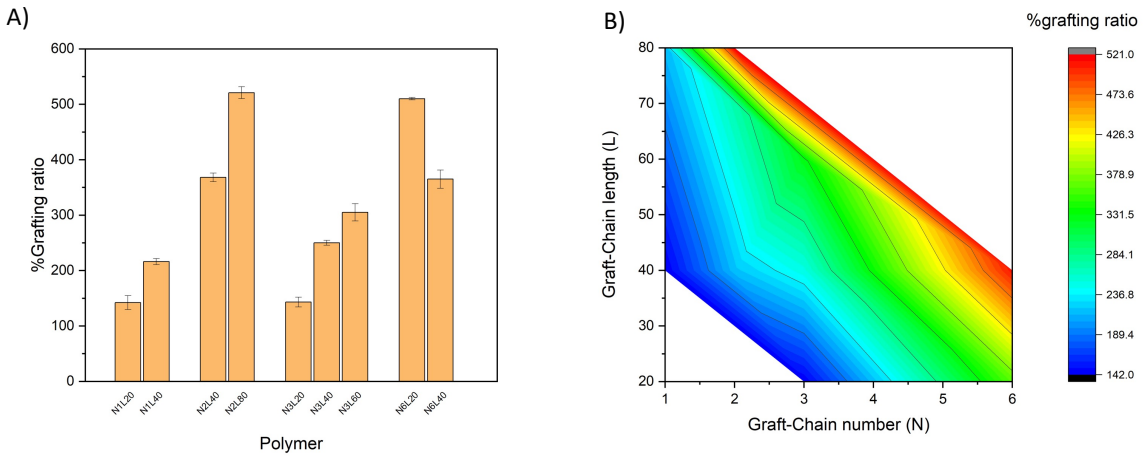

Figure 40 - Grafting ratio (%) of the grafted copolymers (A) and as a function of L and N (B).

Molecular weight

Table 6 shows the number (M_n) and weight (M_w) average molecular weight of the synthesized AP-g-PMETAC. The M_n and M_w of all AP-g-PMETAC polymers were higher than amylopectin (M_n = 4.0×10^5 g/mol; M_w=1.7×10^6 g/mol) and PMETAC (M_n = 1.1×10^6 g/mol; M_w=1.6×10^6 g/mol), confirming that METAC is grafted onto AP. The molecular weight of AP was determined in previous works from the group (Bazoubandi and Soares, 2020; Davey and Soares, 2022).

Table 6 - Molecular weight results obtained from GPC.

AP-g-PMETAC	M_n (10^6 g/mol)	M_w (10^6 g/mol)	Đ
N1L40	4.87	6.12	1.26
N1L80	7.42	10.18	1.37
N2L40	3.64	4.29	1.18
N2L80	4.06	5.51	1.36
N3L20	3.78	4.82	1.28
N3L40	3.83	5.80	1.52
N3L60	3.76	5.07	1.35
N6L20	2.83	3.79	1.34
N6L40	2.96	4.10	1.38

Figure 41 shows the molecular weight of AP-g-PMETAC as a function of the graft chains' number (N) and length (L). As expected, the molecular weight varies proportionally with the graft chain length and inversely with the graft chain number.

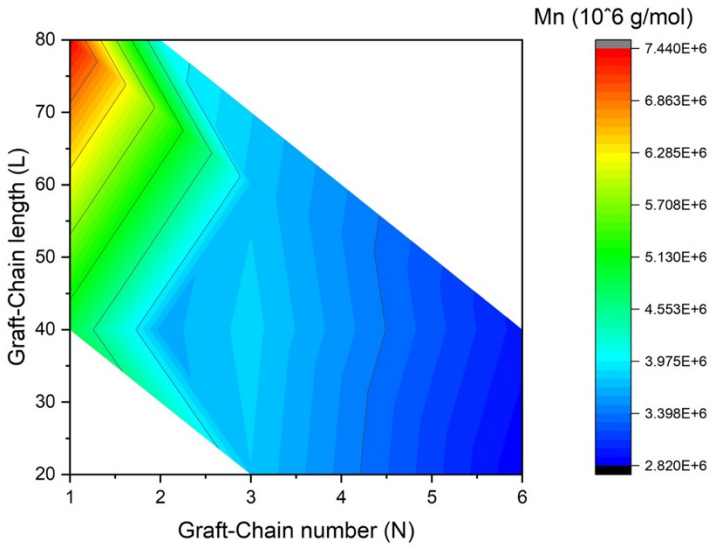

Figure 41 – Number average molecular weight (M_n) of the AP-g-PMETAC copolymers as a function of L and N.

4.3.3 Flocculation tests

A 5 wt.% iron ore tailings suspension was flocculated with AP-g-PMETAC copolymer flocculants. The flocculation tests were designed to evaluate the effect of the variables: molecular weight, percent grafting ratio, graft-chain number (N), and length (L); and different polymer dosages.

Since the AP-g-PMETAC copolymers were made to have different graft-chain numbers (N) and lengths (L), we proposed an illustration for the structural morphologies of the four AP-g-PMETAC groups as shown in Figure 42. Each group has the same number of graft chains but different lengths.

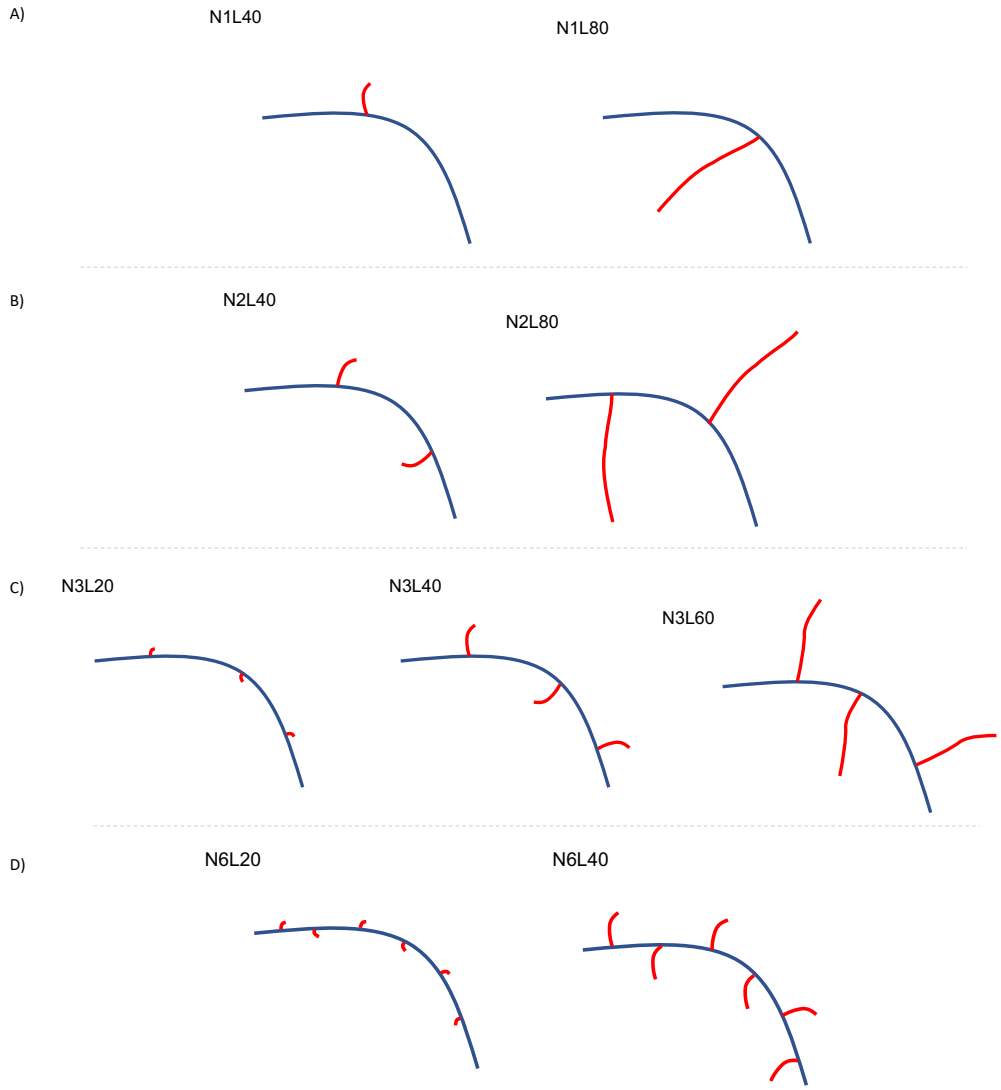

Figure 42 – Scheme of the structural morphology of the various AP-g-PMETAC classified into four groups: N equal to 1 with an L of 40 and 80 (A), N equal to 2 with an L of 40 and 80 (B), N equal to 3 with an L of 20, 40 and 60 (C) and, N equal to 6 with an L of 20 and 40 (D).

Supernatant turbidity, sediment solid content, capillary suction time (CST), and initial settling rate (ISR) were characterized to determine how these variables affect flocculation performance.

Effect on turbidity

The lower the turbidity, the clear the supernatant water is, and the better the performance of the polymer in neutralizing and bridging the suspended particles. In this study, we did not

address the possibility of reusing the water due to the lack of characterization of it after flocculation.

Figure 43 shows turbidity results for each polymer group for all dosages on the left, and only the lowest turbidity results (at 500 and 1000 ppm) on the right. The turbidity of prepared tailings suspensions with 5 wt.% was beyond equipment detection limits (10,000 NTU) and therefore could not be determined. Turbidity decreased sharply from 250 to 500 ppm, then rose again at higher dosages. This was because low dosages (e.g., 250 ppm) of polymeric chains result in small, fragile flocs that cannot provide adequate separation. In contrast, the turbidity increased after 1000 ppm because larger flocs formed faster, giving the polymers less time to capture fine particles. Additionally, other researchers have noted that high doses of charged flocculants favored the colloidal stability of the system due to excessive charge density (Arjmand et al., 2019; Das et al., 2013; Gumfekar et al., 2017).

Figure 43 revealed that clarification performance improved with larger L (evidenced by lower turbidity results) for all groups where N was constant. This was attributed to the higher M_w when grafting lengths increased (L) (see Table 6). In contrast, low molecular weights resulted in small flocs and a low separation efficiency (higher turbidity) (Onen and Gocer, 2019; Vajihinejad et al., 2019b).

In Figure 43B, D, F, and H, higher N values favored flocculation efficiency for most dosages, i.e., the turbidity decreased with increasing graft-chain number (N). By plotting the AP-g-PMETAC with L equal to 40 and different values of N (1, 2, 3, and 6), this result was better observed (See Figure 51, in Appendix B). It was also observed that for N2, N3, and N6 (Figure 43D, F, and H), the flocculant with larger grafts (larger L) had its optimum dosage shifted to 500 ppm. Lower polymer doses may have been possible because larger grafts enhanced strong bridging effects (Hu et al., 2020). These findings revealed that grafted polymeric flocculants with denser and longer graft chains (higher N and L) aided the approach and adsorption of the suspended particles, favoring flocculation at lower dosages. In addition, the denser graft hypothesis also explains the more expressive effect of higher dosages (above 1500 ppm) on turbidity observed in Figure 43E and G. More graft chains along the AP backbone (larger N) enhance the steric repulsion effect, preventing particles, flocs, and other polymer chains from approaching. At higher polymer dosages, this effect is more pronounced, which explains why flocculants with higher N performed relatively poorly in dewatering the solution.

A further illustration of the flocculation can be seen in the photographs of the volumetric cylinders a few minutes after the flocculants were added (Figure 55 - Appendix B).

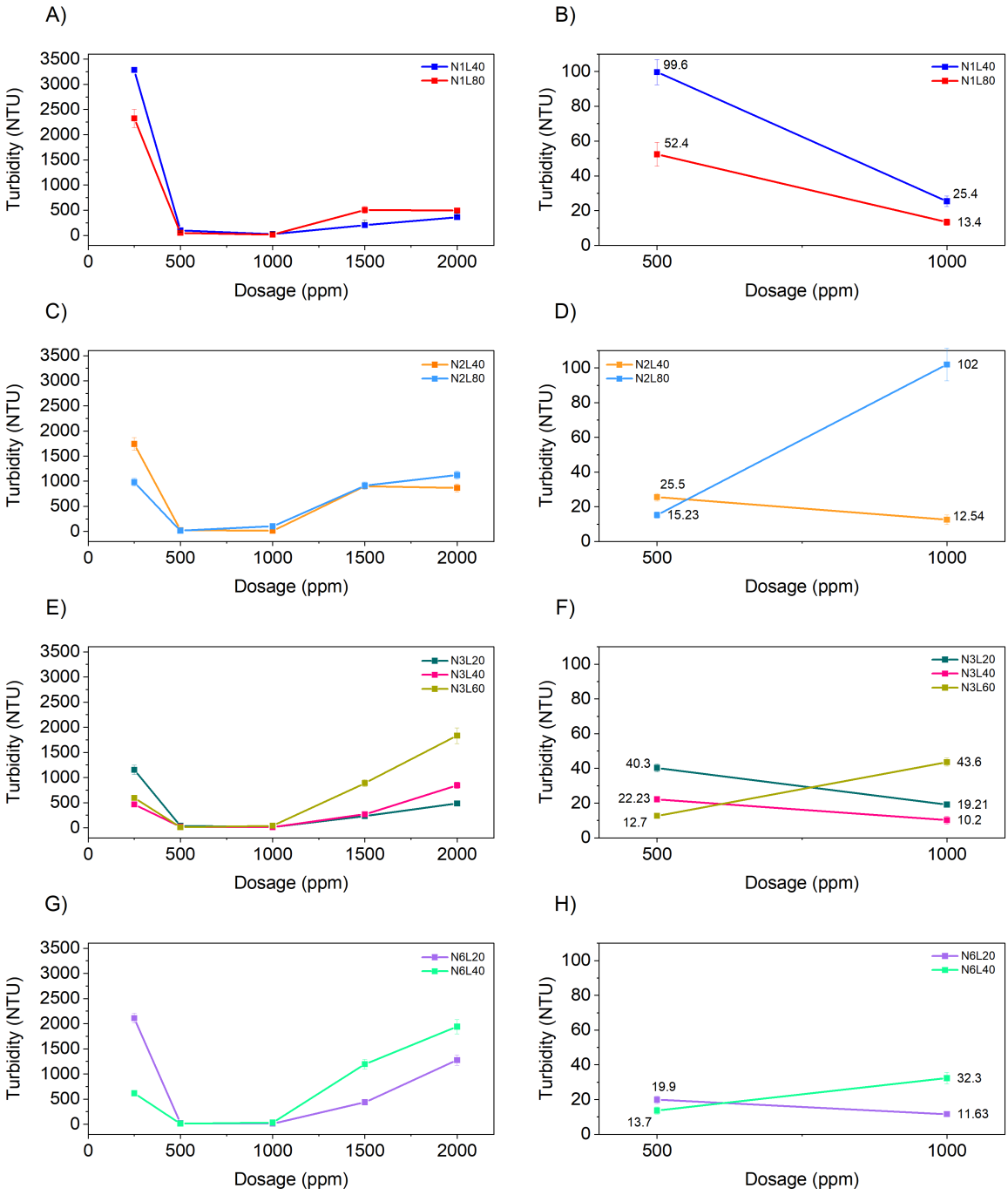

Figure 43 - Supernatant turbidity after 24 hours of flocculation and as a function of polymer dosage. Figures left and right show turbidity for all dosages and the lowest turbidity results at 500 and 1000 ppm, respectively: N1L40 and N1L80 (A-B), N2L40, and N2L80 (C-D), N3L20, N3L40 and N3L60 (E-F) and, N6L20 and N6L40 (G-H).

Effect on solid content

The higher the solids content is, the greater the densification of the sediment, and less water is retained. Figure 44 shows the solid content of the sediment after settling for 24 hours for all the AP-g-PMETAC polymers of each group and at different dosages. The solid content of the thickener underflow stream (≈ 60 wt. %) was used as a reference for our tests.

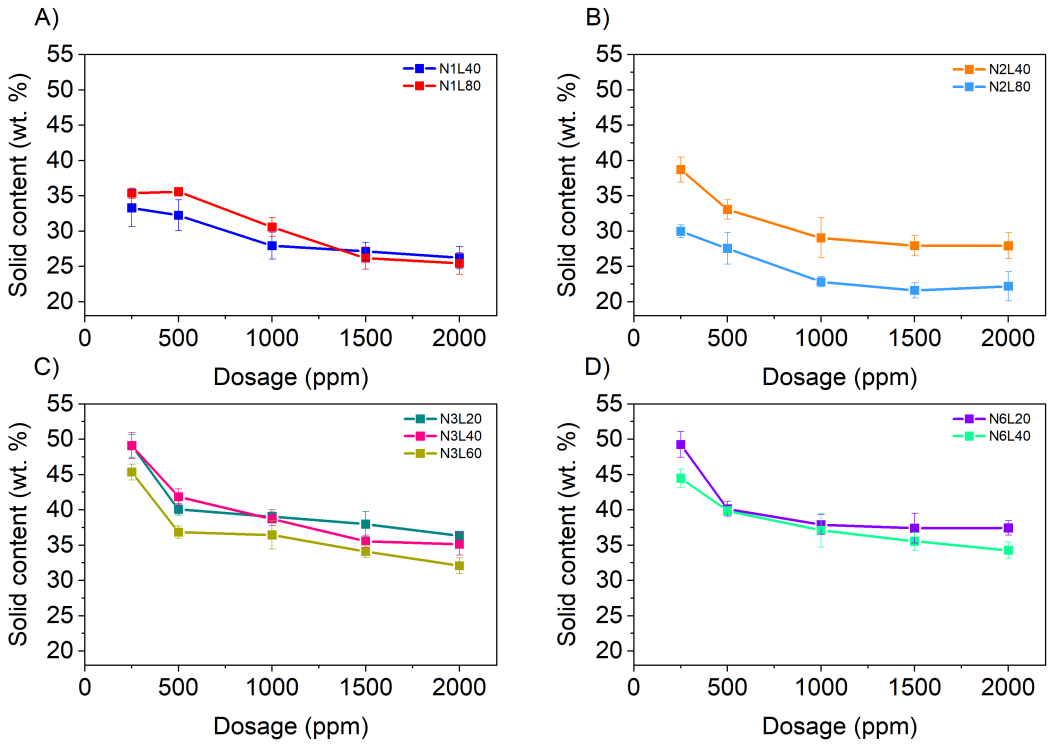

Figure 44 – Solid content (wt. %) after 24 hours of flocculation as a function of dosage and for the polymer: N1L40 and N1L80 (A), N2L40 and N2L80 (B), N3L20, N3L40 and N3L60 (C) and, N6L20 and N6L40 (D).

In Figure 44, for all AP-g-PMETAC polymers, the solid content of the sediment decreased with increasing dosage. Figure 44A shows that N1L80 performed slightly better until 1000 ppm, then retained more water than N1L40 after 1500 ppm. These results were consistent with turbidity shown in Figure 43A, as higher turbidity was observed for N1L80 at higher dosages. This effect is likely because more water tends to be retained for graft copolymers with longer grafts and higher molecular weight, as METAC is a hydrophilic polymer. However, the effect was more pronounced at higher dosages of the flocculant.

Figure 44B, C, and D showed that longer chains (higher L) resulted in sediment with lower solid content in all dosages. The same hindering effect was not observed for turbidity since longer chains enhanced the clarification efficiency (lower turbidity) at low dosages (see

Figure 43). This finding indicated that the AP-g-PMETAC settled suspended particles efficiently at lower dosages; however, the hydrophilic METAC grafts prevented effective sediment dewatering at all dosages.

According to Figure 44C and D, increasing the graft length hindered flocculation efficiency in both cases (lower wt. %). In addition, the denser grafts (higher N) of Figure 44D resulted in higher solids contents at all dosages compared to Figure 44C. The enhancing effect of N was verified when we plotted the AP-g-PMETAC with L equal to 40 (constant) and different values of N (1, 2, 3, and 6), as shown in Figure 52 of the supplementary information (Appendix B). With increasing N, solid content values increased from 1 to 3, while solid content started decreasing with increasing N to 6. It is likely that METAC's hydrophilicity is not dominant when the grafts are smaller and distributed along the AP backbone. Still, there must be a point (possibly for $N > 3$) at which hydrophilicity becomes dominant again. There may be two explanations for these results: shorter grafts allow water molecules to get closer to the amylopectin, which is less hydrophilic than METAC, and higher graft density allows the polymer to form strong bridges with multiple points among the suspended particles, forming more closely packed aggregates.

Effect on initial settling rate

Figure 45 shows the dosage, N, and L effect on the initial settling rate (ISR) of the formed flocs after flocculant addition. Conventional thickeners settle at a low rate when ISR $\leq$ 5 m/h and a high rate when ISR $\geq$ 20 m/h (Pearse, 2003; Witham et al., 2012).

All AP-g-PMETAC copolymers showed a typical ISR behavior of a flocculating polymer and were consistent with the results discussed in Chapter 3. With an optimal flocculant dosage, the ISR reaches a maximum and then declines as the dosage increases. If a particle has about half its surface covered with polymer, other polymer chains can interact with it, facilitating polymer bridges between particles. Polymer dosages below optimum result in insufficient polymer bridging, leading to unlinked particles in suspension supernatants, while doses above optimum cause steric stabilization of particle surfaces, preventing polymer adsorption (Gumfekar et al., 2019; Vajihinejad et al., 2019c).

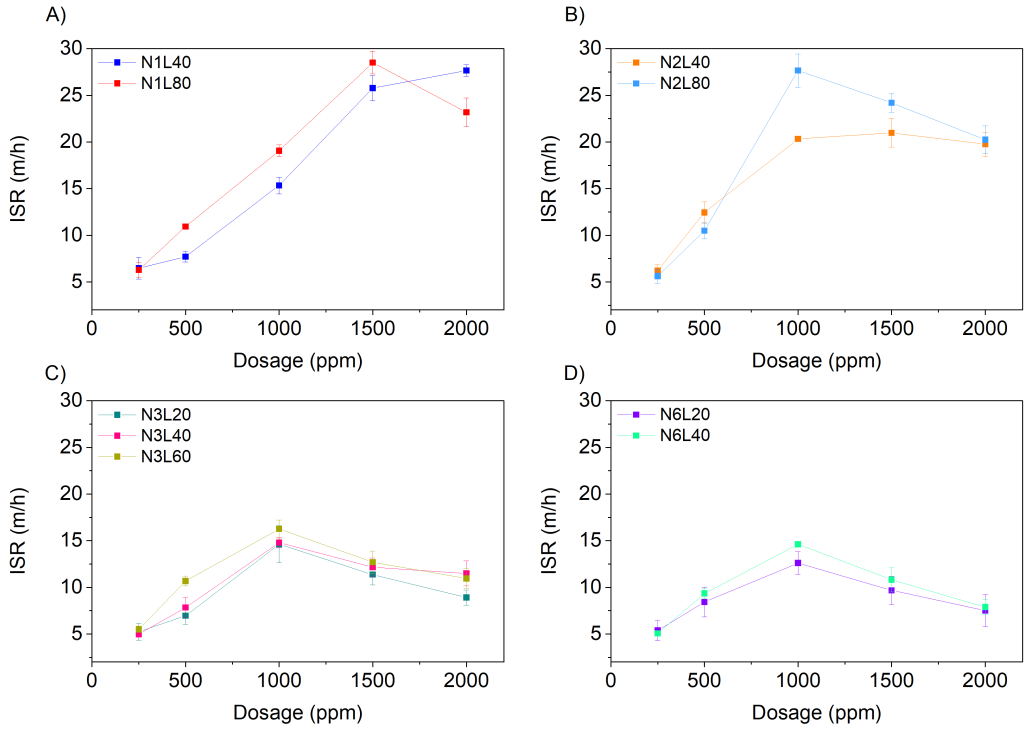

Figure 45 - Initial settling rate (ISR) as a function of dosage and for the polymers: N1L40 and N1L80 (A), N2L40, and N2L80 (B), N3L20, N3L40 and N3L60 (C) and, N6L20 and N6L40 (D).

Figure 45A shows that longer grafts favored the initial settling rate and shifted the optimal dosage (maximum ISR) from 2000 to 1500 ppm. A similar trend was found in Figure 45B, where ISR increased with graft length. These supported our previous observation that the polymers with longer grafts had lower solid content (Figure 44B). Longer grafts produced larger flocs that settled faster and retained more water in concomitance. Furthermore, the increase in molecular weight enhanced the ISR, as discussed in Chapter 3 and elsewhere (Gumfekar et al., 2017; Nguyen and Soares, 2022; Sun et al., 2020).

Figure 45C shows that N2L60, which has a longer chain, had a slightly higher ISR than N3L40 and N3L20. All polymers had the exact optimal dosage of 1000 ppm. Figure 45D shows a similar trend with a higher ISR for longer-chain polymers (N6L40). Both results may be due to the higher M_w when L is increased. However, the effect of L on ISR was more subtle for higher graft-chain numbers. Comparing Figure 45A and B with Figure 45C and D, we observed that ISR decreased for the more grafted copolymer (higher N) at all dosages. The same trend was observed when we plotted the AP-g-PMETAC copolymers with constant L (40) and different values of N (1, 2, 3, and 6), as shown in Figure 53 of the supplementary information (Appendix B). The results are consistent with our hypothesis that stronger bonds between

suspended particles are aided by higher graft density, resulting in smaller and more compact flocs that settle more slowly.

Effect on capillary suction time

Figure 46 shows that the CST decreased with increasing dosage for all AP-g-PMETAC copolymers. In Figure 46A, CST for polymers with longer grafts (N1L80) was slightly lower until 1000 ppm and changed the trend after 1500 ppm. Figures 46B, C, and D showed that the CST was practically the same for all polymer doses in the same group (constant N and different L). In addition, increasing N and keeping L constant did not affect the CST (Figure 54-Appendix B). These results suggested that graft length and number did not affect CST. Thus, we may also observe that the polymers' CSTs didn't change with the increase in molecular weight. A similar result was reported by Vajihinejad et al., (2017), where the molecular weight of the flocculant did not affect the CST. The presence of charge is believed to affect the intermolecular bonds between cationic grafts and water molecules and, therefore, is not capable of affecting sediment dewaterability.

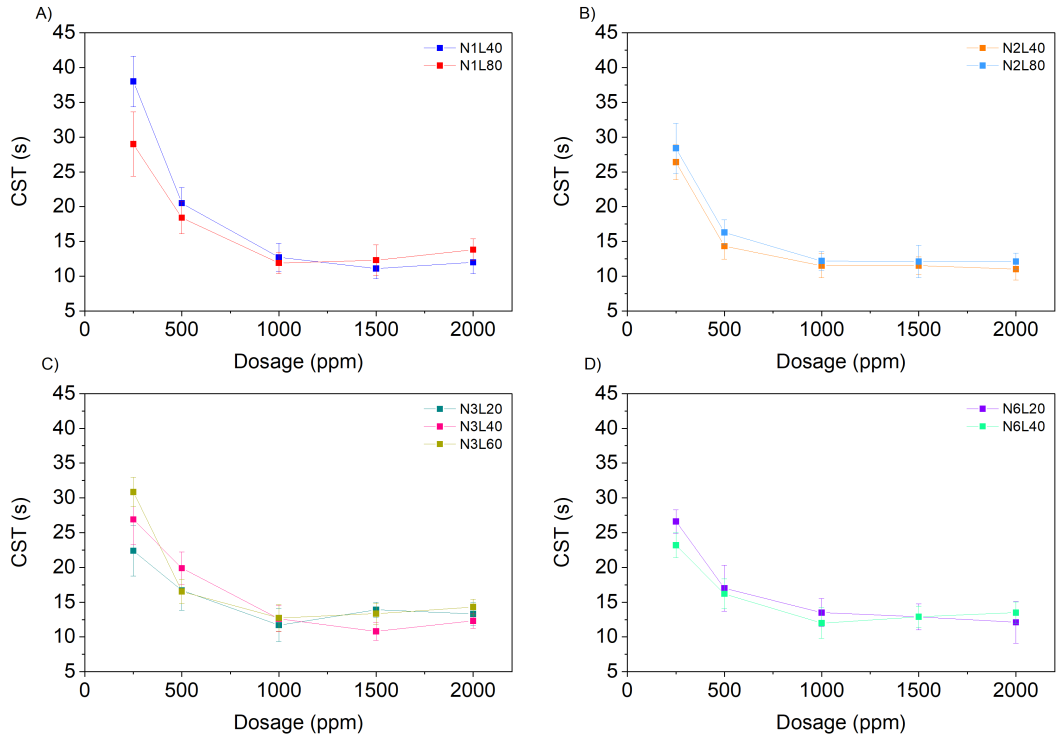

Figure 46 – CST as a function of dosage and for the polymers: N1L40 and N1L80 (A), N2L40 and N2L80 (B), N3L20, N3L40 and N3L60 (C), and N6L20 and N6L40 (D)

4.3.4 Flocculation with PMETAC and AP

In Figure 47, amylopectin and PMETAC are compared regarding flocculation performance.

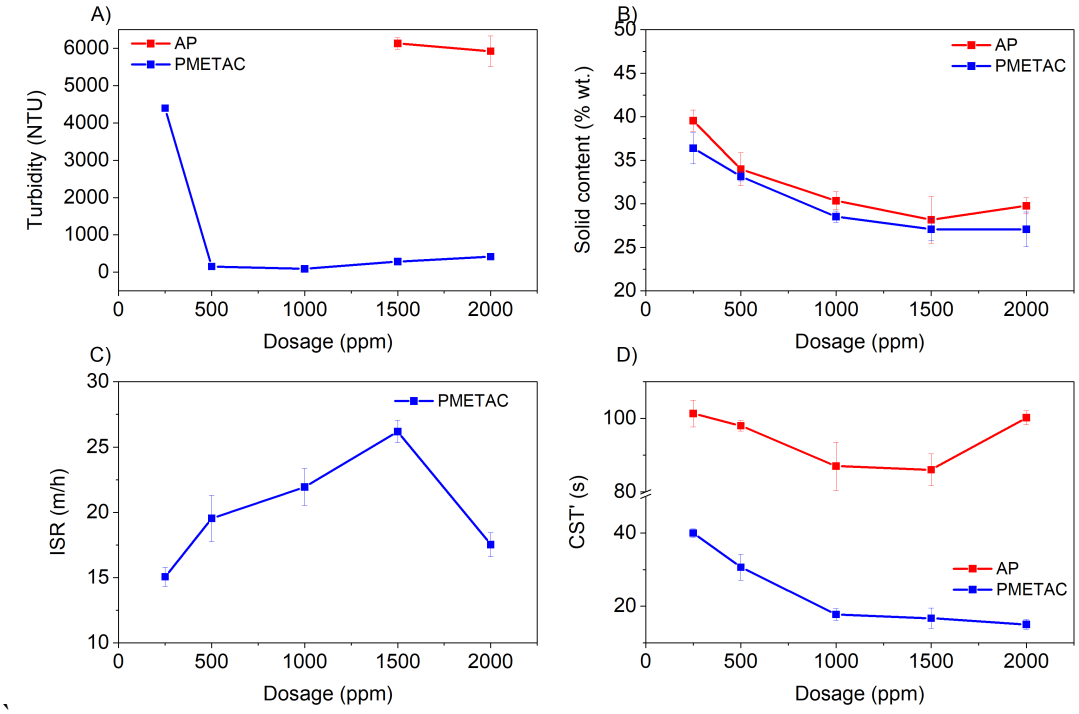

Figure 47 – Results for turbidity (A), solid content (B), ISR (C), and CST (D) for the settling tests using AP and PMETAC as flocculants and in different dosages.

Figure 47A shows the turbidity of the supernatant after flocculation with AP and PMETAC. Turbidity measurements for AP at 250, 500, and 1000 ppm were impossible due to equipment detection limits (10,000 NTU). PMETAC followed the same pattern as AP-g-PMETAC copolymers, where turbidity decreased to the optimal dosage before slightly increasing at higher dosages. PMETAC performed best at 500 and 1000 ppm (lower turbidity), with 153 and 89 NTU, respectively. The lower molecular weight of PMETAC and AP contributed to their inefficiency at separation. The better performance of PMETAC over AP can be attributed to its cationicity, which facilitates the destabilization of negatively charged fine particles.

According to Figure 47B, AP had a slightly higher solid content than PMETAC. The lower solubility of AP in water and the hydrophilicity of PMETAC likely contributed to this result. It is worth noting that PMETAC and AP did not perform better than our best results for

the AP-g-PMETAC with a higher graft-chain number (N) (Figure 44C and D). ISR behavior for PMETAC exhibits a characteristic polymeric flocculant trend, as shown in Figure 47C. Briefly, the ISR increases to the optimal dosage (1500 ppm), followed by a sharp decrease. There was no mudline visible to the naked eye for AP, so the ISR could not be determined. According to Figure 47D, PMETAC sediments had better dewaterability than AP sediments. This might be due to AP's lower molecular weight than PMETAC.

4.3.5 Potential application in mineral tailings treatment

In flocculation processes aiming at tailings treatment, it is desired to obtain a clear supernatant and a densified sediment with minimal water retention. In the previous chapter (Chapter 3), we showed the flocculation performance of two commercial polyacrylamide-based flocculants, widely used in the mineral industry. We concluded that higher molecular weights enhanced the flocculation efficiency, but it was not enough to enable the clarification of the supernatant.

This chapter shows that synthetic monomers can easily be incorporated into the amylopectin backbone to form graft copolymers with high molecular weights (up to 10^7 g/mol). We also demonstrated that grafted chains could be modified in terms of structural parameters (length and number) to improve separation efficiency.

In addition to promoting better clarification of the supernatant, the AP-g-PMETAC copolymers also improved sediment dewaterability. Only 500 ppm of grafted copolymers with higher N allowed the tailings to be clarified to turbidity of 12.7 NTU. It was a remarkable improvement over Commercial PAM, which provided minimum turbidity of 2259 NTU with 1500 ppm added. The dewatering capacity (measured by CST) was also reduced from 130 seconds with PAM to 10.1 seconds with AP-g-PMETAC. The comparison between AP-g-PMETAC and PAM shows that AP-g-PMETAC can provide better performance in the treatment of iron ore tailings than PAM, thereby making it a viable alternative that can therefore be considered a viable alternative to PAM when treating iron ore tailings.

4.4 Conclusions

AP-g-PMETAC flocculants were synthesized and used to treat iron ore tailings suspensions containing 5 wt.% solids. The polymers were fully characterized by TGA, FTIR, NMR, CHNO, and GPC, and the results were compared to those obtained for pure AP or PMETAC.

We showed that graft-chain number (N) and length (L) had a significant effect on the flocculant performance of AP-g-PMETAC as shown by supernatant turbidity, sediment solids content, initial settling rate (ISR), and capillary suction time (CST).

AP-g-PMETAC with denser (higher N) and longer grafts (higher L) performed better at clarification. Low dosages were optimized by these characteristics, which facilitated the suspended particle approach and adsorption. However, for very long grafts, they favored PMETAC's hydrophilic effect on the solid content, resulting in poorer sediment densification. Surprisingly, N and L did not affect CST.

Lower ISRs were associated with denser grafts, and L had no significant effect on ISR. In agreement with our hypothesis, higher graft density facilitates the formation of more bonds between suspended particles, resulting in smaller, more compact flocs that settle more slowly.

AP-g-PMETAC flocculated better than AP and PMETAC due to its higher molecular weight. It was concluded that medium-sized and more distributed grafts resulted in good performances at significantly low dosages, making them an appropriate alternative to flocculating and dewatering iron ore tailings.

Chapter 5

Final considerations and recommendations for future studies.

5.1 Final considerations and contribution to science

The implementation and development of dewatering tailings processes are challenging due to the difficulty of separating fine particles from water. There are no commercially available polymers that can effectively clarify iron ore or other mineral tailings. Therefore, developing polymer flocculants tailored to tailings' specific challenges is crucial for improving dewatering performance and reducing tailings' environmental impact.

To solve this problem, this thesis proposed a natural-based, low-cost, and effective flocculant for iron ore mining treatment. The thesis started by showing that two commercial PAMs with different molecular weights, were unable to clarify supernatant and produce sediment with high solid content and satisfactory dewaterability. In contrast, other polymers designed specifically for oil sand sands performed exceptionally well in flocculating iron ore tailings. Although the sediments with these polymers had low solids contents, these tests revealed that it was possible to develop high-performance polymers compared to the practices in today's industry.

Amylopectin was chosen because it is the major component of starch, a natural material abundant and inexpensive. In addition to providing good clarification results at relatively low dosages, the AP-g-PMETAC copolymers also performed well in terms of supernatant dewatering capacity and initial settling rate, but not so well for sediment densification. A possible solution for this constraint was addressed in the recommendation for future studies.

Although there is still much work to be done, the findings of this work have provided a springboard for future work. Continuity of the work would encompass not just flocculation tests

with other real systems, but also more detailed studies of polymerization mechanisms, as well as mathematical models that describe polymerization by grafting. Even though this study did not focus on mathematical modeling, it deserves to mention that the literature lacks work involving grafting polymerization with natural polymers.

There have been already been some tests conducted, but they are still in the early stages and won't be addressed in this thesis. The first aim is to explore how radicals formed by KPS decomposition attack the amylopectin backbone. Second, METAC is grafted onto the backbone of chitosan. Since amino groups on the backbone of chitosan are protonated, it has a cationic nature, making it a promising natural flocculant.

In conclusion, despite still needing to make significant progress, this thesis has demonstrated the possibility of tailoring flocculants for mineral tailings treatment, as well as achieving significant environmental, economic, and social benefits.

5.2 Future studies

As a result of some questions that emerged during the development of this thesis, we recommend further investigation in several areas:

- **Is grafting possible in all hydroxyl groups of the AGU unit of the amylopectin backbone?**

In most literature, it has been reported that for free radical polymerization with KPS or APS as initiator, the radical attacks only the methyl hydroxyl group (Chen et al., 2016; Kalia and Sabaa, 2013; Pal and Pal, 2012; Salehizadeh et al., 2018; Sarkar et al., 2013; Wang et al., 2013), as illustrated in red in Figure 48.

Based on the characterization of the synthesized AP-g-PMETAC in this work, the initiator attack may have also occurred on the other hydroxyls, allowing for the possible formation of three reactive sites per monomeric unit (AGU) of amylopectin. Nevertheless, this hypothesis could not be validated by only the characterizations performed in these works. Considering this, the study of the grafting mechanism is likely to contribute to more accurate calculations and mathematical modeling of structural parameters such as distribution and length of the grafts.

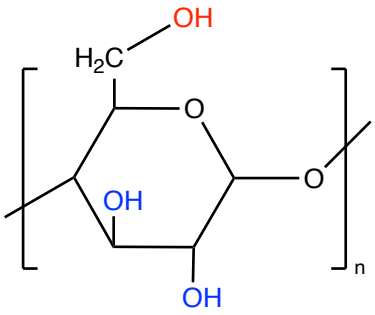

Figure 48 – Amylopectin's hydroxyl groups.

- **The natural polymer backbone is attacked by adding the initiator for a few minutes before the monomer. What is the mechanism and effect of this attack?**

Free radical grafting copolymerization in natural polymers as backbones involves three main steps: 1) dissolution of the natural polymer; 2) addition of the initiator for 10 to 20 minutes; 3) addition of the comonomer to be incorporated into the backbone.

Literature consensus suggests that the initiator is added in the second stage to attack the polymer's backbone and form active sites (generally through hydrogen transfer) for the subsequent reaction with the vinylic group of the comonomer, thus causing the growth of the grafts. Even though this methodology is widely used and adopted in studies on this subject, there are not enough studies in the literature that prove its effectiveness or necessity. Due to their instability and high reactivity, free radicals may not last long enough for the monomer to be added to the medium. The questioning about the method leads us to suggest a study to evaluate the relationship between time and graft parameters, as well as radical attack mechanisms.

- **With AP-g-METAC, could sediments formed in flocculation be densified more effectively?**

By grafting METAC monomers to amylopectin, this study demonstrated a significant improvement in flocculation efficiency over commercial polyacrylamides. In contrast, the hydrophilic properties of METAC overcame the hydrophobic characteristics of amylopectin, resulting in the retention of considerable amounts of water in sediments. To overcome this constraint, hydrophobic comonomers can be incorporated into graft chains. Here, we suggest studying different reaction ratios of METAC and different hydrophobic monomers to determine a tailor-made reaction pathway that provides the best flocculation performance.

- **Can the results be reproduced on a larger scale?**

All flocculation tests in this study were conducted on a laboratory scale using 100 mL volumetric cylinders. Consequently, we suggest that the next step in this research would be to replicate the optimum dosages on a pilot and industrial scale to determine the process' scalability and feasibility.

To scale-up, in general, large investments are required in characterization and monitoring techniques. One solution would be to develop a mathematical model that accounts for operating conditions such as water composition, particle distribution, flocculant dosage, thickener dimensions, and solids content. Applied to large scales, these models could potentially predict results and justify the investment in experiments to validate the model.

- **Does the clarified supernatant have the potential to be reused in iron ore beneficiation?**

It was not possible to discuss whether the clarified supernatant could be reused in the beneficiation process or disposed of in water bodies in this study because the clarified supernatant was not characterized. Characterization of the synthesized polymers would complement the results that suggest the polymers have good performance, thus contributing to the study. Additionally, by knowing the chemical species that remain in the solution, modifications in the polymer can be proposed to attribute affinity between these species.

Appendix A. Supplementary information for Chapter 3

A.1 Turbiscan results for iron ore tailings without flocculants

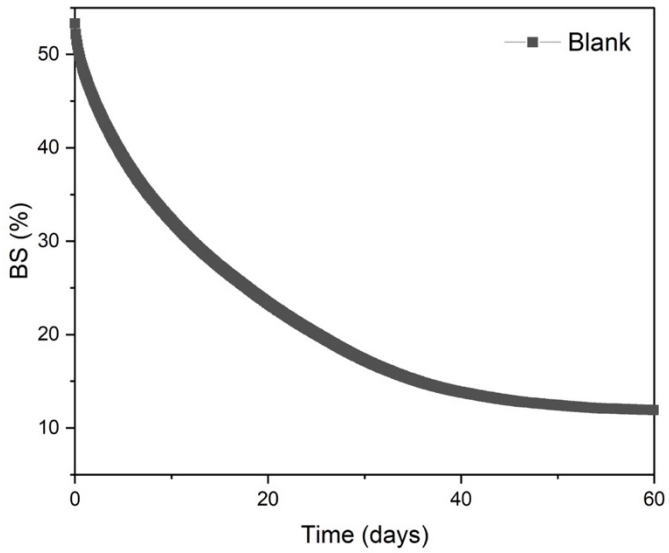

Figure 49 - Backscattering (%) for the colloidal suspension monitored for 60 days

Appendix B. Supplementary information for Chapter 4

B.1 Validation of the purification protocol

Using a mixture of AP and PMETAC, we validated if the Soxhlet extraction with ethanol could remove the PMETAC homopolymers formed during the AP-g-PMETAC synthesis. We added 1.5 g of AP and 75 mL of DI water to the same experimental setup for the polymerization reaction and heated it at 90oC for 1 hour to gelatinize it. In the next step, the suspension was cooled to 70ºC, and PMETAC homopolymer was added at 9 grams. After stirring for 15 minutes, the mixture was cooled to room temperature and dried in a freeze dryer. After that, a 3 g sample was extracted with Soxhlet for 72 hours. Using an elemental analyzer from CHNS, nitrogen content was quantified after 6, 24, 48, and 72 hours. Due to the absence of nitrogen in the AP molecule, N can be used to determine PMETAC concentration in a sample. The nitrogen content is different times are shown in Figure 50

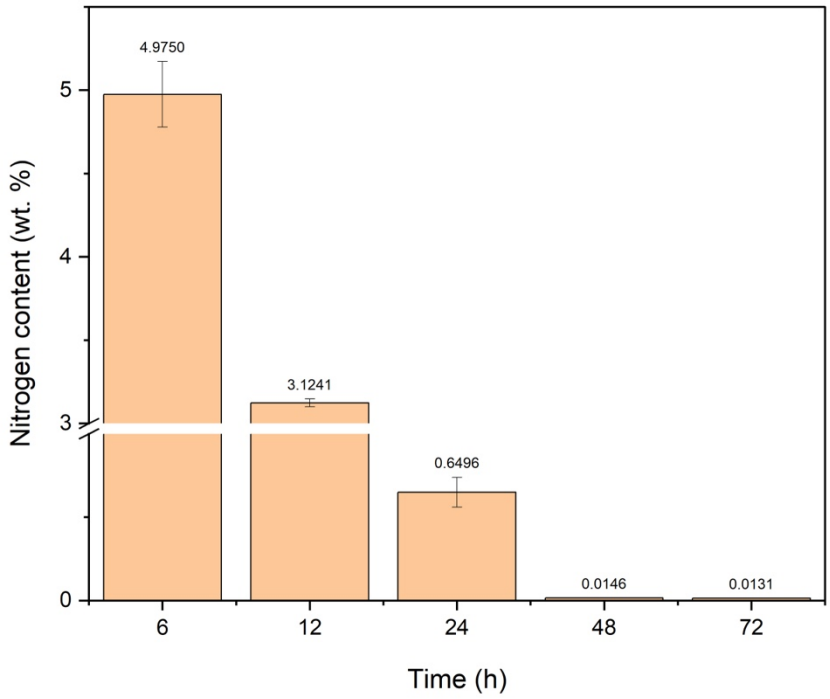

Figure 50 - Nitrogen content of the samples taken from Soxhlet purification at different times.

B.2 Effect of graft-chain length (L) constant and different graft-chain number (N):

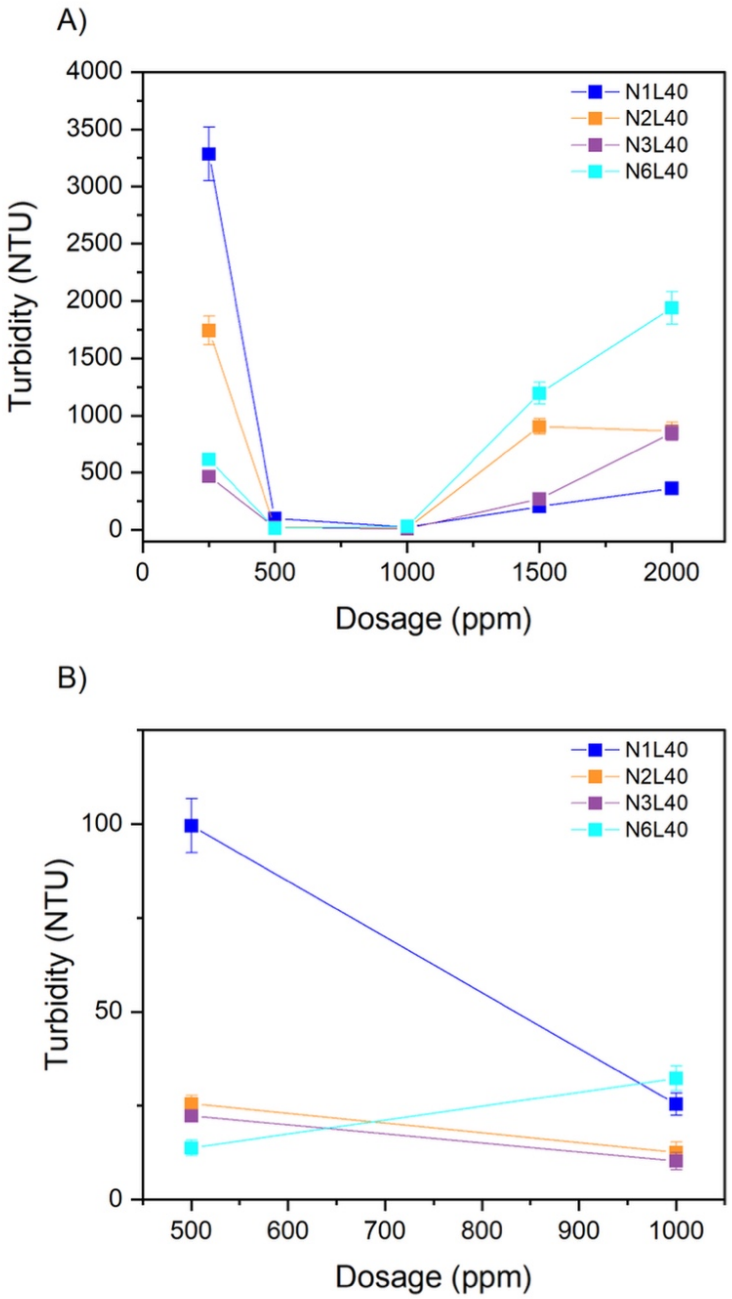

Figure 51 - Supernatant turbidity after 24 hours of flocculation and as a function of polymer dosage for AP-g-PMETAC with graft-chain length (L) constant and graft-chain number (N) varying at 1, 2, 3, and 6.

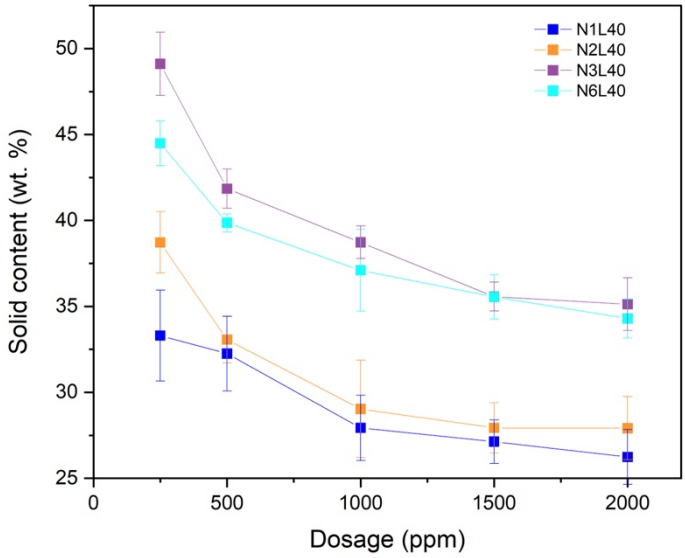

Figure 52 - Solid content (wt. %) after 24 hours of flocculation as a function of dosage for AP-g-PMETAC with graft-chain length (L) constant and graft-chain number (N) varying at 1, 2, 3, and 6: N1L40 N2L40, N3L40 and N6L40.

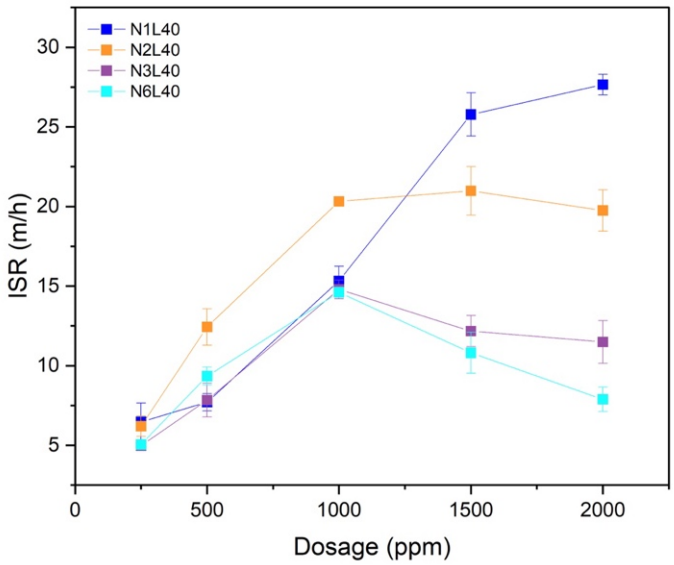

Figure 53 - Initial settling rate (ISR) as a function of dosage for AP-g-PMETAC with graft-chain length (L) constant and graft-chain number (N) varying at 1, 2, 3, and 6: N1L40 N2L40, N3L40 and N6L40.

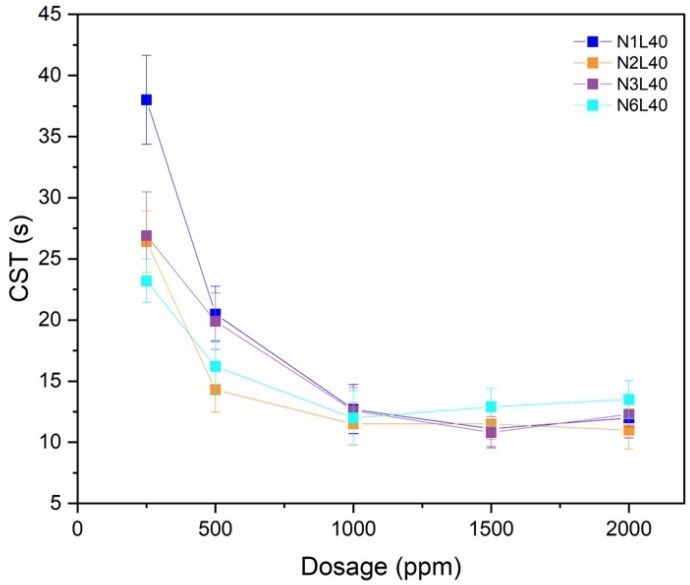

Figure 54 – Capillary suction time (CST) as a function of dosage for AP-g-PMETAC with graft-chain length (L) constant and graft-chain number (N) varying at 1, 2, 3, and 6: N1L40 N2L40, N3L40 and N6L40.

B.3 Flocculation cylinders at different flocculant dosages

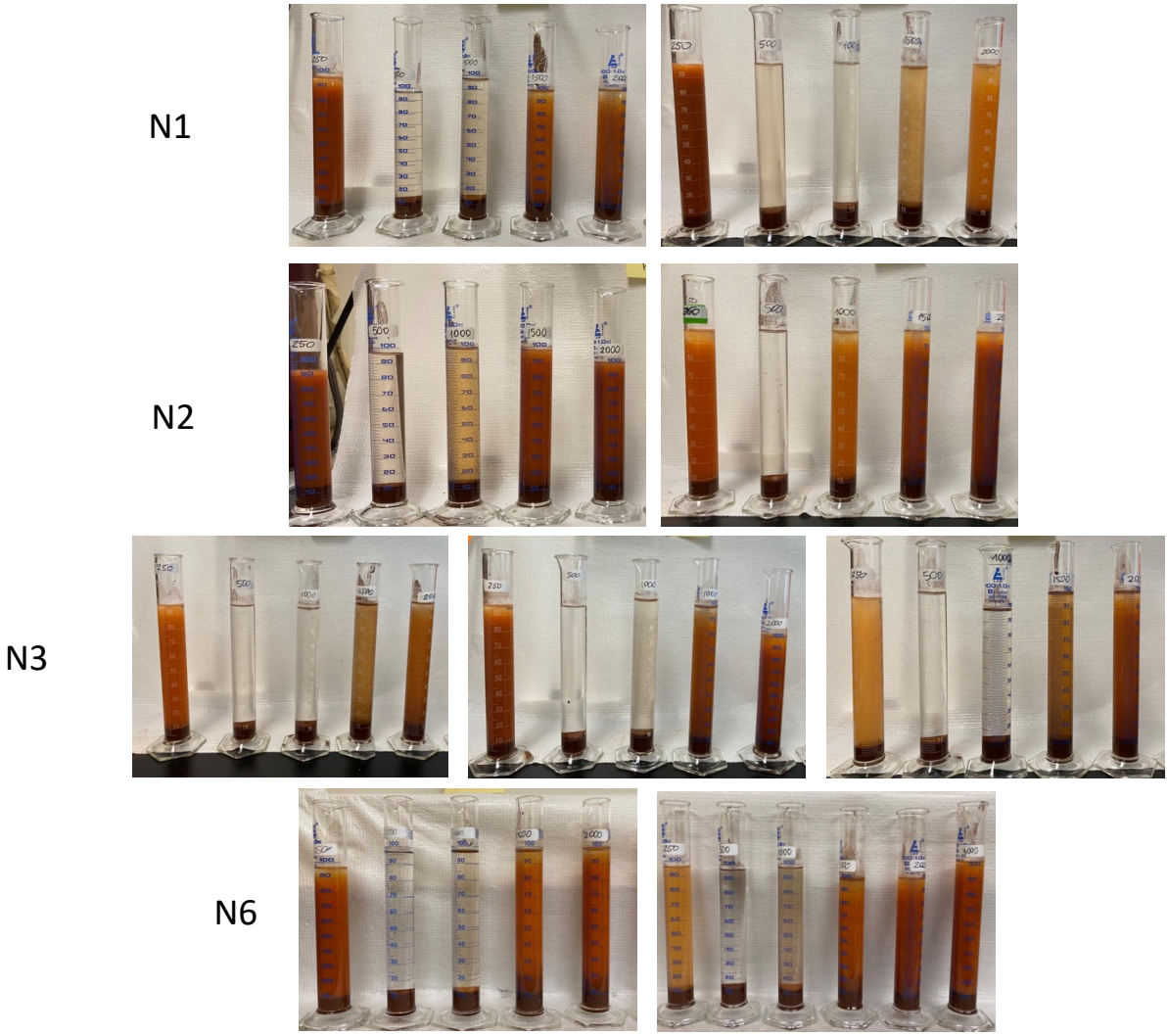

Figure 55 - Photographs of flocculation experiments using different dosages of AP-g-PMETAC.

Bibliography

A. Vidyadhar, N.K.& R.P.B., 2014. Adsorption Mechanism of Mixed Cationic/AnionicCollectors in Quartz–Hematite Flotation System. Miner. Process. Extr. Metall. Rev. 35, 117–125.

Abbasi Moud, A., 2022. Polymer based flocculants: Review of water purification applications. J. Water Process Eng. 48, 102938. https://doi.org/10.1016/j.jwpe.2022.102938

Abdollahi, Z., Frounchi, M., Dadbin, S., 2011. Synthesis, characterization and comparison of PAM, cationic PDMC and P(AM-co-DMC) based on solution polymerization. J. Ind. Eng. Chem. 17, 580–586. https://doi.org/10.1016/j.jiec.2010.10.030

Abu-Zreig, M., Al-Sharif, M., Amayreh, J., 2007. Erosion control of arid land in Jordan with two anionic polyacrylamides. Arid L. Res. Manag. 21, 315–328. https://doi.org/10.1080/15324980701603557

Addai-Mensah, J., Ralston, J., 2004. Interfacial chemistry and particle interactions and their impact upon the dewatering behaviour of iron oxide dispersions. Hydrometallurgy 74, 221–231. https://doi.org/10.1016/j.hydromet.2004.05.002

Adiansyah, J.S., Rosano, M., Vink, S., Keir, G., 2015. A framework for a sustainable approach to mine tailings management: Disposal strategies. J. Clean. Prod. 108, 1–13. https://doi.org/10.1016/j.jclepro.2015.07.139

Andrade, L.C.R., 2014. Caracterização de rejeitos de mineração de ferro, in natura e segregados, para aplicação como material de construção civil. Tese Doutorado. https://doi.org/10.1017/CBO9781107415324.004

Araujo, C.B. de, 2006. CONTRIBUIÇÃO AO ESTUDO DO COMPORTAMENTO DE BARRAGENS DE REJEITO DE MINERAÇÃO DE FERRO. COPPE/UFRJ.

ARINGHIERI, R., PARDINI, G., 1983. INTERACTIONS BETWEEN OH− IONS AND SOIL SURFACES: A KINETIC STUDY. Can. J. Soil Sci. 63, 741–748. https://doi.org/10.4141/cjss83-075

Arjmand, R., Massinaei, M., Behnamfard, A., 2019. Improving flocculation and dewatering performance of iron tailings thickeners. J. Water Process Eng. 31, 100873. https://doi.org/10.1016/j.jwpe.2019.100873

Asare, E., Reis, L.G., Lucas, E.F., Spinelli, L.S., Palhares, T.N., Oliveira, R.S., Soares, J.B.P., Vedoy, D.R.L., 2016. Using acrylamide/propylene oxide copolymers to dewater and densify mature fine tailings. Miner. Eng. 95, 29–39. https://doi.org/10.1016/j.mineng.2016.06.005

Azam, S., Imran, S.A., 2008. A statistical model for Slurry Thickening, in: International Association for Computer Methods and Advances in Geomechanics. Goa, India, pp. 303–307. https://doi.org/10.1109/ISQED.2000.838852

Bahmani-Ghaedi, A., Hassanzadeh, A., Sam, A., Entezari-Zarandi, A., 2022. The effect of residual flocculants in the circulating water on dewatering of Gol-e-Gohar iron ore. Miner. Eng. 179, 107440. https://doi.org/10.1016/j.mineng.2022.107440

Bazoubandi, B., 2018. Synthesis and Characterization of Amylopectin-grafted Polyacrylamide (AP-g-PAM) Flocculants for Dewatering of Oil Sands Mature Fine Tailings (MFT). https://doi.org/10.7939/R3348GX41

Bazoubandi, B., Soares, J.B.P., 2020. Amylopectin-graft-polyacrylamide for the flocculation and dewatering of oil sands tailings. Miner. Eng. 148, 106196. https://doi.org/10.1016/j.mineng.2020.106196

Besra, L., Prasad, A.R., 2007. Coagulation and Flocculation Study of Iron Ore Fines 6395.

Birdi, K.S., 2008. Handbook of Surface and Colloid Chemistry. CRC Press.

Bolto, B., Gregory, J., 2007. Organic polyelectrolytes in water treatment. Water Res. 41, 2301–2324. https://doi.org/https://doi.org/10.1016/j.watres.2007.03.012

Botha, L., Davey, S., Swarnakar, A.K., Soares, J.B.P., Nguyen, B., Rivard, E., 2017. Flocculation of oil sands tailings by hyperbranched functionalized polyethylenes (HB f PE). Miner. Eng. 108, 71–82. https://doi.org/10.1016/j.mineng.2017.02.004

Botha, L., Soares, J.B.P., 2015. The In fl uence of Tailings Composition on Flocculation 93, 1514–1523. https://doi.org/10.1002/cjce.22241

Bowker, L.N., Chambers, D.M., 2015. The risk, public liability & economics of tailings storage facility failures. Cent. Sci. PUBLIC Particip. 1–56.

Bratskaya, S., Schwarz, S., Chervonetsky, D., 2004. Comparative study of humic acids flocculation with chitosan hydrochloride and chitosan glutamate. Water Res. 38, 2955–2961. https://doi.org/10.1016/j.watres.2004.03.033

Carlson, J.J., Kawatra, S.K., 2013. Factors affecting zeta potential of iron oxides. Miner. Process. Extr. Metall. Rev. 34, 269–303. https://doi.org/10.1080/08827508.2011.604697

Chang, L., Wang, F., Guo, Y., Li, J., Gong, Y., Shi, Q., 2021. Green Preparation of Thermochromic Starch-Based Fibers through a Wet-Spinning Process. ACS Appl. Polym. Mater. https://doi.org/10.1021/acsapm.0c01194

Chaturvedi, N., Patra, H.K., 2016. Iron Ore Mining , Waste Generation , Environmental Problems and Their Mitigation through Phytoremediation Technology. Int. J. Sci. Res.

Methodol. 5, 397–420.

Chaves, A.P., 2002. Teoria e Prática do Tratamento de Minérios - Desaguamento, Espessamento e Filtragem, 2nd ed. SIGNUS Editora, São Paulo.

Chen, Q., Yu, H., Wang, L., Abdin, Z. ul, Yang, X., Wang, J., Zhou, W., Zhang, H., Chen, X., 2016. Synthesis and characterization of amylose grafted poly(acrylic acid) and its application in ammonia adsorption. Carbohydr. Polym. 153, 429–434. https://doi.org/10.1016/j.carbpol.2016.07.120

Chen, X., Si, C., Fatehi, P., 2018. Cationic xylan- (2-methacryloyloxyethyl trimethyl ammonium chloride) polymer as a flocculant for pulping wastewater. Carbohydr. Polym. 186, 358–366. https://doi.org/10.1016/j.carbpol.2018.01.068

Cobbledick, J., Zhang, V., Rollings-Scattergood, S., Latulippe, D.R., 2017. Investigation of the role of flocculation conditions in recuperative thickening on dewatering performance and biogas production. Environ. Technol. (United Kingdom) 38, 2650–2660. https://doi.org/10.1080/09593330.2016.1272639

Concha, F., 2014. Solid-Liquid Separation in the Mining Industry, 1st ed. Springer International Publishing. https://doi.org/10.1007/978-3-319-02484-4

Cornell, R.M., Schwertmann, U., 2003. Surface Chemistry and Colloidal Stability, The Iron Oxides. https://doi.org/10.1002/3527602097.ch10

Cox, M., 2006. A Guide Book on the Treatment of Effluents from the minning/metallurgy/paper/platine/textile.

Crowson, P., 2012. Some observations on copper yields and ore grades. Resour. Policy 37, 59–72. https://doi.org/10.1016/J.RESOURPOL.2011.12.004

Das, R., Choudhury, I., 2013. Waste Management in Mining Industry. Indian J. Sci. Res. 4, 139–142.

Das, R., Ghorai, S., Pal, S., 2013. Flocculation characteristics of polyacrylamide grafted hydroxypropyl methyl cellulose: An efficient biodegradable flocculant. Chem. Eng. J. 229, 144–152. https://doi.org/10.1016/j.cej.2013.05.104

Das, S., Patra, P., Singha, K., Biswas, P., Sarkar, S., Pal, S., 2019. Graft copolymeric flocculant using functionalized starch towards treatment of blast furnace effluent. Int. J. Biol. Macromol. https://doi.org/10.1016/j.ijbiomac.2018.12.026

Dash, M, Dwari, R.K., Biswal, S.K., Reddy, P.S.R., Chattopadhyay, P., Mishra, B.K., 2011. Studies on the effect of flocculant adsorption on the dewatering of iron ore tailings. Chem. Eng. J. 173, 318–325. https://doi.org/10.1016/j.cej.2011.07.034

Dash, M., Dwari, R.K., Biswal, S.K., Reddy, P.S.R.R., Chattopadhyay, P., Mishra, B.K., 2011. Studies on the effect of flocculant adsorption on the dewatering of iron ore tailings. Chem. Eng. J. 173, 318–325. https://doi.org/10.1016/j.cej.2011.07.034

Davey, S., Soares, J.B.P., 2022. Amylopectin graft copolymers for oil sands tailings treatment. Can. J. Chem. Eng. 100, 731–751. https://doi.org/10.1002/cjce.24290

Davey, S., Soares, J.B.P., 2021. Amylopectin graft copolymers for oil sands tailings treatment. Can. J. Chem. Eng. 1–21. https://doi.org/10.1002/cjce.24290

Dentel, S.K., Abu-Orf, M.M., Walker, C.A., 2000. Optimization of slurry flocculation and dewatering based on electrokinetic and rheological phenomena. Chem. Eng. J. 80, 65–72. https://doi.org/10.1016/S1383-5866(00)00078-2

Dragunski, D.C., Pawlicka, A., 2001. Preparation and characterization of starch grafted with toluene poly (propylene oxide) diisocyanate. Mater. Res. 4, 77–81. https://doi.org/10.1590/s1516-14392001000200006

Dubey, A., Patra, A.S., Sarkar, A.N., Basu, A., Tripathy, S.K., Mukherjee, A.K., Bhatnagar, A., 2021. Synthesis of a copolymeric system and its flocculation performance for iron ore tailings. Miner. Eng. 165, 106848. https://doi.org/10.1016/j.mineng.2021.106848

Edraki, M., Baumgartl, T., Manlapig, E., Bradshaw, D., Franks, D.M., Moran, C.J., 2014. Designing mine tailings for better environmental, social and economic outcomes: A review of alternative approaches. J. Clean. Prod. 84, 411–420. https://doi.org/10.1016/j.jclepro.2014.04.079

Eisele, T.C., Kawatra, S.K., Ripke, S.J., 2005. Water chemistry effects in iron ore concentrate agglomeration feed. Miner. Process. Extr. Metall. Rev. 26, 295–305. https://doi.org/10.1080/08827500590944063

Elzbieta Czarnecka, Nowaczyk, J., 2020. Semi-Natural Superabsorbents Based on Starch-g-poly(acrylic acid): Modification, Synthesis and Application. Polymers (Basel). 12, 1794.

Espósito, T.J., 2000. Metodologia probabilística e observacional aplicada a barragens de rejeito construídas por aterro hidráulico. Tese Doutorado.

Fan, A., Turro, N.J., Somasundaran, P., 2000. A study of dual polymer flocculation. Colloids Surfaces A Physicochem. Eng. Asp. 162, 141–148. https://doi.org/10.1016/S0927-7757(99)00252-6

Fan, Y., Migliore, N., Raffa, P., Bose, R.K., Picchioni, F., 2019. Synthesis of zwitterionic copolymers via copper-mediated aqueous living radical grafting polymerization on starch. Polymers (Basel). 11, 2–7. https://doi.org/10.3390/polym11020192

Fang, R., Cheng, X.-S., Fu, J., Zheng, Z.-B., 2009. Research on the Graft Copolymerization of EH-lignin with acrylamide. Nat. Sci. 01, 17–22. https://doi.org/10.4236/ns.2009.11004

Flory, P.J., 1953. Principles of Polymer Chemistry, Principles of polymer chemistry. https://doi.org/10.1021/ja01639a090

Formulaction, 2019. Turbiscan Stability Scale-The stability criteria and correlation to visual observation. Toulouse, France.

Galeša, K., Bren, U., Kranjc, A., Mavri, J., 2008. Carcinogenicity of acrylamide: A computational study. J. Agric. Food Chem. 56, 8720–8727. https://doi.org/10.1021/jf800965y

Gidley, M.J., 1985. Quantification of the structural features of starch polysacch. Carbohydr. Res. 139, 85–93.

Gomes, M.A., Pereira, C.A., Peres, A.E.C., 2011. Caracterização tecnológica de rejeito de minério de ferro. Rem Rev. Esc. Minas. https://doi.org/10.1590/S0370-44672011000200016

Grasso*, D., Subramaniam, K., Butkus, M., Strevett, K., Bergendahl, J., 2002. A review of non-DLVO interactions in environmental colloidal systems. Rev. Environ. Sci. Biotechnol. 1, 17–38. https://doi.org/10.1023/A:1015146710500

Gregory, J., O'Melia, C.R., 1989. Fundamentals of flocculation. Crit. Rev. Environ. Control 19, 185–230. https://doi.org/10.1080/10643388909388365

Grilo, C.F., Chassagne, C., Quaresma, V. da S., van Kan, P.J.M., Bastos, A.C., 2020. The role of charge reversal of iron ore tailing sludge on the flocculation tendency of sediments in marine environment. Appl. Geochemistry 117, 104606. https://doi.org/10.1016/j.apgeochem.2020.104606

Guimarães, N.C., 2011. Filtragem de rejeitos de minério de ferro visando a sua disposição em pilhas. UFMG.

Gumfekar, S.P., Rooney, T.R., Hutchinson, R.A., Soares, J.B.P., 2017. Dewatering Oil Sands Tailings with Degradable Polymer Flocculants. ACS Appl. Mater. Interfaces 9, 36290–36300. https://doi.org/10.1021/acsami.7b10302

Gumfekar, S.P., Soares, J.B.P., 2018. Polymer reaction engineering tools to design multifunctional polymer flocculants. Chemosphere 210, 156–165. https://doi.org/10.1016/j.chemosphere.2018.06.175

Gumfekar, S.P., Vajihinejad, V., Soares, J.B.P., 2019. Advanced Polymer Flocculants for Solid–Liquid Separation in Oil Sands Tailings. Macromol. Rapid Commun. 40, 1–18. https://doi.org/10.1002/marc.201800644

Gunson, A.J., Klein, B., Veiga, M., Dunbar, S., 2012. Reducing mine water requirements. J. Clean. Prod. 21, 71–82. https://doi.org/10.1016/j.jclepro.2011.08.020

Guo, K., Gao, B., Pan, J., Shen, X., Liu, C., Yue, Q., Xu, X., 2020. Effects of charge density and molecular weight of papermaking sludge-based flocculant on its decolorization efficiencies. Sci. Total Environ. 723, 138136. https://doi.org/10.1016/j.scitotenv.2020.138136

Hiemenz, P.C., Rajagopalan, R., 1997. Principles of Colloid and Surface Chemistry, 3rd ed. CRC Press.

Ho, C.C., Lee, K.C., 1998. The role of metallic cations on the colloidal stability of tin tailings slurries. Colloids Surfaces A Physicochem. Eng. Asp. 141, 19–27. https://doi.org/10.1016/S0927-7757(98)00200-3

Hogg, R., 2000. Flocculation and dewatering. Int. J. Miner. Process. 58, 223–236. https://doi.org/10.1016/S0301-7516(99)00023-X

Hu, P., Xi, Z., Li, Y., Li, A., Yang, H., 2020. Evaluation of the structural factors for the flocculation performance of a co-graft cationic starch-based flocculant. Chemosphere 240, 124866. https://doi.org/10.1016/j.chemosphere.2019.124866

Hu, P., Zhuang, S., Shen, S., Yang, Y., Yang, H., 2021. Dewaterability of sewage sludge conditioned with a graft cationic starch-based flocculant: Role of structural characteristics of flocculant. Water Res. 189, 116578. https://doi.org/10.1016/j.watres.2020.116578

Huang, M., Liu, Z., Li, A., Yang, H., 2017. Dual functionality of a graft starch flocculant: Flocculation and antibacterial performance. J. Environ. Manage. 196, 63–71. https://doi.org/10.1016/j.jenvman.2017.02.078

IBRAM, 2021. Infografico: Mineracao em números 2021, Infografico: Mineração em números 2021.

Ihle, C.F., Kracht, W., 2018. The relevance of water recirculation in large scale mineral processing plants with a remote water supply. J. Clean. Prod. 177, 34–51. https://doi.org/10.1016/j.jclepro.2017.12.219

ISO, 2017. Geotechnical Investigation and Testing – Identification and Classification of Soil – Part 1: Identification and Description., ISO 14688-1:2017.

Israelachvili, J.N.B.T.-I. and S.F. (Third E. (Ed.), 2011. Intermolecular and Surface Forces. Academic Press, Boston. https://doi.org/https://doi.org/10.1016/B978-0-12-391927-4.10024-6

Jacob H. Masliyah, J.C. and Z.X., 2011. Handbook on Theory and Practice on Bitumen Recovery from Athabasca Oil Sands. Kingsley Knowledge Publishing.

Ji, Y., 2013. Fundamental Understanding of the Flocculation of Mineral Tailings in High Salinity Water.

Jones, H., Boger, D. V., 2012. Sustainability and waste management in the resource industries. Ind. Eng. Chem. Res. 51, 10057–10065. https://doi.org/10.1021/ie202963z

Kalia, S., Sabaa, M.W., 2013. Polysaccharide based graft copolymers, Polysaccharide Based Graft Copolymers. https://doi.org/10.1007/978-3-642-36566-9

Kanungo, S.B., 2005. Effect of some commercial flocculating agents on settling and filtration rates of low grade, fragile manganese ores of Andhra Pradesh. Indian J. Chem. Technol. 12, 550–558.

Keng, J.C.-W., 1974. Surface Chemistry of Some Constant Potential Soil Colloids. UNIVERSITY OF HAWAI.

Kim, H., Lee, B.S., Lee, Y., Lee, J.K., Choi, I.S., 2019. Solid-phase extraction of nerve agent degradation products using poly[(2-(methacryloyloxy)ethyl)trimethylammonium chloride] thin films. Talanta 197, 500–508. https://doi.org/10.1016/J.TALANTA.2019.01.048

Kinnunen, P., Ismailov, A., Solismaa, S., Sreenivasan, H., Räisänen, M.L., Levänen, E., Illikainen, M., 2018. Recycling mine tailings in chemically bonded ceramics – A review. J. Clean. Prod. 174, 634–649. https://doi.org/10.1016/j.jclepro.2017.10.280

Kobayashi, M., Terada, M., Terayama, Y., Kikuchi, M., Takahara, A., 2010. Direct synthesis of well-defined poly[{2-(methacryloyloxy)ethyl} trimethylammonium chloride] brush via surface-initiated atom transfer radical polymerization in fluoroalcohol. Macromolecules 43, 8409–8415. https://doi.org/10.1021/ma1014897

Kokhanovsky, A.A., Weichert, R., 2001. Multiple light scattering in laser particle sizing. Appl. Opt. 40, 1507. https://doi.org/10.1364/ao.40.001507

Kolya, H., Sasmal, D., Tripathy, T., 2017. Novel Biodegradable Flocculating Agents Based on Grafted Starch Family for the Industrial Effluent Treatment. J. Polym. Environ. 25, 408–418. https://doi.org/10.1007/s10924-016-0825-0

Kolya, H., Tripathy, T., 2013. Grafted polysaccharides based on acrylamide and N,N-dimethylacrylamide: Preparation and investigation of their flocculation performances. J. Appl. Polym. Sci. 127, 2786–2795. https://doi.org/10.1002/app.37603

Konduri, M.K.R., Fatehi, P., 2017. Influence of pH and ionic strength on flocculation of clay suspensions with cationic xylan copolymer. Colloids Surfaces A Physicochem. Eng. Asp. 530, 20–32. https://doi.org/10.1016/j.colsurfa.2017.07.045

Kosmulski, M., 2021. The pH dependent surface charging and points of zero charge. IX. Update. Adv. Colloid Interface Sci. 296, 102519. https://doi.org/10.1016/j.cis.2021.102519

Kossoff, D., Dubbin, W.E., Alfredsson, M., Edwards, S.J., Macklin, M.G., Hudson-Edwards,

K.A., 2014. Mine tailings dams: Characteristics, failure, environmental impacts, and remediation. Appl. Geochemistry 51, 229–245. https://doi.org/10.1016/j.apgeochem.2014.09.010

Kumari, A., Gajbhiye, P., Rayasam, V., 2019. Comparative Evaluation of Natural and Synthetic Flocculants on Selective Metal Recovery from Low-Grade Iron Ore Slimes. Trans. Indian Inst. Met. 72, 2567–2579. https://doi.org/10.1007/s12666-019-01726-9

Lakshmipathiraj, P., Narasimhan, B.R.V., Prabhakar, S., Bhaskar Raju, G., 2006. Adsorption of arsenate on synthetic goethite from aqueous solutions. J. Hazard. Mater. 136, 281–287. https://doi.org/10.1016/j.jhazmat.2005.12.015

Lanthong, P., Nuisin, R., Kiatkamjornwong, S., 2006. Graft copolymerization, characterization, and degradation of cassava starch-g-acrylamide/itaconic acid superabsorbents. Carbohydr. Polym. 66, 229–245. https://doi.org/10.1016/j.carbpol.2006.03.006

LaRue, R.J., Cobbledick, J., Aubry, N., Cranston, E.D., Latulippe, D.R., 2016. The microscale flocculation test (MFT)—A high-throughput technique for optimizing separation performance. Chem. Eng. Res. Des. 105, 85–93. https://doi.org/10.1016/J.CHERD.2015.10.045

Laskowski, J.S., Ralston, J., 2015. Colloid Chemistry in Mineral Processing, ISSN. Elsevier Science.

Lawrence, A.S.C., 1951. Colloid science, Nature. https://doi.org/10.1038/168800a0

Lee, C.H., Liu, J.C., 2001. Sludge dewaterability and floc structure in dual polymer conditioning. Adv. Environ. Res. 5, 129–136. https://doi.org/10.1016/S1093-0191(00)00049-6

Lee, L.T., Somasundaran, P., 1989. Adsorption of Polyacrylamide on Oxide Minerals. Langmuir 5, 854–860. https://doi.org/10.1021/la00087a047

Lee, L.T., Somasundaranh, P., 1989. Adsorption of Polyacrylamide on Oxide Minerals. Adsorpt. J. Int. Adsorpt. Soc. 10027, 854–860.

Leite, A. da M.C., Reis, É.L., 2020. Cationic starches as flocculants of iron ore tailing slime. Miner. Eng. 148, 106195. https://doi.org/10.1016/j.mineng.2020.106195

Leong, Y.K., 2021. Controlling the rheology of iron ore slurries and tailings with surface chemistry for enhanced beneficiation performance and output, reduced pumping cost and safer tailings storage in dam. Miner. Eng. 166, 106874. https://doi.org/10.1016/j.mineng.2021.106874

Levitt, D.B., Pope, G.A., Jouenne, S., 2011. Chemical degradation of polyacrylamide polymers under alkaline conditions. SPE Reserv. Eval. Eng. 14, 281–286. https://doi.org/10.2118/129879-PA

Li, H., Long, J., Xu, Z., Masliyah, J.H., 2008. Effect of molecular weight and charge density on the performance of polyacrylamide in low-grade oil sand ore processing. Can. J. Chem. Eng. 86, 177–185. https://doi.org/10.1002/cjce.20029

Liang, G., Zhao, Q., Liu, B., Du, Z., Xia, X., 2021. Treatment and reuse of process water with high suspended solids in low-grade iron ore dressing. J. Clean. Prod. 278, 123493. https://doi.org/10.1016/j.jclepro.2020.123493

Lin-Vien, D., Colthup, N.B., Fateley, W.G., Grasselli, J.G.B.T.-T.H. of I. and R.C.F. of O.M. (Eds.), 1991. APPENDIX 3 - A Summary of Characteristic Raman and Infrared Frequencies. Academic Press, San Diego, pp. 477–490. https://doi.org/https://doi.org/10.1016/B978-0-08-057116-4.50027-4

Liu, Z., Wei, H., Li, A., Yang, H., 2017. Evaluation of structural effects on the flocculation performance of a co-graft starch-based flocculant. Water Res. 118, 160–166. https://doi.org/10.1016/j.watres.2017.04.032

Lobato, F., 2012. Recursos hídricos e a economia verde – setor privado.

Lu, Q., Yan, B., Xie, L., Huang, J., Liu, Y., Zeng, H., 2016a. Science of the Total Environment A two-step fl occulation process on oil sands tailings treatment using oppositely charged polymer fl occulants. Sci. Total Environ. 565, 369–375. https://doi.org/10.1016/j.scitotenv.2016.04.192

Lu, Q., Yan, B., Xie, L., Huang, J., Liu, Y., Zeng, H., 2016b. A two-step flocculation process on oil sands tailings treatment using oppositely charged polymer flocculants. Sci. Total Environ. 565, 369–375. https://doi.org/10.1016/j.scitotenv.2016.04.192

Luz, A.B. da, Sampaio, J.A., França, S.C.A., 2010. Introdução ao tratamento de minérios, 5th ed, Tratamento de Minérios. CETEM/MCT, Rio de Janeiro. https://doi.org/10.1017/CBO9781107415324.004

Lv, X., Song, W., Ti, Y., Qu, L., Zhao, Z., Zheng, H., 2013. Gamma radiation-induced grafting of acrylamide and dimethyl diallyl ammonium chloride onto starch. Carbohydr. Polym. 92, 388–393. https://doi.org/10.1016/J.CARBPOL.2012.10.002

M., D., S., B., 2016a. Synthesis, characterization and application of acryloyl chitosan anchored copolymer towards algae flocculation. Carbohydr. Polym. 152, 459–467. https://doi.org/10.1016/j.carbpol.2016.07.031

M., D., S., B., 2016b. Synthesis, characterization and application of acryloyl chitosan anchored copolymer towards algae flocculation. Carbohydr. Polym. 152, 459–467. https://doi.org/10.1016/J.CARBPOL.2016.07.031

Mamghaderi, H., Aghababaei, S., Gharabaghi, M., Noaparast, M., Albijanic, B., Rezaei, A., 2021. Investigation on the effects of chemical pretreatment on the iron ore tailing dewatering. Colloids Surfaces A Physicochem. Eng. Asp. 625, 126855.

https://doi.org/10.1016/j.colsurfa.2021.126855

Mandal, B., Rameshbabu, A.P., Soni, S.R., Ghosh, A., Dhara, S., Pal, S., 2017. In Situ Silver Nanowire Deposited Cross-Linked Carboxymethyl Cellulose: A Potential Transdermal Anticancer Drug Carrier. ACS Appl. Mater. Interfaces. https://doi.org/10.1021/acsami.7b10716

Maurice, N.; Kenneth, C., 2003. Principles of Mineral Processing. Sme. https://doi.org/ISBN 0-87335-167-3

McGuire, M.J., Addai-Mensah, J., Bremmell, K.E., 2006. The effect of polymer structure type, pH and shear on the interfacial chemistry, rheology and dewaterability of model iron oxide dispersions. Colloids Surfaces A Physicochem. Eng. Asp. 275, 153–160. https://doi.org/10.1016/j.colsurfa.2005.09.034

Mengual, O., Meunier, G., Cayre, I., Puech, K., Snabre, P., 1999. Characterisation of instability of concentrated dispersions by a new optical analyser: The TURBISCAN MA 1000. Colloids Surfaces A Physicochem. Eng. Asp. 152, 111–123. https://doi.org/10.1016/S0927-7757(98)00680-3

Mishra, S., Mukul, A., Sen, G., Jha, U., 2011. Microwave assisted synthesis of polyacrylamide grafted starch (St-g-PAM) and its applicability as flocculant for water treatment. Int. J. Biol. Macromol. 48, 106–111. https://doi.org/10.1016/j.ijbiomac.2010.10.004

Moad, G., 2011. Chemical modification of starch by reactive extrusion. Prog. Polym. Sci. 36, 218–237. https://doi.org/10.1016/j.progpolymsci.2010.11.002

Moran, D.A., Soares, J.B.P., 2017. Starch-based composites using mature fine tailings as fillers. Can. J. Chem. Eng. 95, 1901–1908. https://doi.org/10.1002/cjce.22904

Mpofu, P., 2003. Surface Chemistry and Improved Dewatering of Clay Dispersions 224.

Mudd, G.M., 2008. Sustainability reporting and water resources: A preliminary assessment of embodied water and sustainable mining. Mine Water Environ. 27, 136–144. https://doi.org/10.1007/s10230-008-0037-5

Nanda, D., Mandre, N.R., 2022. Studies on Performance Evaluation of Modified Polymer on Iron Ore Fines by Selective Flocculation Process. J. Sustain. Metall. 8, 488–500. https://doi.org/10.1007/s40831-022-00509-9

Nanda, D., Mandre, N.R., 2019. Mechanism of polymeric adsorption in selective flocculation of low-grade iron ore. Sep. Sci. Technol. 00, 1–10. https://doi.org/10.1080/01496395.2019.1708936

Napper, D.H., 1983. Polymeric Stabilization of Colloidal Dispersions. J. Dispers. Sci. Technol. 6, 497. https://doi.org/10.1080/01932698508943966

Nasser, M.S., James, A.E., 2007. Effect of polyacrylamide polymers on floc size and rheological behaviour of kaolinite suspensions. Colloids Surfaces A Physicochem. Eng. Asp. 301, 311–322. https://doi.org/10.1016/j.colsurfa.2006.12.080

Nasser, M.S., James, A.E., 2006. The effect of polyacrylamide charge density and molecular weight on the flocculation and sedimentation behaviour of kaolinite suspensions. Sep. Purif. Technol. 52, 241–252. https://doi.org/10.1016/j.seppur.2006.04.005

Ng, J.K.H., 2018. Study of Thermoresponsive Hybrid Polymer for Oil Sands Applications.

Nguyen, B., Soares, J.B.P., 2022. Effect of the branching morphology of a cationic polymer flocculant synthesized by controlled reversible-deactivation radical polymerization on the flocculation and dewatering of dilute mature fine tailings. Can. J. Chem. Eng. 100, 790–799. https://doi.org/10.1002/cjce.24329

Nilsson, G.S., Bergquist, K.E., Nilsson, U., Gorton, L., 1996. Determination of the degree of branching in normal and amylopectin type potato starch with 1H-NMR spectroscopy: Improved resolution and two-dimensional spectroscopy. Starch/Staerke 48, 352–357. https://doi.org/10.1002/star.19960481003

Nittala, A.K., 2017. Smart Polymers as Flocculants for Oil Sands Tailings Treatment.

Olatunji, O.N., Du, J., Hintz, W., Tomas, J., 2016. Application of particle sedimentation analysis in sterically-stabilized TiO2 particles stability assessment. Adv. Powder Technol. 27, 1325–1336. https://doi.org/10.1016/j.apt.2016.04.027

Oliveira, L.P. De, 2017. Chitosan-Based Flocculants for Mature Fine Tailings Treatment.

Onen, V., Gocer, M., 2019. The effect of single and combined coagulation/flocculation methods on the sedimentation behavior and conductivity of bentonite suspensions with different swelling potentials. Part. Sci. Technol. 37, 823–830. https://doi.org/10.1080/02726351.2018.1454993

Osborn, I., 2015. Application of Temperature-Responsive Polymers to Oil Sands Tailings Management.

Ouachtak, H., Akhouairi, S., Ait Addi, A., Ait Akbour, R., Jada, A., Douch, J., Hamdani, M., 2018. Mobility and retention of phenolic acids through a goethite-coated quartz sand column. Colloids Surfaces A Physicochem. Eng. Asp. https://doi.org/10.1016/j.colsurfa.2018.02.071

Ozturk, O.F., Demirci, S., Sengel, S.B., Sahiner, N., 2018. Highly regenerable ionic liquid microgels as inherently metal-free green catalyst for H2 generation. Polym. Adv. Technol. https://doi.org/10.1002/pat.4254

Pal, S., Ghorai, S., Dash, M.K., Ghosh, S., Udayabhanu, G., 2011. Flocculation properties of polyacrylamide grafted carboxymethyl guar gum (CMG-g-PAM) synthesised by

conventional and microwave assisted method. J. Hazard. Mater. 192, 1580–1588. https://doi.org/10.1016/j.jhazmat.2011.06.083

Pal, S., Pal, A., 2012. Synthesis and characterizing a novel polymeric flocculant based on amylopectin-graft-polyacrylamide-graft-polyacrylic acid [(AP-g-PAM)-g-PAA]. Polym. Bull. 69, 545–560. https://doi.org/10.1007/s00289-012-0744-8

Pan, Z., Somasundaran, P., Turro, N.J., Jockusch, S., 2004. Interactions of cationic dendrimers with hematite mineral. Colloids Surfaces A Physicochem. Eng. Asp. 238, 123–126. https://doi.org/https://doi.org/10.1016/j.colsurfa.2004.01.019

Pattanaik, A., 2021. Application of Colloids and Its Relevance in Mineral Engineering, in: Rashed, R.V.E.-M.N. (Ed.), . IntechOpen, Rijeka, p. Ch. 10. https://doi.org/10.5772/intechopen.95337

Pearse, M.J., 2003. Historical use and future development of chemicals for solid–liquid separation in the mineral processing industry. Miner. Eng. 16, 103–108. https://doi.org/10.1016/S0892-6875(02)00288-1

Peixoto, C.L.P., 2012. Proposta De Nova Metodologia De Desaguamento De Rejeitos Em Polpa. UFOP.

Petronilho, S., Oliveira, A., Domingues, M.R., Nunes, F.M., Coimbra, M.A., Gonçalves, I., 2021. Hydrophobic starch-based films using potato washing slurries and spent frying oil. Foods. https://doi.org/10.3390/foods10122897

Quast, K., 2012. Effects of Pretreatments on the Zeta Potential Characteristics of a Hematite Ore. Int. J. Min. Eng. Miner. Process. 1, 47–55. https://doi.org/10.5923/j.mining.20120102.05

Rodrigues, A.B., 2017. Riscos da disposição de rejeitos de mineração e técnicas alternativas de disposição.

Rooney, T.R., Gumfekar, S.P., Soares, J.B.P., Hutchinson, R.A., 2016. Cationic Hydrolytically Degradable Flocculants with Enhanced Water Recovery for Oil Sands Tailings Remediation. Macromol. Mater. Eng. 301, 1248–1254. https://doi.org/10.1002/mame.201600230

Rostami Najafabadi, Z., Soares, J.B.P., 2021. Flocculation and dewatering of oil sands tailings with a novel functionalized polyolefin flocculant. Sep. Purif. Technol. 274. https://doi.org/10.1016/j.seppur.2021.119018

Rötzer, N., Schmidt, M., 2018. Decreasing metal ore grades-Is the fear of resource depletion justified? Resources 7. https://doi.org/10.3390/resources7040088

Salehizadeh, H., Yan, N., Farnood, R., 2018. Recent advances in polysaccharide bio-based flocculants. Biotechnol. Adv. 36, 92–119.

https://doi.org/10.1016/j.biotechadv.2017.10.002

Sánchez, J., Mendoza, N., Rivas, B.L., Basáez, L., Santiago-García, J.L., 2017. Preparation and characterization of water-soluble polymers and their utilization in chromium sorption. J. Appl. Polym. Sci. 134, 1–10. https://doi.org/10.1002/app.45355

Sarkar, A.K., Mandre, N.R., Panda, A.B., Pal, S., 2013. Amylopectin grafted with poly (acrylic acid): Development and application of a high performance flocculant. Carbohydr. Polym. 95, 753–759. https://doi.org/10.1016/j.carbpol.2013.03.025

Shrimali, K., Jin, J., Hassas, B.V., Wang, X., Miller, J.D., 2016. The surface state of hematite and its wetting characteristics. J. Colloid Interface Sci. 477, 16–24. https://doi.org/10.1016/j.jcis.2016.05.030

Siah, C., Robinson, J., Fong, M., 2014. A review on application of flocculants in wastewater treatment. Process Saf. Environ. Prot. https://doi.org/10.1016/j.psep.2014.04.010

Singh, R.P., Pal, S., Rana, V.K., Ghorai, S., 2013. Amphoteric amylopectin: A novel polymeric flocculant. Carbohydr. Polym. 91, 294–299. https://doi.org/10.1016/j.carbpol.2012.08.024

Siyamak, S., Laycock, B., Luckman, P., 2020. Synthesis of starch graft-copolymers via reactive extrusion: Process development and structural analysis. Carbohydr. Polym. 227, 115066. https://doi.org/10.1016/j.carbpol.2019.115066

Sponchioni, M., Capasso Palmiero, U., Manfredini, N., Moscatelli, D., 2019. RAFT copolymerization of oppositely charged monomers and its use to tailor the composition of nonfouling polyampholytes with an UCST behaviour. React. Chem. Eng. 4, 436–446. https://doi.org/10.1039/c8re00221e

Sun, G., Zhang, M., He, J., Ni, P., 2009. Synthesis of amphiphilic cationic copolymers poly[2-(methacryloyloxy)ethyl trimethylammonium chloride-co-stearyl methacrylate] and their self-assembly behavior in water and water-ethanol mixtures. J. Polym. Sci. Part A Polym. Chem. https://doi.org/10.1002/pola.23517

Sun, X., Ma, L., Tan, X., Wang, K., Liu, Q., 2020. Influence of molecular weight on polyacrylic acid flocculation of sub-micron titanium dioxide. Colloids Surfaces A Physicochem. Eng. Asp. 603, 125195. https://doi.org/10.1016/j.colsurfa.2020.125195

Sweedman, M.C., Tizzotti, M.J., Schäfer, C., Gilbert, R.G., 2013. Structure and physicochemical properties of octenyl succinic anhydride modified starches: A review. Carbohydr. Polym. 92, 905–920. https://doi.org/10.1016/j.carbpol.2012.09.040

Tizzotti, M.J., Sweedman, M.C., Tang, D., Schaefer, C., Gilbert, R.G., 2011. New 1H NMR procedure for the characterization of native and modified food-grade starches. J. Agric. Food Chem. 59, 6913–6919. https://doi.org/10.1021/jf201209z

Tonietto, A; Silva, J.J.M.., 2011. Valoração de danos nos casos de mineração de ferro no Brasil.

Rev. Bras. Crim. 1, 31–38.

Torquato, N.C., Luz, J.A.M. da, 2011. Espessadores no beneficiamento de minério de ferro. Rem Rev. Esc. Minas 64, 91–96. https://doi.org/10.1590/S0370-44672011000100012

Vajihinejad, V., Guillermo, R., Soares, J.B.P., 2017. Dewatering Oil Sands Mature Fine Tailings (MFTs) with Poly(acrylamide-co-diallyldimethylammonium chloride): Effect of Average Molecular Weight and Copolymer Composition. Ind. Eng. Chem. Res. 56, 1256–1266. https://doi.org/10.1021/acs.iecr.6b04348

Vajihinejad, V., Gumfekar, S.P., Bazoubandi, B., Rostami Najafabadi, Z., Soares, J.B.P., 2019a. Water Soluble Polymer Flocculants: Synthesis, Characterization, and Performance Assessment. Macromol. Mater. Eng. https://doi.org/10.1002/mame.201800526

Vajihinejad, V., Gumfekar, S.P., Bazoubandi, B., Rostami Najafabadi, Z., Soares, J.B.P., 2019b. Water Soluble Polymer Flocculants: Synthesis, Characterization, and Performance Assessment. Macromol. Mater. Eng. 304, 1–43. https://doi.org/10.1002/mame.201800526

Vajihinejad, V., Gumfekar, S.P., Bazoubandi, B., Rostami Najafabadi, Z., Soares, J.B.P., 2019c. Water Soluble Polymer Flocculants: Synthesis, Characterization, and Performance Assessment. Macromol. Mater. Eng. 304, 1–43. https://doi.org/10.1002/mame.201800526

Vedoy, D.R.L., Soares, J.B.P., 2015. Water-soluble polymers for oil sands tailing treatment: A Review. Can. J. Chem. Eng. https://doi.org/10.1002/cjce.22129

Velásquez-Barreto, F.F., Miñano, H.A., Alvarez-Ramirez, J., Bello-Pérez, L.A., 2021. Structural, functional, and chemical properties of small starch granules: Andean quinoa and kiwicha. Food Hydrocoll. 120, 106883. https://doi.org/10.1016/J.FOODHYD.2021.106883

Vidyadhar, A., Kumari, N., Bhagat, R.P., 2014. Adsorption Mechanism of Mixed Cationic/Anionic Collectors in Quartz-Hematite Flotation System. Miner. Process. Extr. Metall. Rev. 35, 117–125. https://doi.org/10.1080/08827508.2012.723649

Wang, C., Harbottle, D., Liu, Q., Xu, Z., 2014. Current state of fine mineral tailings treatment: A critical review on theory and practice. Miner. Eng. 58, 113–131. https://doi.org/10.1016/j.mineng.2014.01.018

Wang, F., Chang, L., Wang, L., Gong, Y., Guo, Y., Shi, Q., Quan, F., 2022. In-situ compatibilized starch/polyacylonitrile composite fiber fabricated via dry-wet spinning technique. Int. J. Biol. Macromol. 212, 412–419. https://doi.org/10.1016/j.ijbiomac.2022.05.091

Wang, J.P., Chen, Y.Z., Ge, X.W., Yu, H.Q., 2007. Gamma radiation-induced grafting of a cationic monomer onto chitosan as a flocculant. Chemosphere 66, 1752–1757. https://doi.org/10.1016/j.chemosphere.2006.06.072

Wang, J.P., Yuan, S.J., Wang, Y., Yu, H.Q., 2013. Synthesis, characterization and application of a novel starch-based flocculant with high flocculation and dewatering properties. Water Res. 47, 2643–2648. https://doi.org/10.1016/j.watres.2013.01.050

Wang, L., Shen, J., Men, Y., Wu, Y., Peng, Q., Wang, X., Yang, R., Mahmood, K., Liu, Z., 2015. Corn starch-based graft copolymers prepared via ATRP at the molecular level. Polym. Chem. 6, 3480–3488. https://doi.org/10.1039/c5py00184f

Wang, S., 2014. Fundamental Study on Polymer Flocculation Behavior in Saline Solutions.

Wang, S., 2011. Understanding Stability of Water-in-Diluted Bitumen Emulsions by Colloidal Force Measurements.

Wang, S., Hou, Q., Kong, F., Fatehi, P., 2015. Production of cationic xylan-METAC copolymer as a flocculant for textile industry. Carbohydr. Polym. 124, 229–236. https://doi.org/10.1016/j.carbpol.2015.02.015

Wang, S., Kong, F., Gao, W., Fatehi, P., 2018. Novel Process for Generating Cationic Lignin Based Flocculant. Ind. Eng. Chem. Res. 57, 6595–6608. https://doi.org/10.1021/acs.iecr.7b05381

Water, O.S.P., 2011. Application of Coagulation-Flocculation Process for Treating Oil Sands Process-Affected Water.

Wei, H., Gao, B., Ren, J., Li, A., Yang, H., 2018. Coagulation/flocculation in dewatering of sludge: A review. Water Res. 143, 608–631. https://doi.org/10.1016/J.WATRES.2018.07.029

Wills, B.A., Napier-Munn, T., 2005. Froth flotation. Wills' Miner. Process. Technol. 267–352. https://doi.org/10.1016/b978-075064450-1/50014-x

Witham, M.I., Grabsch, A.F., Owen, A.T., Fawell, P.D., 2012. The effect of cations on the activity of anionic polyacrylamide flocculant solutions. Int. J. Miner. Process. 114–117, 51–62. https://doi.org/10.1016/J.MINPRO.2012.10.007

Wolff, A.P., 2009. Caracterização De Rejeitos De Minério De Ferro De Minas Da Vale. Diss. apresentada ao Programa Pós- Grad. do Dep. Eng. Minas da Esc. Minas da Univ. Fed. Ouro Preto, como parte Integr. dos requisitos para obtenção do título mestre em Eng. Miner. Área.

Xu, R., Zou, W., Wang, T., Huang, J., Zhang, Z., Xu, C., 2022. Adsorption and interaction mechanisms of Chi-g-P(AM-DMDAAC) assisted settling of kaolinite in a two-step flocculation process. Sci. Total Environ. 816, 151576. https://doi.org/10.1016/j.scitotenv.2021.151576

Yang, Y., Wu, A., Klein, B., Wang, H., 2019. Effect of primary flocculant type on a two-step flocculation process on iron ore fine tailings under alkaline environment. Miner. Eng. 132,

14–21. https://doi.org/10.1016/j.mineng.2018.11.053

Yang, Z., Wu, H., Yuan, B., Huang, M., Yang, H., Li, A., Bai, J., Cheng, R., 2014. Synthesis of amphoteric starch-based grafting flocculants for flocculation of both positively and negatively charged colloidal contaminants from water. Chem. Eng. J. 244, 209–217. https://doi.org/https://doi.org/10.1016/j.cej.2014.01.083

Yi, L., Li, K.Z., Liu, D.X., 2013. Degradation of polyacrylamide: A review. Adv. Mater. Res. 800, 411–416. https://doi.org/10.4028/www.scientific.net/AMR.800.411

Zuquette, L., 2015. Geotecnia ambiental, 1st ed. Elsevier Editora Ltda., Rio de Janeiro.